

**THE ROLE OF CIRCULAR RNA CDRIAS IN MACROPHAGE
MEDIATED CARDIAC INJURY AND REPAIR**

A Dissertation
Submitted to
the Temple University Graduate Board

In Partial Fulfillment
of the Requirements for the Degree
DOCTOR OF PHILOSOPHY

By
Carolina Gonzalez
August 2024

Examining Committee Members:

Raj Kishore, Advisory Chair, Cardiovascular Science
Douglas Tilley, Cardiovascular Science
Conchi Estaras, Cardiovascular Science
Sadia Mohsin, Cardiovascular Science
Prasanna Krishnamurthy, External Member, University of Alabama

©
Copyright
2024

by

Carolina Gonzalez
All Rights Reserved

ABSTRACT

Introduction: Myocardial infarction is the most common form of acute cardiac injury attributed to heart failure. Despite advancements in prognosis and treatment, acute MI (AMI) still bears a considerable mortality rate within the initial year, with a significant portion of patients succumbing within the initial 30 days post-MI. The overall prognosis hinges on factors such as the extent of heart muscle damage, duration of the inflammatory response, and the efficacy of administered treatments in mitigating myocardial cell death and injury. This underscores the need for deeper mechanistic understanding and development of targeted therapies for cardiovascular diseases.

In response to cardiac injury, macrophages are initially recruited to the infarcted myocardium and undergo phenotypic change from pro-inflammatory (M1) macrophages in the early stage to an anti-inflammatory (M2) macrophages phenotype in the later stage, orchestrating the initiation, maintenance, and eventual resolution of the inflammatory response. However, in chronic ischemia or severe infarction, continuous cardiomyocyte death prolongs pro-inflammatory macrophage activation resulting in robust secretion of pro-inflammatory cytokines perpetuating the inflammatory response and resulting in increased myocardial damage. Despite some understanding, further research is needed on the mechanisms and factors influencing macrophage function during injury. Circular RNAs are newly discovered non-coding RNA generated from protein-coding genes ubiquitously expressed in mammalian tissue, highly conserved among species, and recently implicated in the possible regulation of macrophage activation. However, their role in immunomodulation during cardiovascular injury remains unknown.

Objective: This study focused on determining the specific role of circ-cdr1as in phenotypic switching between pro-, and anti-inflammatory macrophages and to determine whether functional regulation of circ-cdr1as modulates macrophage function post-cardiac injury.

Methods and Results: We performed circular RNA microarray analyses to assess circular RNA transcriptome changes using RNA isolated from bone marrow derived macrophages (BMDM) polarized to a M1 phenotype by $\text{INF}\gamma$ and $\text{TNF}\alpha$ or a M2 phenotype by IL-10, IL-4, and TGF- β . Following RNA isolation, samples are treated with RNaseR for enrichment of circular RNA and removal of linear RNA. We identified circRNAs differentially expressed in pro-and anti-inflammatory macrophages, including circRNA cdr1as (circ-cdr1as). RT-qPCR analysis revealed circ-cdr1as was one of the most downregulated in pro-inflammatory macrophages and significantly upregulated in anti-inflammatory macrophages *in vitro*. We established a circ-cdr1as overexpression system by generating a circ-cdr1as plasmid using pc3.1 plasmid with flanking regions that allows circularization of specified sequence for *in vitro* studies. For knockdown of circ-cdr1as, we used small hairpin RNA targeting the splicing junction found only in circular RNA. RT-qPCR and fluorescence activated cell sorting (FACS) analyses showed that overexpression of circ-Cdr1as increased transcription of anti-inflammatory markers and percentage of CD206+ (M2 macrophage marker) cells in naïve and pro-inflammatory macrophages *in vitro*. Meanwhile, knockdown decreased transcription of anti-inflammatory markers and increased the percentage of CD86+ (M1 macrophage marker) cells in naïve and anti-inflammatory macrophages *in vitro*. Disease enrichment analysis based on IPA system of the diseases associated with circular RNA involved in macrophage polarization indicated that cardiac fibrosis and cardiac enlargement as the top diseases. Therefore, we investigated

the expression levels of circ-cdr1as in the heart after myocardial infarction (MI) injury in a mouse model. RT-qPCR analysis revealed downregulation of circ-cdr1as in the heart 3 days post MI, suggesting a possible physiological role for circ-cdr1as in MI pathophysiology. We isolated fibroblast, cardiomyocytes, CD31+ endothelial cells, and F4/80+ macrophages and investigated the transcriptional changes of circ-cdr1as to determine if it is cell-type specific. RT-qPCR analysis showed no significant difference in transcription of circ-cdr1as in fibroblast and endothelial cells. However, in cardiomyocytes and macrophages there was a significant downregulation of circ-cdr1as. To understand the role of circ-cdr1as modulated macrophages in post-MI cardiac repair *in vivo*, we overexpressed circ-cdr1as in fluorescently labeled BMDMs and directly injected them into the ischemic myocardium immediately following MI surgery. FACS and immunohistochemistry analyses showed that these macrophages retained their anti-inflammatory phenotype during the initial stages of cardiac injury, and in the later stages improved cardiac left ventricular (LV) functions and reduced infarct size. Since circ-cdr1as was also decreased in cardiomyocytes post-MI, we additionally generated circ-cdr1as adeno associated virus 9 (circ-cdr1as-AAV-9) vectors to overexpress circ-cdr1as in mouse hearts. We performed tail vein injections of circ-cdr1as-AAV9 vectors 14 days prior to MI and conducted physiological and histological studies. Administration of circ-cdr1as-AAV9 significantly improved post-MI LV functions including ejection fraction (%EF) and fractional shortening (%FS) at 21-28D post MI, decreased infarct size, and improved angiogenesis. Interestingly, in the initial stages of cardiac injury, overexpression of circ-cdr1as reduced cardiomyocyte apoptosis and increased percentage of anti-inflammatory macrophages at injury site. Lastly, emerging evidence suggests that some circular RNAs

function as microRNA (miR) sponges. Therefore, we investigated this mechanism to assess whether circular cdr1as invokes phenotypic changes in macrophages in both the steady-state and injured heart by acting as a sponge for miRNA to inhibit its function. Circ-cdr1as contains over 70 binding sites for miR-7, a microRNA known to exacerbate inflammation in lung related diseases through inhibition of KLF4. Pull-down assay indicated that circ-cdr1as directly interacts with miR-7. We found a reciprocal relationship between circ-cdr1as and miR-7 in macrophages and in the heart 3 days post-MI. Overexpression of miR-7 by miR-7-5p mimic increased the percentage of pro-inflammatory marker CD86 in naïve, pro-, and anti-inflammatory macrophages and upregulated transcription of pro-inflammatory markers. Meanwhile, inhibition of miR-7 had the opposite effect. We also found that expression of miR-7 target gene, KLF4, was reduced when macrophages were treated with miR-7 and increased when miR-7 was inhibited.

Conclusions: In summary, this study suggests that circ-cdr1as plays a key role in regulating anti-inflammatory phenotype of macrophages through the modulation of miR-7 and its targets and exogenous delivery of circ-cdr1as may improve LV function over time. Therefore, circ-cdr1as may potentially be developed as an anti-inflammatory regulator in tissue inflammation after cardiac injury.

For Yoli, Mom, and Dad

who believed in me before I believed in myself.

For my baby girl Athena, we didn't start this journey, but we finished it together.

ACKNOWLEDGEMENTS

Nothing is ever done alone. I am incredibly grateful for the support I have received from my family and friends throughout my Ph.D. Collectively, you filled me with high spirits and held me up when I needed it most. Particularly, my mother and father that taught me to question everything, love learning, and to have the tenacity to accomplish my passions. I cannot express the amount of gratitude I have for my best friends and partner that have stuck by my side throughout all the long nights studying and challenges I have faced along every step. Finally, I am forever grateful to my loyal companion Rocky, whom I adopted during my third year and has never left my side. I love you all.

I am eternally grateful to my Ph.D. mentor and department chair, Dr. Raj Kishore. Throughout my Ph.D., Raj has been an outstanding mentor and provided me with incredible training, support, feedback, and patience. From the moment I joined his research group, Raj gave me the freedom and guidance to decide what I wanted to research and to develop into an independent resourceful critical thinking scientist. Thank you for molding me into the scientist I am today.

I am thankful to every member in the lab, past and present, for all the technical support and mentoring along the way. I learned to ask the right questions, design my experiments accordingly, and work as a team to help each other along the way. Cindy, your resourcefulness, and ability to manage this team is invaluable and I am tremendously grateful for all the help troubleshooting. May, thank you for always sharing your snacks with me when I am too busy to have lunch.

I would like to thank my research advisory committee: Drs. Douglas Tilley, Sadia Mohsin, and Conchi Estaras for their insightful comments, constructive criticism, and

valuable suggestions, which have significantly enriched the content and methodology of this study. Your guidance has helped me develop as a scientist and obtain a better understanding of the techniques, experiments, and methodology behind my research questions. Additionally, I would like to thank my external examiner, Dr. Prasanna Krishnamurthy, a distinguished researcher in the field of cardiovascular science focusing on understanding the underlying mechanisms of cardiovascular diseases with extensive expertise in cardiac inflammation, for taking the time and effort to be part of my committee.

Lastly, I want to thank everyone for your unwavering support, encouragement, and understanding throughout my journey as this work would not have been possible without all of you.

FUNDING

Carolina Gonzalez was partially supported by the National Institutes of Health (National Heart, Lung, and Blood Institute) F31 pre-doctoral fellowship HL162543-01(to Carolina Gonzalez), NIH T32-HL091804; HL091983, HL143892, HL134608 and HL147841 (to Raj Kishore).

TABLE OF CONTENTS

	Page
ABSTRACT.....	iii
DEDICATION	vii
ACKNOWLEDGMENTS	viii
FUNDING.....	x
LIST OF TABLES	xvi
LIST OF FIGURES	xvii
LIST OF ABBREVIATIONS	xix
 CHAPTER	
1. IMMUNE RESPONSE DURING CARDIAC INJURY	1
1.1 The Prevalence of Cardiovascular Disease and Pathophysiology of Cardiac Injury.....	1
1.2 Role of Innate Immune Cells in Cardiac Injury.....	3
1.3 Cross Talk between Macrophages and Cardiac cells.....	6
1.4 Challenges with Immunomodulation Therapy for Cardiac Injury and Potential of Non-coding RNAs as a Therapeutic Approach	7
2. THE ROLE OF CIRCULAR RNA IN INFLAMMATION AND CARDIOVASCULAR DISEASE.....	10
2.1 Circular RNA Biogenesis and Regulatory Roles.....	10
2.1.1 Methods for Detecting Circular RNAs	10
2.1.2 Circular RNA Databases	11
2.1.3 Proposed Models of Circular RNA Biogenesis	12
2.1.4 Expression of Circular RNAs	15

2.1.5	Regulatory Functions of Circular RNAs	17
2.2	Circular RNA as Regulators in Cardiac Physiology and Disease.....	23
2.2.1	Circular RNAs in Coronary Artery Disease	24
2.2.2	Circular RNAs in Atherosclerosis.....	26
2.2.3	Circular RNAs in Cardiac Hypertrophy	27
2.2.4	Circular RNAs in Cardiomyopathy	28
2.2.5	Circular RNAs in Cardiac Fibrosis.....	30
2.2.6	Circular RNAs in Cardiac Senescence	31
2.2.7	Circular RNAs in Myocardial Infarction.....	32
2.3	Circular RNAs in Immune Regulation	34
2.3.1	Circular RNAs in the Innate Immune Response.....	35
2.3.2	Role of Circular RNAs in Neutrophils	36
2.3.3	Role of Circular RNAs in Dendritic Cells.....	36
2.3.4	Role of Circular RNAs in Macrophages.....	38
2.3.5	Circular RNAs in the Adaptive Immune Response	39
2.3.6	Circular RNAs in Infectious Diseases	40
2.3.7	Circular RNAs in Autoimmune Diseases	41
2.3.8	Circular RNAs in Cancer Immunology	42
2.4	Summary and Objective	45
3.	THE ROLE OF CIRCULAR RNA CDR1AS IN MODULATION OF MACROPHAGE PHENOTYPE	47
3.1	Introduction.....	47
3.2	Methods	49
3.2.1	Bone Marrow Cell Isolation and Monocyte Culture	49

3.2.2 Polarization of BMDMs.....	49
3.2.3 RNA Isolation	50
3.2.4 Circular RNA Microarray and Microarray Data Analysis.....	50
3.2.5 Generation of circ-cdr1as Overexpression Plasmid and <i>in vitro</i> Overexpression in BMDMs.....	51
3.2.6 Lentivirus Short Hairpin RNA Construction and <i>in vitro</i> Knockdown of circ-cdr1as in BMDMs	53
3.2.7 FACS analysis and Cell Sorting.....	54
3.2.8 Reverse Transcription and RT-qPCR.....	55
3.2.9 CircRNA-miRNA-mRNA Interaction Network	55
3.2.10 TargetScan and Gene Ontology Analysis	56
3.2.11 Statistical Analysis.....	56
3.3 Results.....	56
3.3.1 Circular RNA Profiling in Pro- and Anti- Inflammatory Macrophages.....	56
3.3.2 Gene Interaction Networks and Disease Enrichment Analysis.....	57
3.3.3 Validation of the Top Ten Highly Conserved and Differentially Expressed CircRNAs	61
3.3.4 Overexpression of circ-cdr1as Increases Transcription of Anti- inflammatory markers and Percentage of CD206+ cells <i>in vitro</i>	63
3.3.5 Knockdown of circ-cdr1as Decreases Transcription of Anti- inflammatory markers and Increases Percentage of CD86+ cells <i>in vitro</i>	65
3.3.6 CircRNA Cdr1as-miRNA-mRNA Network and GO Enrichment Analysis.....	69
3.4 Discussion.....	69

3.5 Conclusion.....	74
4. CIRCULAR RNA CDR1AS MODULATES MACROPHAGE PHENOTYPE AND CARDIAC REPARATIVE FUNCTION AND IMPROVES POST-INJURY CARDIAC REPAIR.....	76
4.1 Introduction.....	76
4.2 Methods.....	78
4.2.1 Animal Models	78
4.2.2 Myocardial Infarction Surgery	79
4.2.3 Circ-cdr1as Expression Plasmid and AAV Construction.....	80
4.2.4 Left Ventricle Heart Tissue Collection and Cardiac Cell Isolations.....	81
4.2.5 Echocardiography.....	82
4.2.6 FACS Analysis of Cardiac Cells and Bone Marrow Derived Macrophages.....	83
4.2.7 Tissue Preparation and Immunohistochemistry.....	84
4.2.8 Cell Culture and <i>in vitro</i> Studies	86
4.2.9 <i>Ex Vivo</i> Overexpression of Circ-cdr1as in BMDMs	87
4.2.10 Pull Down Assay	87
4.2.11 RNaseR Treatment, Reverse Transcription, and RT-qPCR.....	88
4.2.12 Statistical Analysis.....	89
4.3 Results.....	89
4.3.1 Circular RNA cdr1as is Downregulated in Post-MI Hearts	89
4.3.2 <i>Ex Vivo</i> Overexpression of circ-cdr1as in Bone Marrow Derived Macrophages Retain their M2 Macrophage Phenotype when Injected in Post-MI Hearts	90

4.3.3 Injection of circ-cdr1as Overexpressing BMDMs into the Ischemic Myocardium Improved LV Function and Reduced Infarct Size	93
4.3.4 Administration of AAV9 circ-cdr1as by Tail Vein Injection Enhanced Cardiac circ-cdr1as Expression After Injury.....	94
4.3.5 Administration of AAV9 circ-cdr1as Attenuates LV Dysfunction and Reduces Infarct Size Post-MI	97
4.3.6 Cardiac Overexpression of circ-cdr1as Reduces Cardiomyocyte Apoptosis and Increases Anti-Inflammatory Macrophages 5 days Post-MI.....	99
4.3.7 Circular RNA cdr1as Modulates miR-7 Expression in Injured Hearts and BMDMs	101
4.3.8 MicroRNA-7 target KLF4 is Upregulated in BMDMs Treated with anti-miR-7	103
4.4 Discussion	104
4.5 Conclusion	110
5. CONCLUDING REMARKS AND SIGNIFICANCE	111
REFERENCES	115

LIST OF TABLES

Table	Page
4.1 Antibodies for FACS analysis	84
4.2 Primary antibodies for immunohistochemistry	85
4.3 Secondary antibodies for immunohistochemistry	85

LIST OF FIGURES

Figure	Page
1.1 Cellular microenvironment post-myocardial infarction.....	3
1.2 The three phases of infarcted myocardium healing and remodeling	8
2.1 Proposed models of circRNA biogenesis.....	16
2.2 Regulatory functions of circRNAs.....	24
2.3 Circular RNAs in cardiovascular disease	34
2.4 Circular RNAs in immune regulation.....	44
3.1 Characterization of bone marrow derived macrophages (BMDM) stimulated to pro-inflammatory or anti-inflammatory phenotype compared to naïve macrophages	58
3.2 Microarray analysis of differentially expressed circular RNAs in bone marrow derived macrophages	59
3.3 Ingenuity pathway analysis for differentially expressed circular RNAs between pro-inflammatory and anti-inflammatory macrophages	60
3.4 Top 10 differentially expressed and conserved circRNAs in BMDMs	62
3.5 Parent gene <i>cdr1</i> is unaffected in polarized BMDMs.....	63
3.6 Transcriptional changes in naïve, pro-inflammatory, and anti-inflammatory macrophages with scrambled control or overexpression plasmid	64
3.7 Overexpression of circ- <i>cdr1as</i> upregulates expression of anti-inflammatory markers in naïve macrophages and pro-inflammatory macrophages	66
3.8 Transcriptional changes in naïve, pro-inflammatory, and anti-inflammatory macrophages treated with scrambled control or lentivirus circ- <i>cdr1as</i> shRNA.....	67
3.9 Knockdown of circular <i>cdr1as</i> downregulates expression of anti-inflammatory markers in naïve or polarized anti-inflammatory macrophages	68
3.10 Predicted circular RNA <i>cdr1as</i> -miRNA-mRNA targets and top 3 associated functions.....	70

4.1 Circular RNA cdr1as expression in sham and MI hearts.....	90
4.2 GFP+ circ-cdr1as overexpressing macrophages retain M2-like phenotype in ischemic heart.....	92
4.3 Circ-cdr1as overexpressing macrophages injected into the myocardium improved cardiac function and reduced infarct size 28 days post-MI in mice	95
4.4 Validation of circ-cdr1as overexpression in the heart after tail vein injection.....	96
4.5 AAV9 circ-cdr1as tail vein injection improves cardiac function and reduces infarcted area in mice	98
4.6 Cardiac overexpression of circ-cdr1as reduces cardiomyocyte cell death enhances anti-inflammatory macrophages 5 days post-MI	100
4.7 Reciprocal relationship between miR-7 and circ-cdr1as in injured hearts and macrophages	102
4.8 Changes in expression of miR-7b-3p target KLF4 in the heart 3D post-MI and in BMDMs	104
4.9 Graphical Summary	110

LIST OF ABBREVIATIONS

AAV	Adeno-associated Virus
AGO	Argonaute
AMI	Acute Myocardial Infarction
ANOVA	Analysis of Variance
ANRIL	Antisense Noncoding RNA in the INK 4 locus
Arg-1	Arginase
α SMA	Alpha Smooth Muscle Actin
BM	Bone Marrow
BM-MNCs	Bone marrow-derived mononuclear cells
BMDMs	Bone Marrow Derived Macrophages
CACR	Caspase-1-Associated CircRNA
CAD	Coronary Artery Disease
CAF	Cancer associated Fibroblast
CDR1	Cerebellum Degeneration-related Protein 1
CDR1as	Cerebellar Degeneration-related Protein 1 Antisense
CDIP1	Cell Death Inducing Protein
CDK2	Cell Division Protein Kinase 2
CircRNA	Circular RNA
CiRNA	Intronic circRNA
Circ-CDR1as	Circular Cerebellar Degeneration-related Protein 1 Antisense
CHD	Coronary Heart Disease
CHI3I3	Chitinase-3-like protein 1

CMs	Cardiomyocytes
CO	Cardiac Output
CTGF	Connective Tissue Growth Factor
CVD	Cardiovascular Disease
DCs	Dendritic Cells
DNA	Deoxyribonucleic Acid
dsRNA	Double Stranded RNA
Dox	Doxorubicin
Echo	Echocardiography
ECM	Extracellular Matrix
EC	Endothelial Cells
EDV	End Diastolic Volume
ESD	End Systolic Volume
EF	Ejection Fraction
EndMT	Endothelial-to-Mesenchymal Transition
EcRNA	Exonic circRNA
ElcRNA	Exonic-Intronic circRNAs
EPIC	Estimating the Proportion of Immune and Cancer Cells
FACS	Fluorescence Activated Cell Sorting
FC	Fold Change
FS	Fractional Shortening
FUS	Fused in Sarcoma
GFP	Green Fluorescent Protein

GSEA	Gene Set Enrichment Analysis
GO	Gene Ontology
HCV	Hepatitis C Virus
HF	Heart Failure
HUVECs	Human Umbilical Vein Endothelial Cells
IL	Interleukin
INF γ	Interferon gamma
IPKB	Ingenuity Pathway Knowledge Base
I/R	Ischemia/reperfusion
IPA	Ingenuity Pathway Analysis
IRES	Internal Ribosome Entry Site
KEGG	Kyoto Encyclopedia of Genes and Genomes
KLF4	Krüppel-like factor 4
KSHV	Kaposi's Sarcoma Herpesvirus
LAD	Left Anterior Descending Artery
LDL	Low Density Lipoprotein
LPS	Lipopolysaccharide
Lrp6	Lipoprotein Receptor 6
lncRNAs	Long non-coding RNAs
LV	Left Ventricle
LVID	Left-ventricular Internal Diameter
LVPWT	Left-ventricular Posterior Wall Thickness
M ϕ	Macrophages

MAVS	Mitochondrial Antiviral Signal
MCP-1	Monocyte Chemoattractant Protein-1
MCFs	Mouse Cardiac Fibroblast
MDM	Monocyte-Derived Macrophages
MEFs	Mouse Embryonic Fibroblast
MI	Myocardial Infarction
miRNAs	MicroRNAs
Mbl	Muscleblind
MMD	Moyamoya Disease
MMP	Matrix Metalloproteinase
MS	Multiple Sclerosis
MT1-MMP	Membrane Type 1 Matrix Metalloproteinase
NKs	Natural Killer cells
NF κ B	Nuclear Factor Kappa B
NRG1	Neuregulin- 1
NIH	National Institutes of Health
NIICD	Notch1 Intracellular Domain
ncRNA	Non-Coding RNA
NRVM	Neonatal Rat Cardiomyocyte
Ox-LDL	Oxidized Low-Density Lipoprotein
PARP	Poly ADP Ribose Polymerase
PBMCs	Peripheral Blood Mononuclear Cells
PBS	Phosphate Buffered Saline

PCR	Polymerase chain reaction
PDK1	Phosphoinositide-Dependent Protein Kinase 1
PES1	Pescadillo Homologue 1
PFA	Paraformaldehyde
piRNA	Piwi-interacting RNAs
pre-mRNA	Precursor mRNA
PTEN	Phosphatase and tensin homolog
QKI	Quaking homolog, KH domain RNA binding protein
RA	Rheumatoid Arthritis
RBM20	RNA Binding Motif protein 20
qPCR	Quantitative Polymerase Chain Reaction
rRNAs	Ribosomal RNAs
RBP	RNA Binding Protein
RNA	Ribonucleic Acid
RNA-seq	RNA sequencing
ROS	Reactive Oxygen Species
RT-qPCR	Reverse Transcription Quantitative Polymerase Chain Reaction
siRNA	Small Interfering RNA
SEM	Standard Error of the Mean
shrRNA	Short Hairpin RNA
Sry	Sex Determining Region Y
snRNAs	Small Nuclear RNAs
snRNP	Small Nuclear Ribonucleoprotein

STAT	Signal Transducer and Activator of Transcription
SOCS1	Suppressor of Cytokine Signaling 1
SSBP1	Single Stranded DNA Binding Protein 1
S1pr1	Shingosine 1-phosphate Receptor
TAC	Transverse Aortic Constriction
TGF- β	Transforming Growth Factor beta
TIME	Tumor Immune Microenvironment
TLR4	Toll-Like Receptor 4
TNF α	Tumor Necrosis Factor α
tRNAs	Transfer RNAs
VEGF	Vascular Endothelial Growth Factor
VSMCs	Vascular Smooth Muscle Cells
WGA	Wheat Germ Agglutinin
WT	Wild-type

CHAPTER 1

IMMUNE RESPONSE DURING CARDIAC INJURY

1.1 The Prevalence of Cardiovascular Disease and Pathophysiology of Cardiac Injury

Cardiovascular disease (CVD) is the leading cause of morbidity and mortality, both globally and in the United States (1). CVD accounts for more than 20 million deaths globally and more than 900,000 deaths in the United States annually. Additionally, the economic burden is significant, with estimated direct costs of CVD in the United States to be about 254.3 billion each year (1). There are several distinct pathologies that are grouped under CVD that include coronary heart disease (CHD), heart failure (HF), stroke, and hypertension. It is estimated that roughly 48.6% of Americans suffer from at least one form of CVD (1). Myocardial Infarction (MI) is the most common form of acute cardiac injury attributed to heart failure, characterized by persistent inflammation leading to dysfunctional remodeling. MI is defined as sudden ischemic death of myocardial tissue caused by decreased or complete obstruction of blood flow to a portion of the myocardium, usually caused by rupture of vulnerable plaque (2). Following injury, molecular signaling pathways regulate processes such as inflammation, fibrosis, and hypertrophy, which collectively contribute to adverse myocardial remodeling, impaired cardiac function, and the progression of heart failure.

Prolonged MI deprives the myocardium of oxygen leading to extensive cardiomyocyte death as a result of calcium overload, oxidative stress, and myocardial dysfunction (3). This leads to the release of damage-associated molecular patterns and pro-inflammatory cytokines to initiate an inflammatory response. Additionally, endothelial cells participate in the inflammatory response by expressing adhesion molecules and

secreting cytokines and chemokines. This aids in the recruitment and adhesion of leukocytes promoting their extravasation into the injured tissue and enhance the inflammatory response. As infiltrating leukocytes clear debris, there is a shift to suppress inflammation and promote regeneration (4). As the infarcted area heals, surviving cardiomyocytes undergo hypertrophy to compensate for the loss of tissue. Meanwhile, fibroblasts proliferate, undergo phenotypic transformation into myofibroblast, and deposit extracellular matrix proteins, such as collagen, to preserve the structural integrity of the infarcted ventricle. This process, known as fibrosis, helps to stabilize the myocardium but will impair cardiac function leading to adverse remodeling (5). Heart remodeling is then characterized by dilation, segmental hypertrophy of remaining viable tissue, and cardiac dysfunction (4). Therefore, impairment in the contractile function of the heart results in decreased cardiac output, impaired systolic and diastolic function, and ultimately lead to heart failure (Fig 1.1).

The current most effective treatment following myocardial infarction involves immediate myocardial reperfusion through primary percutaneous coronary intervention and coronary artery bypass grafting. This approach mitigates injury severity to preserve viable myocardium and limit the extent of the infarction. The overall prognosis depends on the extent of heart muscle damage, length of inflammatory response, (6) and the impact the treatment itself had on myocardial cell death and injury (4). Despite advances in treatment, acute MI (AMI) still carries a mortality rate of 20% within the first year after MI, with over 50% of patients dying within the first 30 days post-MI (7). Hence, gaining deeper insight into the underlying mechanisms of CVD will aid in the development of targeted therapies for cardiovascular diseases.

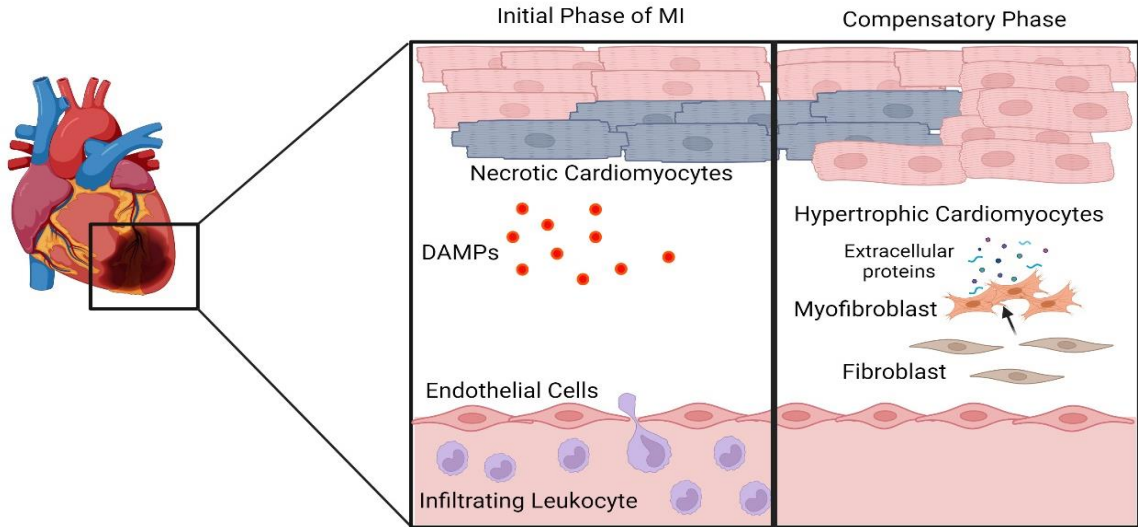


Figure 1.1. Cellular microenvironment post-myocardial infarction. In the initial phase following cardiac injury, dying cardiomyocytes release damage associated molecular patterns to recruit leukocytes to the site of injury. Endothelial cells begin to express extracellular proteins to allow the binding and extravasation of leukocytes to injury. In the later stages, inflammation is suppressed, and surviving cardiomyocytes undergo hypertrophy. Fibroblasts proliferate and phenotypically switch to myofibroblast, depositing extracellular matrix proteins to protect the structural integrity of the infarcted ventricle. (Illustration created in Biorender)

1.2 Role of Innate Immune Cells in Cardiac Injury

The link between heart failure and inflammation was first described in 1990 by Levine et al., who reported elevated levels of tumor necrosis factor in heart failure patients with a reduced ejection fraction (8). Numerous studies thereafter corroborated this finding, revealing elevated levels of inflammatory mediators in patients experiencing acute decompensated heart failure and heart failure patients with preserved ejection fraction, suggesting a consistent inflammatory response present in all the manifestations of heart failure (9-11). In response to cardiac injury, both innate and adaptive immune responses are activated to provide the heart with a short-term adaptation to stress. However, prolonged dysregulated inflammatory response can lead to collateral myocardial damage that contributes to left ventricular (LV) dysfunction and adverse LV remodeling (12).

During the first few days after cardiac injury, inflammatory signals promote adhesive interactions between leukocytes and endothelial cells. CXC chemokines mediate infiltration of neutrophils and C-C motif chemokine monocyte chemoattractant protein-1 (MCP-1) induces infiltration of monocytes. Selectins mediate leukocyte capture and rolling on the endothelial surface then interaction between ICAM-1 and integrins mediate firm adhesion of leukocytes to the endothelial layer (13). Neutrophils are one of the earliest leukocytes to infiltrate the infarcted myocardium, peaking around 12-24 hours (14). They mediate tissue damage by releasing matrix-degrading enzymes and reactive oxygen species (ROS) (15).

Monocytes then migrate to the injured heart where they differentiate into macrophages in a chemokine C-C motif receptor 2 (CCR2) dependent manner and are the predominant leukocyte type from days 2-7 post-injury (16). Monocytes/macrophages are crucial in the maintenance and resolution of inflammatory response. The recruited macrophages produce a sequential spectrum of cytokines, chemokines, and growth factors that exert both pro- and anti-inflammatory effects mediating wound healing and LV remodeling (4,11,13,15).

Pro-inflammatory (M1) macrophages will peak around the third day after MI. M1 macrophages are traditionally associated with a pro-inflammatory response and are referred to as classically activated macrophages, induced by Interferon gamma (IFN γ), Lipopolysaccharides (LPS), and Tumor Necrosis Factor α (TNF α) (17). When stimulated, M1 macrophages secrete high levels of pro-inflammatory cytokines such as TNF-alpha and interleukins (IL) IL-12, IL23, IL-1, and IL-6. They are characterized by efferocytosis, the scavenging of damaged tissue, and high antigen presenting capacity (11,16).

At approximately day 5-7 post-MI, clearance of apoptotic cells by macrophages and secretion of anti-inflammatory mediators including IL-4, IL-10, and transforming growth factor beta (TGF- β) promote polarization to anti-inflammatory M2 macrophages, working to resolve inflammation and repair cardiac tissue (18). M2 macrophages exhibit an anti-inflammatory, pro-regenerative phenotype and secrete high levels of anti-inflammatory cytokines, including IL-10 and growth factors such as Vascular Endothelial Growth Factor (VEGF), and inhibit leukocyte recruitment (11,17). During the resolution of inflammation stage, the macrophage population is maintained by local proliferation stimulated by growth factors (Figure 1.2). Meanwhile, these macrophages will produce myeloid-derived growth factor (MYGDF), a growth factor able protect cardiomyocytes from cell death (19).

Moreover, macrophages that reside within the heart (CCR2- resident macrophages) also participate in various forms of tissue remodeling and cardiac regeneration; however, to a lesser extent than recruited CCR2+ macrophages (20). CCR2- macrophages represent a tissue resident population that is maintained by local proliferation, and CCR2+ macrophages originate from infiltrating bone marrow derived monocytes. Differential gene expression analysis comparing CCR2- and CCR2+ macrophages revealed that genes associated with inflammatory pathways such as Interleukin-2/Signal Transducer and Activator of Transcription 5 (IL2/STAT5), IL-6/STAT3, and Tumor Necrosis Factor/ Nuclear Factor kappa B (TNF/NF κ B) signaling are upregulated in CCR2+ macrophages. Whereas genes associated with epithelial mesenchymal transition, coagulation, myogenesis, IL-2/STAT5 signaling were upregulated in CCR2- macrophages. Generally, CCR2+ macrophages express chemokines, cytokines, and mediators of IL-1, NF κ B and IL-6 signaling. Meanwhile, CCR2- macrophages express growth factors,

extracellular matrix components and conduction genes (20). Despite their functional differences, both circulating and tissue-resident macrophages are able to uniquely change phenotypes to either a pro-inflammatory M1 or anti-inflammatory M2 phenotype. Despite numerous studies describing the dynamic changes in macrophage phenotype, the signals and molecular mechanisms involved in these phenotypic changes remain to be completely elucidated.

1.3 Cross Talk between Macrophages and Cardiac cells

Macrophages are pivotal in the inflammatory response following MI, contributing to subsequent damage and the recuperative process. Apart from their acknowledged function in the immune response, macrophages participate in crosstalk with other cardiac cells such as cardiomyocytes, fibroblast, immune cells, and endothelial cells to dictate the inflammatory and repair processes (4). Specific efferocytosis receptors on macrophages are key regulators of CM efferocytosis including MerTk receptor, important for the identification of CMs, and expression of integrin-related proteins CD47 and CD72 in CM that can impair efferocytosis (21). Macrophages are also able to secrete cytokine oncostatin, a key regulator of CM proliferation and cardiac regeneration through the gp130/Src/Yap-Notch and Yap-ctgf/Areg pathways (4). Additionally, CCR2- resident macrophages can express high levels of the sodium channel, SCN9A, and sodium channel modulator, FGF13, suggesting that macrophages can modulate the electrical activity of cardiomyocytes (20,22).

Both M1 and M2 macrophages facilitate the fibrotic response. M1 macrophages recruit fibroblasts by CCL7 and CCL9 mediated signaling. Meanwhile, M2 macrophages secrete high levels of TGF β 1 to upregulate transcription of alpha smooth muscle actin (α -

SMA) resulting in fibroblast differentiation into myofibroblast, which secrete extracellular matrix components (ECM) to facilitate tissue repair (23). Sustained activation of macrophages leads to continuous secretion of growth factors and cytokines leading to continued breakdown of the ECM as well as overproduction of the ECM components by myofibroblast that can promote adverse remodeling and fibrotic scar tissue (Figure 1.2) (11).

The crosstalk between macrophages and cardiac endothelial cells (ECs) plays a regulatory role in vascular remodeling post-MI. Macrophages increase expression of membrane type 1 matrix metalloproteinase (MT1-MMP) resulting in activation of TGF β 1 to promote paracrine SMAD2-mediated signaling in endothelial cells and endothelial-to-mesenchymal transition (EndMT) (24). Macrophages and ECs also interact through sphingosine 1-phosphate receptor (S1pr1) in a contact dependent manner to promote the proliferation of M2 macrophages in the infarcted myocardium (25).

1.4 Challenges with Immunomodulation Therapy for Cardiac Injury and Potential of Non-coding RNAs as a Therapeutic Approach

In cases of chronic ischemia or severe infarction during which continuous cardiomyocyte death leads to prolonged M1 macrophage activation, efferocytotic ability is reduced. Additionally, the robust secretion of pro-inflammatory cytokines prolonging inflammatory response leads to increased damage to the myocardium. This is particularly the case in patients suffering from underlying chronic inflammatory diseases such as diabetes and obesity (11,26).

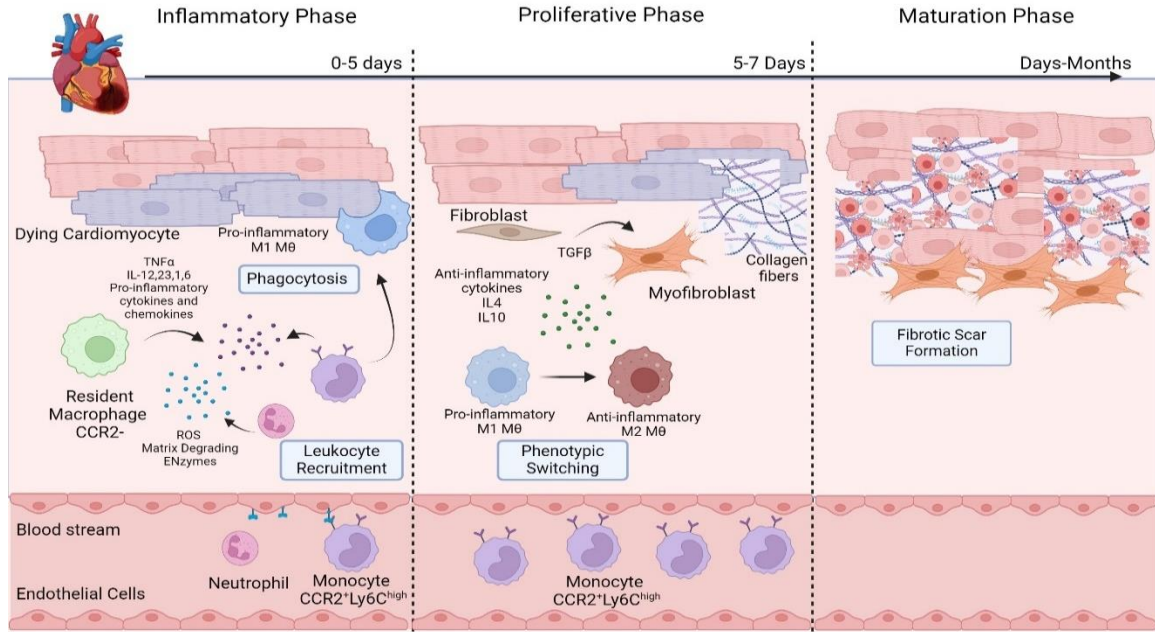


Figure 1.2. The three phases of infarcted myocardium healing and remodeling. In the initial days following cardiac injury (inflammatory phase), inflammatory signals recruit leukocytes. Endothelial cells express selectins and integrins to facilitate extravasation. Neutrophils are the first to infiltrate and peak around 12-24 hours. Neutrophils release matrix degrading enzymes and ROS. CCR2⁺ monocytes are recruited and peak around 2-7 days after injury. Pro-inflammatory cytokine secretion promotes monocytes to switch to pro-inflammatory macrophages and secrete high levels of pro-inflammatory cytokines. M1 macrophages recruit fibroblast CCL7 and CCL9 mediated signaling. As they continue to clear dead cells, in response to anti-inflammatory signals they undergo phenotypic switch to anti-inflammatory macrophages. These macrophages secrete anti-inflammatory cytokines and TGFβ to promote fibroblast to become myofibroblast. Myofibroblast then deposits collagen fibers leading to fibrotic scar formation. (Illustration created by Biorender)

Given the importance of macrophages in inflammation, proliferation, and tissue repair after MI, they represent a potential therapeutic target. There have been attempts to target the immune response following cardiac injury to either deplete monocytes post-MI or impair monocyte function and mobilization (11,15,16). For example, neutralizing anti-CC chemokine monocyte chemoattractant protein-1 antibody to prevent macrophage infiltration (27), depleting B-lymphocyte cells with CD20 specific monoclonal antibody to prevent recruitment of Ly6C^{high} monocytes (28), and treatment with clodronate-loaded

liposomes to deplete circulating monocytes post-MI (29). However, the unintended consequences of these approaches resulted in prolonged cardiac inflammation due to insufficient clearance of tissue debris and impaired tissue remodeling. Therefore, shifting the focus from selective elimination to direct immunomodulation targeting macrophage phenotypic switching to promote an anti-inflammatory M2 phenotype at an earlier stage in cardiac injury could promote repair and regeneration without these unintended consequences.

In recent years, non-coding RNAs (ncRNAs) were discovered to be involved in CVD, gathering interest in their potential to be used for diagnosis and targeted therapy (30-35). NcRNAs are ribonucleic acids transcribed from deoxyribonucleic acid (DNA) that are not translated into proteins. They include microRNAs (miRNAs), long non-coding RNAs (lncRNAs), circular RNAs (circRNAs), transfer RNAs (tRNAs), ribosomal RNAs (rRNAs), small nuclear RNAs (snRNAs), and piwi-interacting RNAs (piRNA) (36). Overall, ncRNAs play a role in stability of mRNA, translation initiation, and regulation of post-translational modification. Dysregulation of lncRNAs are associated with cardiac pathological hypertrophy, metabolic syndrome, and cell fate programming and development dysregulation (37). Recently, we and others have demonstrated the role of non-coding RNAs, including lncRNAs and miRNAs, to play a role in modulation of cardiomyocyte apoptosis, inflammation, angiogenesis, and fibrosis (31,38-44). In particular, circular RNAs (circRNAs) have recently emerged as promising candidates for targeted therapy due to their circular structure that confers resistance to exonucleases, their capability to regulate gene expression by modulating miRNA activity, sequester proteins by acting as protein sponges, and differential expression in CVD and immune cells (34,39,45-47).

CHAPTER 2

THE ROLE OF CIRCULAR RNA IN INFLAMMATION AND CARDIOVASCULAR DISEASE

2.1 Circular RNA Biogenesis and Regulatory Roles

Advances in high-throughput RNA sequencing (RNA-seq) have identified novel non-coding transcripts such as microRNAs (miRNA), long non-coding RNAs (lncRNAs), and circular RNAs (circRNAs) that have been found to influence various biological process, including onset and development of disease (48-50). Recently, the newest member of the long non-coding RNA family, circRNAs, are recognized to be involved cardiovascular disease and the inflammatory response (39,45,47,51-54). Circular RNA are covalently closed transcripts that are formed when the precursor mRNA (pre-mRNA) splicing machinery backsplice to join a downstream 5' splice site to an upstream 3' splice site. The unique characteristic of circRNAs to lack free terminals allow circRNAs to be resistant to exoribonuclease degradation and have longer half-lives compared to their linear counterpart (48,55,56).

2.1.1 Methods for Detecting Circular RNAs

Current methods for the detection of circRNAs include high throughput RNA sequencing (RNA-seq) with depletion of ribosomal RNA to enhance sequencing of non-polyadenylated RNA species and microarray analysis that specifically targets back-splicing junctions (57). The use of RNA-seq is recommended for the novel discovery of circRNAs since it will only require a small number of read counts. However, it may be inefficient in providing an accurate analysis of differential expression of specific quantification of circRNAs (58). Microarray implements known circular junction sequence-specific probes to only detect known circRNAs. However, one of the

disadvantages of microarray is the need for high input of total RNA compared to RNA-seq. After identification of circRNAs by either RNA-seq or microarray, Reverse Transcription- quantitative polymerase chain reaction (RT-qPCR) is used for validation using divergent primers to prevent amplification of other RNA species (57,59) and northern blot using sequence-specific probes that target the back-splicing junctions of circRNAs (60). These methods utilize treatment with RNaseR for the enrichment of circRNAs considering that circRNAs lack free terminals and therefore resistant to RNaseR exonuclease degradation (57).

2.1.2 Circular RNA Databases

As a result of several studies identifying a vast amount of circRNAs, specialized databases have been created to unify data sets from published studies. These databases include: circBase, CircInteractome, CIRCpedia, CircR2Disease, and Circ2Traits. circBase, established by Glažar P et al., contains data from humans, mice, *C. elegans*, and *Latimeria* organisms. It provides gene description, genomic position, circRNA ID, and tissue/cell line a particular circRNAs is expressed in (61). CircInteractome, established by Dudekula et al., combines numerous features from other databases (starebase 2.0, circBase, Primer3, and TargetScan 7.0) to provide information about circRNAs binding factors (miRNAs and RBPs), facilitate in divergent primer design, and aid in small interfering RNA (siRNA) design that target circRNA of interest (62). CIRCpedia, established by Zhang et al., is a database that contains identified alternative backsplicing and alternative splicing in circRNAs from six different species from over 180-RNA seq datasets. Additionally, this database incorporates conservation analysis of circRNA between human and mice (63). Circ2Traits, established by Ghosal et al., is a database for circRNAs that is predicted to

associate with a disease based on the likelihood that a particular circRNA will interact with a disease associated miRNA or based on mapping disease associated single nucleotide polymorphism sites on circRNA loci. This data base also provides miRNA-circRNA-mRNA-lncRNA interactome networks for any disease of interest (64). Lastly, CircR2Disease, established by Fan et al., is a database for circRNA dysregulation in disease. This database identified circRNAs relevant to gene regulation in the transcriptional, post-transcriptional, and translational levels. Additionally, this database includes circRNA-disease association, name of disease, expression levels of circRNA, methods of detection, circ-RNA disease connection, and associated publications (65). Overall, these databases provide crucial information from conservation, expression, primer design, to associated diseases.

2.1.3 Proposed Models of Circular RNA Biogenesis

Circular RNAs can be categorized based on the region from the pre-mRNA they were derived from. Exonic circRNA (EcRNA) originates from exonic regions, intronic circRNA (CiRNA) is derived from intronic regions, and exon-intronic circRNAs (EicRNA) emerge from both regions. Additionally, these circular RNAs will differ in structure, location, and function. The most abundant type of circRNA is exonic circRNA and is primarily located in the cytoplasm (49,56,66,67). Meanwhile, intronic circRNA are generally found in the nucleus and participate as transcriptional regulators of the parental genes by interaction with RNA polymerase II (Figure 2.1E) (68,69).

There are currently proposed models that explain circRNA formation. In canonical linear splicing, the spliceosome machinery removes introns from pre-mRNA and joins exons together for form a single stranded RNA that is protected from degradation by

the addition of a 5' cap and poly (A) tail (Figure 2.1D). In backsplicing, there are two main proposed models for exon circularization, “lariat-driven circularization” or “intron pairing driven circularization.” In “lariat-driven circularization,” alternative splicing leads to an exon or intron containing lariat that can promote circularization (Figure 2.1A). The exons are then back spliced by the spliceosome and modulated by both *cis* and *trans* regulators (70). In “intron-pairing-driven-circularization,” direct RNA base pairing of reverse complementary sequences, such as Alu repeats (most abundant primate-specific repeats) across introns that are flanking exons are brought into proximity to promote circularization (Figure 2.1B) (71). In “lariat-driven circularization,” canonical splicing occurs prior to backsplicing, whereas in “intron-pairing-driven-circularization” the backsplicing occurs first (48). In some cases, flanking introns can contain binding sites for RNA binding proteins (RBPs) such as Quaking (QKI) (71) or Muscleblind (Mbl) that facilitate RBPs to bind and dimerize to form a looped structure promoting circularization (Figure 2.1C). Quaking protein is an RBP that belongs to the signal transduction and activation of RNA family and Muscleblind (Mbl) is an RNA splicing factor that regulates pre-mRNA alternative splicing (71). Alternative splicing and competing RNA pairing across different flanking introns can promote varying exonic circRNAs derived from a single gene locus (55,72). On the other hand, circular intronic RNAs (ciRNAs) can be self-splicing derived or spliceosomal-derived (73). In the self-splicing group I, introns are located within genomic ribosomal RNA regions and the group I introns recruit an external guanosine as a nucleophile to initiate splicing (74). In self-splicing group II, the introns autocatalytically splice themselves from precursor RNAs by transesterification (75,76). On the other hand, in spliceosomal-derived circular intronic RNAs, a 2' to 5' lariat is formed during intron

excision that is then additionally degraded from their 3' end up the branch point (Figure 2.1A). Further degradation beyond the branch point depends on a 7-nt GU rich motif near the 5' splice site and 11-nt C-rich motif near the branch point (69).

Furthermore, studies have also investigated factors that play a role in the inhibition of circRNAs formation. Notably, ADAR1, an RNA editing enzyme, can catalyze adenosine in the reverse complementation region of introns to inosine, untying of the pairing structure, and preventing the splicing site from approaching to inhibit circRNA formation. ATP dependent RNA helicase A (DHX9) can bind to inverted complementary repeats (*Alu*) and unwinds dsRNA helical structures to prevent the looping of intron sequences and thereby, preventing circular RNA biogenesis (77). In hepatocellular carcinoma, Cleavage and Polyadenylation Specific Factor 4 (CPSF4), core component of the 3' end processing complex, that specifically recognizes the polyadenylation signal sequences (PAS: AAUAAA or variants: AUUAAA, AAUAUA, AAUGAA, AAUAAU, and AAGAAA) in circRNAs and catalyzes cleavage by the CPSF4 complex to reduce expression of circRNAs (78).

Studies have suggested that the formation of circular RNA can occur co-transcriptionally or post-transcriptionally (79,80). Studies in *Drosophila* found a substantial number of circRNAs as chromatin-bound (nascent) RNA from fly heads and mutant RNA polymerase II with slower elongation rate in favor of co-transcriptional splicing increased the ratio of linear to circRNA (Figure 2.1E), suggesting that circRNA biogenesis occurs co-transcriptionally (71,79). In the case that circularization occurs co-transcriptionally, circRNA biogenesis can compete with pre-mRNA splicing resulting in reduce expression of their linear counterpart (71). On the other hand, studies have also

reported that pre-mRNA requires a stable 3' end to promote circularization (81) and that circRNA processing might largely occur post-transcriptionally rather than co-transcriptionally (82,83). Metabolic tagging of nascent RNAs with 4-thiouridine (4sU) during circRNA biogenesis demonstrated that a significant portion of circRNAs were detected only after transcriptional completion of their host pre-mRNA (84).

2.1.4 Expression of Circular RNAs

Total RNA high-throughput sequencing libraries depleted of ribosomal RNAs identified that circRNAs are ubiquitously expressed in viruses, bacteria, plants, and mammalian tissue and are highly conserved among species (47,55,85-87). Although the majority of circRNAs are expressed at low levels due to inefficiency of back-splicing compared to canonical splicing. In some cases, exonic circRNAs have been identified to be expressed at higher levels than their associated linear mRNAs (88,89). Deep RNA sequencing from a variety of normal and malignant human cells identified a substantial fraction of the spliced transcription from hundreds of genes are circular RNA(89). In humans, they are highly expressed in the brain (90) , exosomes, and peripheral blood (91). Studies exploring circRNA expression profiles using RNA-seq data in adult and fetal tissues (colon, heart, kidney, liver, lung, and stomach) identified a total of 8,120 (adult tissue) and 25,933 (fetal tissue) circular RNA. The abundance and relative expression level of circRNAs changed throughout development and they were found to be higher in fetal tissue compared to adult tissue. For at least 1,000 circRNAs identified in each adult tissue type, they reported 36.97-50.04% were tissue-specific (92).

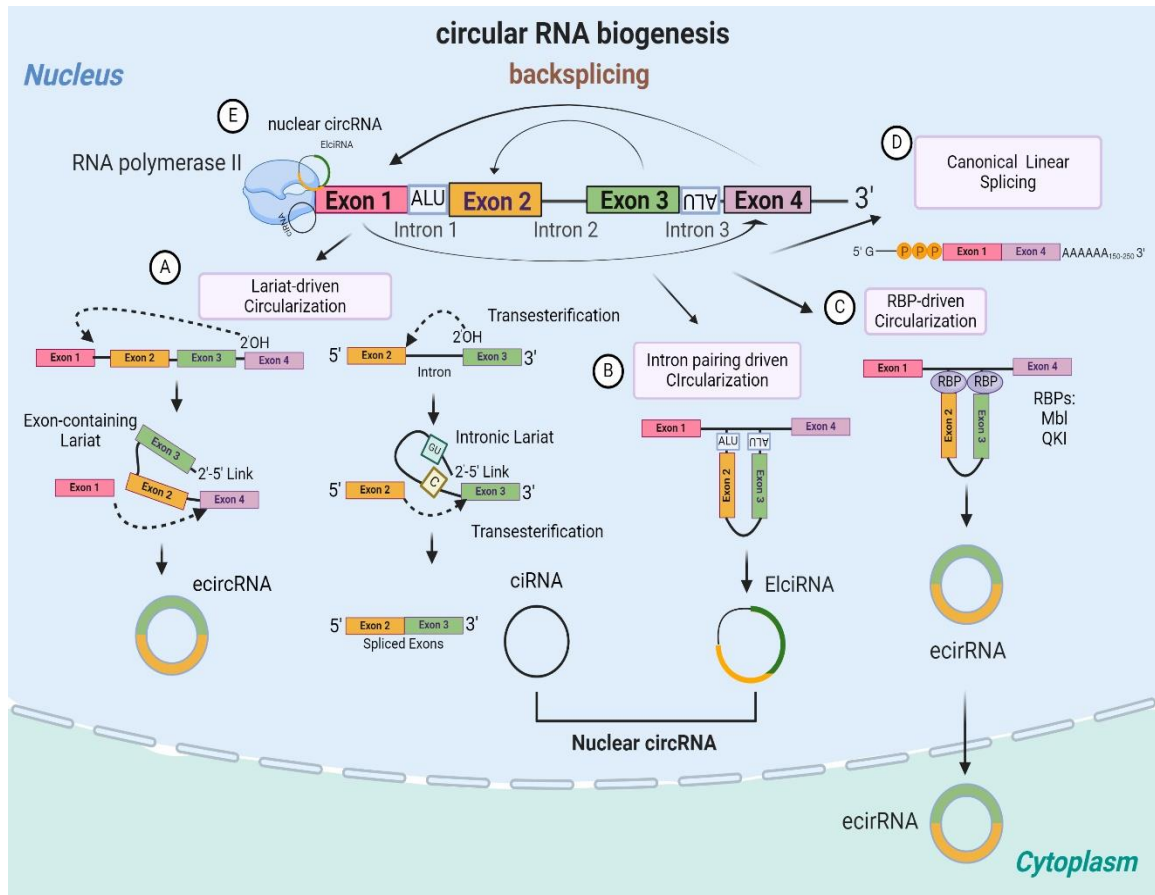


Figure 2.1. Proposed models of circRNA biogenesis. Circular RNAs are covalently closed circular RNA generated from backsplicing events mediated by the spliceosomal machinery. (A) Lariat-driven circularization, backsplicing produces an intronic lariat or exon-containing lariat. An upstream branch point adenosine 2' hydroxyl group nucleophilically attacks the 3' splice site of the downstream exon to form a lariat structure. The downstream exon 3' hydroxyl group then attacks the 5' splice acceptor of the exon to circularize it. Exon-containing lariats produce an exonic circular RNA (ecircRNA) that translocates to the cytoplasm. Whereas intronic lariats produce intronic circular RNA (ciRNA) that remain in the nucleus, degradation beyond the branch point will depend on the GU rich and C-rich motifs in the lariat. (B) In intron pairing driven circularization, direct RNA base pairing of reverse complementary sequences (Alu repeats) occurs in the intronic regions flanking the exons to promote circularization of exonic-intronic circular RNA (ElciRNA) that will remain in the nucleus. (C) RBP-driven circularization, RBPs such as QKI or Mbl bind and dimerize to form a looped structure to promote circularization. (D) Canonical pre-mRNA linear splicing, spliceosome machinery removes introns from pre-mRNA to join exons together and addition of a 5' cap and poly-A tail protects mRNA from degradation. (E) Nuclear circRNAs can regulate transcription of parental gene by binding to the U1 component of the spliceosomal machinery to recruit RNA polymerase II. (Illustration created in Biorender)

Deep RNA sequencing on ribosomal-depleted RNA from 12 human hearts, 25 mouse hearts, and human embryonic stem cell-derived cardiomyocytes identified 3,017 circRNAs found within human and mouse. They performed a 28- day differentiation time course of the human embryonic stem cell-derived cardiomyocytes and found that circRNAs were also differentially expressed throughout development. Interestingly, circRNAs expression levels correlated with their linear counterpart; however, some circRNAs were expressed in higher levels compared to the linear RNA (cardiac genes: Titin, RyR2, and DMD) (86). In a more extensive study, circRNA expression was analyzed in neonatal or adult rats, in sham or after transverse aortic constriction (TAC) mice, and in failing or non-failing human hearts. They identified over 9,000 circular RNAs present in all species, most notably several circRNAs derived from the Titin gene. Overall, they corroborated previous findings that circRNAs expression is differentially expressed throughout development with lower circRNAs expression in the adult rat heart. Additionally, they report an increase in circRNAs expression in the mouse and human failing hearts, in which under disease conditions a re-expression of fetal genes tends to occur (47). Additionally, the level of circRNA expression does not always correlate with the expression level of its linear counterpart, suggesting that expression is regulated and the spliceosome can differentiate between canonical linear splicing and backsplicing (55).

2.1.5 Regulatory Functions of Circular RNAs

The functions of circRNAs are still largely unclear. However, circRNAs have been implicated in distinct biological functions such as regulators of transcription/translation, sequesters of miRNA/RBP, and cell-cell communication through exosomes (Figure 2.2). Exon-intronic circRNAs regulate gene expression in the nucleus

by interacting with U1 small nuclear ribonucleoprotein (snRNP) to form a complex that associates with RNA polymerase II at the promoter region of the parental gene to promote transcription of parental gene. Blocking of the ElciRNA-U1 snRNP complex impaired the interaction with RNA polymerase II resulting in reduced parent gene transcription (93). Intronic circRNAs are also retained in the nucleus and regulate transcription of parental gene by association with elongation RNA polymerase II machinery (Figure 2.1E) (69). The potential translational function of circRNAs remains a subject of significant debate. Polysome profiling analysis of RNaseR resistance RNAs and mass spectrometry suggest that circRNAs have protein coding ability. Additionally, there are numerous reports that suggest circRNAs contain internal ribosome entry sites (IRES) or N6-methyladenosine (m6A) residues to promote the translational function of circRNAs (56,82,94-96). A study revealed that a single m6A motif is sufficient to promote translation initiation in human cells (95). Another study described a group of circRNAs that could be translated *in vivo* from *Drosophila melanogaster*. This group performed ribosome foot-printing from the fly heads to identify circRNAs associated with translating ribosomes (ribo-circRNAs). These circRNAs were found to share a start codon with the hosting mRNA and that isoform circMbl3 produced a 37.04 kDa protein that was detected by mass spectrometry (Figure 2.2D) (97). A recent study found that exogenous circRNAs are able bypass cellular sensors and avoid triggering an immune response in RIG-I and Toll-like receptor competent cells and circRNA packaged in a lipid-nanoparticle could effectively be translated *in vivo* without provoking an RNA-mediated innate immune response (94). One study identified circRNAs that could be translated in HeLa cells, a human epithelial cell line derived from cervical adenocarcinoma, in the absence of an IRES site, poly-A tail, or a cap structure.

These circRNAs produced a protein product by utilizing the rolling circle amplification mechanism in which synthesis of nucleic acids occur on a circular template (96). Contrary to these findings, studies that performed ribosome profiling of circRNAs containing protein coding sequences did not find evidence of translation (98-100). One extensive study using ribosome profiling, proteomics analysis, and cross-species analysis found that circRNAs with start codons from the protein-coding host genes did not translate (98). This finding was further validated by another study in which deep ribosome-footprinting sequencing and mass spectrometry analysis of hematopoietic cells did not provide evidence for translation (99). Moreover, circRNAs can also modulate translation of their linear counterpart by interacting with RBPs to regulate translation. Abdelmohsen et al., identified circRNAs that bind to RBP HuR in human carcinoma HeLa cells, specifically, circPABPN1 suppressed HuR binding to PABPN1 mRNA to prevent PABPN1 translation (101).

The most established function of circRNAs located in the cytoplasm is acting as sequesters of miRNAs or RBPs to modulate transcriptional regulation for miRNA target genes, and processing and stability of mRNA (49,102-104). Notably, one of the most studied circRNA to function as a miRNA sponge is cerebellar degeneration-related protein 1 antisense RNA (Circ-cdr1as), known to contain over 70 binding sites for miR-7. Circ-cdr1as is comprised of a single exon, highly conserved, and highly expressed in the mammalian brain (49,82,104). One study knocked out circ-cdr1as in the mammalian brain using CRISPR-Cas 9 system utilizing two single-guide RNAs designed to bind upstream of the Circ-cdr1as splice sites indicated that knockout of circ-cdr1as lead to dysfunction of excitatory synaptic transmission that is associated with neuropsychiatric disorders (105).

Additionally, in a diabetic mouse model, circ-cdr1as overexpression improved insulin secretion in pancreatic islet cells by inhibition of miR-7 (106). Functional studies on zebrafish showed that overexpression of circ-cdr1as induced developmental defects in the midbrain through miR-7 dysregulation (104). Sex Determining Region Y (Sry) circRNA acts as a miR-138 sponge containing 16 binding sites. Their interaction was further confirmed using biotin-labelled miR-138 effectively captured Sry circRNA (104). Furthermore, circHIPK3 contains 19 miRNA binding sites for nine different miRNAs and through luciferase screening was revealed to bind to miR-124, a tumor suppressor, to upregulate cell proliferation and migration in hepatocellular carcinoma (107,108). However, it should be noted that most circRNAs in mammals lack enrichment of binding sites for specific miRNAs and so, some studies suggest that the general function of circRNAs may not be as miRNA sponges (39,67,98,109-111). Screening for circRNA enriched with argonaute (AGO)-bound regions, a protein that is part of the RNA-induced silencing complex known to directly bind with miRNA, provided evidence of circRNAs not primarily functioning as miRNA sponges in HEK-293 cells (110). In addition to this, loss of function experiments in human umbilical vein endothelial cells (HUVECs) (109), and *in silico* analysis on predicted 8mer target sites across different species (98), and mutations of predicted miRNA binding sites for circFndc3b has no effect on the function *in vitro* and *in vivo* (39), support the notion that circRNAs may not primarily regulate miRNAs. However, whether circRNAs may indirectly regulate miRNA or have a different function altogether remains to be explored.

Circular RNAs also interact with regulatory RBPs acting as protein sponges, decoys, scaffolds, and recruiters (Figure 2.2 C) (46,112-114). Circ-Foxo3 has been implicated to play a role in the cell cycle by interacting with cell division protein kinase 2 (CDK2) and cyclin dependent kinase inhibitor 1 (p21) resulting in depletion of available CDK2 and p21 and cell cycle arrest at the G1/S phase (113). CircANRIL forms a stem-loop structure to mimic ribosomal RNA to bind to pescadillo homologue 1 (PES1), essential 60S ribosomal assembly factor, and thereby, blocking PES1 interaction with PeBoW complex (Pes1, Bop1, WDR12) that is necessary for biogenesis of the 60S ribosomal subunit in vascular smooth muscle cells and macrophages (46). Furthermore, Circ-Amotl1 can act as a protein decoy by binding and retaining c-myc in the nucleus and upregulating expression of c-myc targets to promote tumorigenicity (114). Additionally, circ-Amotl1 and circ-Foxo3 can function as protein scaffolds to aid in the co-localization of enzymes and their substrates (115). Circ-Amotl1 binding to PDK1 and AKT1 leads to phosphorylation of AKT (pAKT) and nuclear translocation in which pAKT upregulates proliferation associated factors and downregulates expression of pro-apoptotic proteins (115,116). Additionally, circ-Foxo3 can bind to p63 and E3 ubiquitin-protein ligase Mdm2 to promote Mdm2 induced p53 ubiquitination and degradation. This prevented Mdm2 from inducing Foxo3 ubiquitination and degradation triggering cancer cell apoptosis (116). In conclusion, the intricate interplay between circular RNAs and RNA-binding proteins underscores their multifaceted roles in gene regulation, offering promising avenues for further exploration in both cell physiology and disease development.

Exosomes play a crucial role in facilitating cell-to-cell communication. They are tiny shuttles carrying bioactive cargos, including lipids, proteins, and nucleic acids, from

numerous cell types that can modify several cellular bioactivities. Exosomes are nanosized extracellular vesicles with a lipid bilayer formed through inward budding of the endosomal membrane. They accumulate in multi vesicular bodies and then are released into the extracellular space where they can be taken up by neighboring cells or transported through body fluids to remote locations (117). High-throughput RNA-seq revealed RNA populations in exosomes and identified enrichment of circRNAs in exosomes derived from human cancer xenografts (118), and cells lines HeLa, 293T, and U-2 OS cells (119). Li et al.(118), conducted an expression profile of serum exosomal circRNAs in colorectal cancer patients and healthy donors. They found significant differential expression, including the absence of 67 circRNAs and 257 new circRNAs times compared to healthy donors(118). Considering that circRNAs are miRNA sponges and miRNAs are also abundant in exosomes, the relationship between circRNAs-miRNAs in exosomes was investigated. The level of circ-cdr1as was significantly downregulated in exosomes after treatment with miR-7 mimic in HEK293T and MCF-7 cell lines. Additionally, the exo-circ-cdr1as retained biological activity as circ-cdr1as could still function as a miRNA sponge (118). These findings demonstrate that sorting of circRNAs within exosomes is regulated. Furthermore, it has been speculated that circRNAs resistance to enzymatic degradation may result in the accumulation of circRNAs within the cell and so, they may be packaged into exosomes to reduce the accumulation of circRNAs and to assist with circRNA clearance. As a result of this, circular RNAs can be found in several body fluids including serum/plasma providing evidence for their potential as biomarkers of disease (Figure 2.2E) (120-125). One study assessed expression levels of circRNAs MICRA on the peripheral blood at the time of reperfusion in acute MI patients and healthy patients and found lower levels of circRNAs

MICRA associated with higher risk of developing left ventricular dysfunction post-AMI (120). Additionally, in patients with coronary artery disease (CAD), there is differential expression of circRNAs in the peripheral blood and microarray analysis identified hsa_circ_0124644 and hsa_circ_0098964 as potential biomarkers for diagnosing CAD (124). In a case-control study of 100 patients with or without hypertension found a close correlation between circRNAs and hypertension based on differential expression in tissues and body fluids from hypertensive patients compared to healthy patients. Of the 287 circRNAs that were differentially expressed, hsa_circ_0037911 was the most significantly elevated in hypertensive patients and could potentially serve as a novel biomarker for hypertension (125,126). In conclusion, circRNAs are attributed as being highly conserved across tissues, released during physiological responses, enclosed in extracellular vesicles, and detectable in body fluids, rendering them promising candidates as biomarkers for disease.

2.2 Circular RNA as Regulators in Cardiac Physiology and Disease

Circular RNAs are abundant in the eukaryotic transcriptome and participate in various biological processes. Numerous circRNAs have been identified to be important for cardiovascular development and disease (52,127,128). Overall studies have shown differential expression of circRNA in failing mouse, rat, and human hearts (39,47). Circular RNAs have been implicated to play a role in cardiovascular diseases such as coronary artery disease, atherosclerosis, cardiac hypertrophy, cardiomyopathy, cardiac fibrosis, cardiac senescence, and myocardial infarction (Figure 2.3).

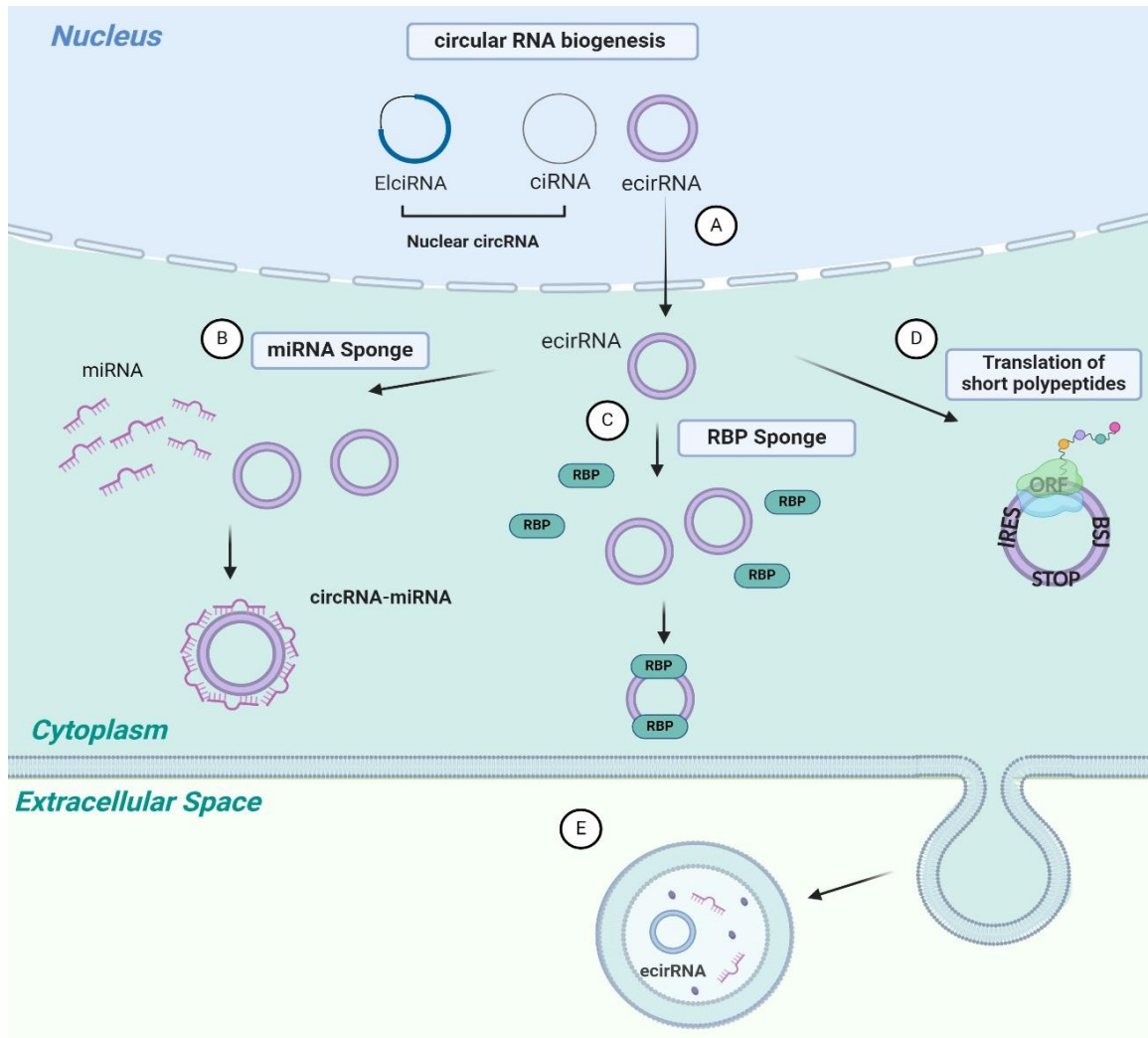


Figure 2.2 Regulatory functions of circRNAs. (A) Exonic circRNA (ecircRNA) is translocated to the cytoplasm. (B) ecircRNA can sequester miRNA acting as a miRNA sponge. (C) ecircRNA can function as RBP sponges. (D) CircRNAs may contain internal ribosome entry sites or m6A residues to promote translation of a short polypeptide. (E) ecircRNA can be packaged into microvesicles, detected in several body fluids, and levels of circRNAs within microvesicles are altered in disease states. Therefore, they may function as biomarkers of disease. (Illustration created in Biorender)

2.2.1 Circular RNAs in Coronary Artery Disease

Coronary Artery Disease is one of the most common forms of CVD (129). Despite current diagnostic tools and treatment strategies, prognosis is still poor. Therefore, there is a need for sensitive biomarkers for early diagnosis of CAD. Studies have suggested the use

of circRNA profiling as a potential novel class of biomarker for CAD. CircRNA transcriptome profiling by microarray analysis in peripheral blood mononuclear cells (PBMCs) of 24 CAD male patients and 7 healthy patients identified circular RNA differential expression. Specifically, hsa_circ_0001879 and hsa_circ_0004104 were further validated by qRT-qPCR in 412 CAD and 290 healthy patients. These circRNAs were significant higher expression levels in CAD and univariate and multivariate logistic regression analysis identified these circRNAs as predictors of CAD. Gain of functions studies on human monocytic cell line (THP-1)-derived macrophages showed overexpression of hsa_circ_0004104 upregulated pro-atherosclerotic gene expression and downregulated anti-atherosclerotic gene expression (130). Additionally, another study investigating circRNA profiling in peripheral blood of 12 CAD or healthy patients followed by verification in 30 CAD or healthy patients identified hsa_circ_0124644 upregulation in CAD patients. Multivariable logistic models combining conventional risk factors with established biomarkers validated hsa_circ_0124644 as a potential diagnostic biomarker with high sensitivity and specificity (124). Interestingly, circular RNA profiling in exosomes derived from plasma of CAD or healthy patients indicated differential expression of circRNA with 164 circRNAs upregulated and 191 circRNAs downregulated. Multivariate logistic regression models were analyzed with consideration of risk factors (age, gender, smoking history, diabetes, hypertension, and TC and HDL levels) and demonstrated that circular RNA hsa_circ_0005540 was significantly associated with CAD. in bodily fluids. These In conclusion, increasing evidence has defined circRNAs as highly conserved in tissues, secreted during a physiological response, packaged into extracellular vesicles, and detected characteristics make them promising biomarkers for disease (131).

2.2.2 Circular RNAs in Atherosclerosis

Atherosclerosis is a persistent inflammatory condition that affects the arteries, characterized by plaque formation from accumulation of low-density lipoprotein, fibrous substances, and inflammatory cells on the inner linings of the arteries. Over time, plaque buildup will lead to narrowing and hardening of the arteries, impeding blood flow, and resulting myocardial infarction (132). Notably, a class of novel circular RNA products from the Antisense Noncoding RNA in the INK4 locus (ANRIL) was found to be associated with atherosclerotic vascular disease. CircANRIL is downregulated in the serum of patients with coronary artery disease. Overexpression of circANRIL increased apoptosis and reduced proliferation. Mechanistically, circANRIL binds to PES to impair exonuclease-mediated pre-rRNA processing and ribosome biogenesis resulting in induced nucleolar stress and p53 activation in vascular smooth muscle cells. Therefore, circANRIL may promote atheroprotection by suppressing proliferation of cells in atherosclerotic plaques (46). Vascular smooth muscle cells (VSMCs) are a vital component of blood vessels and proliferation can prevent the rupture of the plaque fiber cap to increase plaque stability. Meanwhile, VSMCs apoptosis will promote thinning of the fibrous cap leading to plaque vulnerability. A study investigated circRNA-miRNA interactions of the lipoprotein receptor 6 (Lrp6), a gene that is highly expressed in vessels and implicated in vascular pathology, found circ_Lrp6 to act as a miRNA sponge for miR-145. Circ_Lrp6 sequestering of miR-145 resulted in VSMC migration, proliferation, and differentiation (133).

Another circular RNA that regulates VSMCs is circNRG-1 that sequesters miR-193b-5p to prevent its inhibition of neuregulin-1 (NRG1), an epidermal growth factor that suppresses proliferation and promotes apoptosis of VSMCs (134). Additionally, VSMCs induced treated with oxidized Low-density lipoprotein (ox-LDL) showed a significant upregulation of circCHFR. This circRNA regulates FOXO1 expression by sequestering miR-370 and the transcription factor FOXO1 promotes cyclin D1 expression leading to increased proliferation and migration of VSMCs (135). CircCHFR can also sequester miR-214 to upregulate Wnt3 expression to promote VSMC proliferation and migration (136). Nevertheless, despite these reports indicating the potential roles of circRNA in atherosclerosis, the underlying role of circRNAs have not been fully elucidated, and further research is necessary.

2.2.3 Circular RNAs in Cardiac Hypertrophy

Pathological cardiac hypertrophy often occurs as a result of myocardial damage manifesting as increase in myocardial cell volume increased cardiac fibrosis, and loss of myocardial cells. When pathological myocardial hypertrophy is decompensated, dysfunctional ventricular remodeling occurs leading to heart failure (137). One of the most characterized circRNA is heart-related circular RNA (HRCR) is found to be repressed in hypertrophy and heart failure (138). HRCR directly binds to miR-223 in cardiomyocytes to sequester miR-223, a miRNA known to induce cardiac hypertrophy by inhibition of the protein apoptosis inhibitor with a CARD domain. Overexpression of HRCR attenuated cardiomyocyte hypertrophy *in vitro* and adenoviral delivery of HRCR in mice also repressed cardiac hypertrophy *in vivo* (138). On the other hand, circRNA circSlc8a1 functions as pro-hypertrophic by sequestering miR-133 to enhance cardiac hypertrophy.

Adeno-associated virus vector system 9 (AAV9) short hairpin RNA (shRNA) against circSlc8a1 attenuated cardiac hypertrophic *in vivo* (139). Notably, another circRNA, circNlgn, encodes a short polypeptide, Nlgn 173, to promote cardiac fibroblast proliferation and exacerbating pressure-overload-induced-cardiac hypertrophy. This polypeptide interacts with structural protein LaminB1 to facilitate nuclear localization in order to bind to inhibitor of growth protein 4, and serum and glucocorticoid-inducible kinase 3 promoters, resulting in increased collagen deposition, cardiac fibroblast proliferation, and reduced cardiomyocyte survival in left ventricular pressure overload mouse model (140). In summary, a small number of studies have examined the role of circRNAs in cardiac hypertrophy but highlight the potential for circRNA targeting as a means for treating hypertrophy.

2.2.4 Circular RNAs in Cardiomyopathy

Cardiomyopathy is characterized as thickening, stiffness, or enlargement of the heart chamber walls that affect the ability of the heart to pump blood around the body. In the case of dilated cardiomyopathy, there is an enlargement of the cardiac chamber accompanied by systolic myocardial dysfunction. One study investigating RNA binding motif protein 20 (RBM20), protein essential for splicing of cardiac genes, which is lost during dilated cardiomyopathy identified circRNA production from the parent titin gene was significantly altered. They performed ribosomal depleted RNA sequencing from human hearts and RBM20-null mice found 6 circRNAs (cTTN1, cTTN2, cTTN3, cTTN4, cTTN5, and cCAMK2D) that were significantly downregulated in response to dilated cardiomyopathy (141). In Doxorubicin-induced cardiomyopathy, which arises from long-term treatment with the chemotherapeutic drug anthracycline doxorubicin (Dox) and

manifests as dilated cardiomyopathy, overexpression of circAmotl1 was found to attenuate dox-induced cardiomyopathy. CircAmotl1 directly binds to phosphoinositide-dependent protein kinase 1 (PDK1) and AKT to induce AKT phosphorylation leading to p-AKT nuclear translocation. Therefore, activating the AKT signaling pathway and attenuating the cumulative effects of dox-induced cardiomyopathy (115). Additionally, circRNA profiling of the left ventricular cardiac tissue of healthy or heart failure patients and from mice with or without left ventricular pressure overload induced cardiac remodeling, identified significant downregulation of circINSR. Further analysis in dox-induced cardiomyopathy in patients and mice confirmed this downregulation. Mechanistically, circINSR binds to single stranded DNA binding protein 1 (SSBP1) protein to regulate mitochondrial function in cardiomyocytes and prevent cell death (142). In addition to doxorubicin-induced cardiomyopathy, circRNAs also regulate diabetic induced cardiomyopathy. Diabetic cardiomyopathy is a diabetes associated cardiovascular complication, characterized by cardiomyocyte metabolic dysfunction, myocardial interstitial fibrosis, and cardiac dysfunction. A recent study identified caspase-1-associated circRNA (CACR) to be highly upregulated in high-glucose treated cardiomyocytes and in the serum of diabetic patients. CircCACR acts to sequester miR-214-3p and prevent inhibition of caspase-1 by miR-214-3p. CircRNA CACR silencing alleviated high-glucose-induced cardiomyocyte pyroptosis (143). Another circular RNA reported to play a role in diabetic cardiomyopathy is circHIPK3. This circular RNA is downregulated in diabetic patients and in AC16 human cardiomyocyte cell line. CircHIPK3 decreases expression levels of mRNA and protein of tumor suppressor gene Phosphatase and Tensin homolog (PTEN) to protect cardiomyocytes from high glucose-induced cell apoptosis. However, further studies are

needed to establish if circHIPK3 affects transcription of mRNA stability of PTEN and how PTEN regulates cardiomyocyte apoptosis (144). Overall, these studies indicate the involvement of circRNAs in the pathology of cardiomyopathy. However, future studies are needed to fully elucidate the clinical significance and the mechanisms of circRNA on cardiomyopathy.

2.2.5 Circular RNAs in Cardiac Fibrosis

The severity of cardiac fibrosis correlates with higher long-term mortality in patients with CVD. Cardiac fibrosis is the result of excess deposition of extracellular matrix in the cardiac muscle resulting from cardiac injury and it is the main component of adverse ventricular remodeling and heart failure (128). Recently, two circular RNAs, CircRNA_010567 and CircRNA_000203, reported to function as miRNA sponges were found to be upregulated in the myocardium of diabetic mice and in angiotensin II (Ang-II) induced cardiac fibroblast (145,146). CircRNA_010567, promotes myocardial fibrosis by sequestering miR-141 to prevent the inhibition of TGF- β 1. Silencing of this circular RNA resulted in upregulation of miR-141, downregulation of TGF- β 1, and suppression of fibrosis-associated proteins in cardiac fibroblasts (145). In addition to this, circRNA_000203 sequesters miR26b-5p and miR-140-3p to prevent miRNA inhibition of fibrosis-associated genes (Col1a2, Col3a1 and α -SMA) in Ang-II treated neonatal mouse ventricular cardiomyocytes. Overexpression of circRNA_000203 also increased cell size and expression of atrial natriuretic peptide. Mechanistically, CircRNA_000203 is able to sequester miRNAs, miR-26b-5p and miR-140-3p, to prevent binding with Gata4, a pro-hypertrophic transcription factor, to promote hypertrophic growth (146,147). Although circHIPK3 has previously been shown to protect cardiomyocytes from high glucose-

induced cell apoptosis, this circular RNA functions to promote cardiac fibroblast proliferation and migration. CircHIPK3 expression is highly upregulated in cardiac fibroblast treated with Ang-II and sequesters miR-29b-3p to enhance expression of miR-29b-3p targeting genes (α -SMA, COL1A1, COL3A1) (148). On the other hand, circNFIB expression is downregulated in primary adult cardiac fibroblast treated with TGF- β 1. Forced expression of circNFIB in primary adult cardiac fibroblast and NIH3T3 fibroblast cell line decreased cell proliferation by sequestering miR-33, a miRNA known to positive regulate cardiac fibrosis. Interestingly, overexpression of circNFIB did not regulate fibroblast proliferation in cardiac fibroblast not treated with TGF- β 1 (149). However, its role in cardiac fibrosis remains largely unknown and necessitates future study. Understanding functions of circRNAs in cardiac fibrosis might provide key insights of the underlying mechanism of cardiac fibrosis is important for treatment cardiac fibrosis.

2.2.6 Circular RNAs in Cardiac Senescence

Senescence refers to the gradual decline in bodily function, often culminating in death, occurring at either the cellular or organismal level. On the cellular level, cell cycle progression is arrested, typically triggered by factors such as telomerase shortening or stress induced cell death. Notably, a study found an increased expression of circFOXO3 in older hearts compared to younger hearts (150). This circRNA is derived from transcription factor FOXO3 and acts as a scaffold to modulate P21 and CDK2 interactions to repress cell cycle progression (113). CircFOXO3 was reported to be highly expressed in various cell lines including mouse embryonic fibroblasts (MEFs), mouse cardiac fibroblasts (MCFs), NIH3T3 fibroblasts, B16 cells, and primary cardiomyocytes. Additionally, circFOXO3 expression was also increased in dox-induced cardiomyopathy mouse model.

Interestingly, circFOXO3 directly interacted with senescence associated proteins ID1, E2F1, HIF-1 α , and FAK; meanwhile, the linear counterpart did not. Mechanistically, circFOXO3 association with senescence associated proteins prevented their translocation to the nucleus or mitochondria (FAK), sequestering them to the cytoplasm to arrest their functions and promote senescence (150). The number of different regulatory mechanisms of circ-Foxo3 indicates that the stress response pathways of circRNAs may be different each time depending on the stressors. Another well characterized circRNA, Circ-cdr1as, has been implicated to upregulate cardiomyocyte apoptosis by activating the Hippo signaling pathway in diabetic cardiomyopathy. Knockdown of Circ-cdr1as using small interfering RNA protected cardiomyocytes from apoptosis induced by high glucose treatment. FOXO3 acts as a transcription factor of Cdr2as to regulate the transcription of this circular RNA (151). Another circRNA implicated in cardiac senescence is circNCX1, a circular RNA abundantly expressed in cardiomyocytes and upregulated in stress induced cardiomyocyte apoptosis. CircNCX1 sequesters miR-133a-3p, preventing the inhibition of pro-apoptosis factor cell death inducing protein (CDIP1) (152). In summary, these studies demonstrate possible regulatory roles of circRNAs in cardiac senescence and pave the way for further investigation into circRNA as a potential therapeutic avenue for cardiac senescence.

2.2.7 Circular RNAs in Myocardial Infarction

Acute myocardial infarction remains one of the leading causes of morbidity and mortality globally. During acute MI, cardiomyocyte apoptosis and necrosis trigger the inflammatory response to facilitate clearance of dead cells. Early reperfusion therapy improves survival rates; however, it leads to myocardial ischemia reperfusion injury and

can further risk the development of heart failure. Circ-cdr1as has been shown to increase cardiac infarct size and cardiomyocyte apoptosis 24h after cardiac injury by permanent ligation of the left anterior descending (LAD) artery. Circ-cdr1as functions to sequester miR-7 and prevent miRNA inhibition of pro-apoptotic targets poly ADP ribose polymerase (PARP) and member of the SP/KLF family of transcription factors SP1 (51). Overexpression of circHIPK3 in a MI mouse model attenuated cardiac dysfunction and decreased fibrotic area. CircHIPK3 sequestered miR-133 to promote angiogenesis, increasing connective tissue growth factor (CTGF) expression in ECs. In cardiomyocytes, circHIPK3 did not act as a miRNA sponge for miR-133. Rather it regulated CM proliferation by direct interaction with Notch1 intracellular domain (NICD) to promote its stability and nuclear translocation (153). Additionally, circRNA circNFIIX was found to be highly expressed in the adult heart of humans, rats, and mice. Downregulation of this circular RNA during MI resulted in increased angiogenesis and attenuated cardiomyocyte apoptosis. CircNFIIX facilitates the degradation of YBX1 through ubiquitination by E3 ubiquitin ligase NEDD4L, leading to the suppression of Cyclin A2 and B1. Loss of function of circNFIIX resulted in increased angiogenesis and enhanced cardiomyocyte survival following MI (154). Lastly, our lab identified circFndc3b to be significantly downregulated in ischemic cardiomyopathy patients and mice with myocardial infarction. Interestingly, this circular RNA does not function as a miRNA sponge. Rather, circFndc3b interacts with RNA binding protein fused in sarcoma (FUS) to regulate VEGF expression. Overexpression of circFndc3b enhances angiogenic activity, reduces endothelial apoptosis, and improves cardiomyocyte survival (39). These studies highlight the potential of therapeutically targeting circRNAs to promote cardiac function and remodeling post-MI.

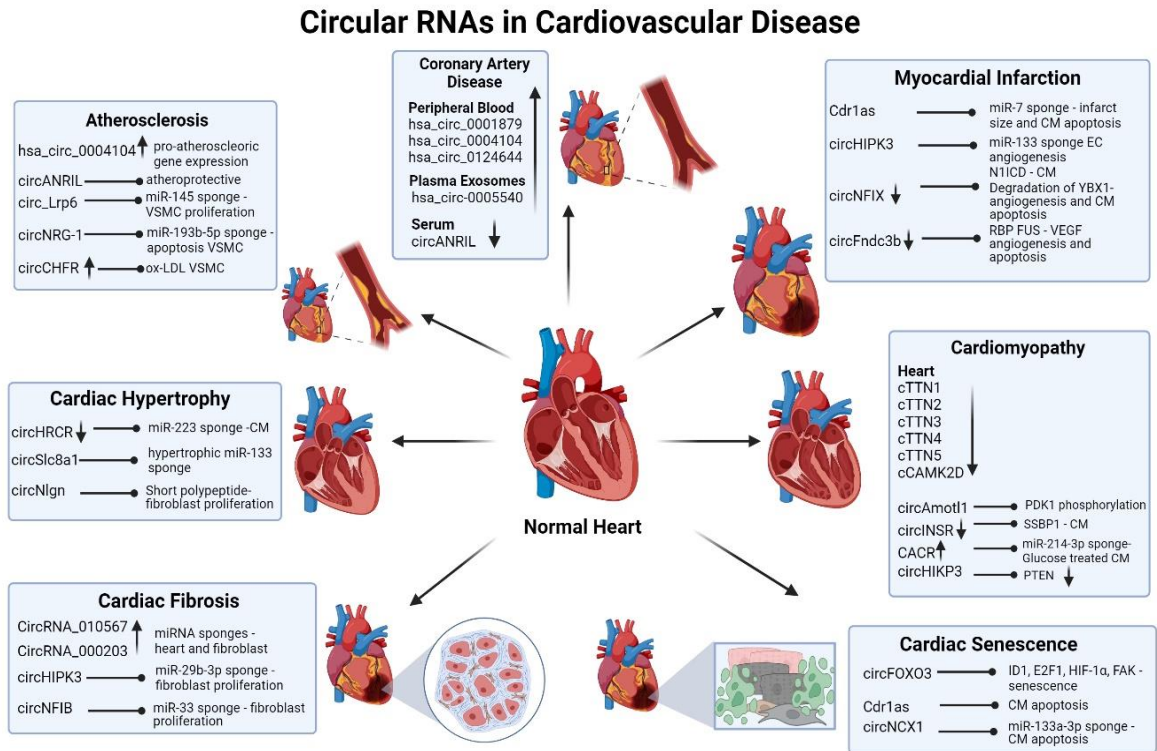


Figure 2.3. Circular RNAs in cardiovascular disease. The regulation of circRNAs involved in coronary artery disease, cardiac fibrosis, MI, atherosclerosis, cardiomyopathy, cardiac senescence, and cardiac hypertrophy. (Illustration created in Biorender)

2.3 Circular RNAs in Immune Regulation

The immune system is a complex network that maintains internal homeostasis by immune regulation. Recent studies have suggested non-coding RNA circular RNA play a role in immune response (Figure 2.4). Circular RNA expression profile in peripheral blood mononuclear cells (PBMCs) from patients infected with tuberculosis indicated dysregulated expression in these patients (155). Reports suggest that circRNAs are directly involved in immune regulation. One study has shown that the delivery of purified exogenous circRNA stimulates a greater innate immune response than that stimulated by linear RNA with the same sequence. The circRNAs in this study were generated by the *in vitro* production of circRNAs with autocatalytic introns and transfection resulted in portent

induction of innate immunity genes (45). They further concluded that cells could distinguish endogenous circRNA from exogenous circRNAs by whether they contain an N6-methyladenosine modification. Circular RNAs lacking this modification are able to activate RNA pattern recognition receptor RIG-I in the presence of lysine-63-linked polyubiquitin chain to promote RIG-I polymerization and activation. This then leads to the filamentation of adaptor protein mitochondrial antiviral signal (MAVS) and dimerization activation of downstream transcription factor IRF3 to promote expression of genes involved in immune response (156). Although these few studies point to the view that circRNAs are involved in immune regulation, how they act in this important context remains largely unknown.

2.3.1 Circular RNAs in the Innate Immune Response

Immunity can fall into innate and adaptive immunity. Innate immunity is an intricate network that regulates the immediate response to pathogens while avoiding autoimmunity. It is the first line of defense against pathogens and gives rise to antigen-specific adaptive immune response. Innate immunity is primarily composed of neutrophils, dendritic cells (DCs), natural killer cells (NKs), and Macrophages (M ϕ). Meanwhile, adaptive immunity is highly specific and is comprised primarily of T and B lymphocytes.

Endogenous circRNAs are reported to form 16-26 bp imperfect RNA duplexes and bind to double stranded RNA (dsRNA)- activated protein kinase (PKR) to function as endogenous PKR inhibitors. Forced expression of the ds-RNA containing circRNA in PBMCs and T cells from patients with autoimmune disease systemic lupus erythematosus attenuated PKR phosphorylation resulting in suppressed INF- β and Type I IFN induced genes expression (157).

2.3.2 Role of Circular RNAs in Neutrophils

Neutrophils are vital components of the immune system. They are the first immune cells to migrate to the site of injury and facilitate the initiation of the immune response. They function to kill and degrade engulfed pathogens and release extracellular traps for the extracellular capture of foreign pathogens to prevent the spread of infection. In Moyamoya disease (MMD), neutrophils are involved in the inflammatory response and development of vascular lesions. In MMD, neutrophil extracellular traps contribute to endothelial damage and exacerbated inflammatory response within the affected blood vessels. MMD is an uncommon cerebrovascular disorder that affects the terminal ends of the internal carotid artery resulting in abnormal fragile vascular network at the base of the brain. Circular RNA expression profile in patients with MMD have revealed differential expression patterns compared to healthy patients. Additionally, analysis of circRNA expression in neutrophils from MMD patients remained consistent with previous findings. The differentially expressed circRNAs contributed to metabolism, angiogenesis, and immune response (158).

2.3.3 Role of Circular RNAs in Dendritic Cells

Dendritic cells are highly effective antigen-presenting cells. Once DCs reach the maturation state they can present and process antigens, migrate, and co-stimulate T cells. A key circular RNA involved in modulating DC function is circSnx5, found to regulate DC-driven immunity and tolerance. Gain of function studies indicated a suppression of DC activation; meanwhile, loss of function promoted activation to an inflammatory phenotype. CircSnx5 sequesters miR-644 to prevent inhibition of miRNA target suppressor of cytokine signaling 1 (SOCS1). Administration of overexpressing circSnx5-DCs protected

against acute rejection of cardiac allograft after cardiac transplantation in mice. The allografts showed reduced infiltration of inflammatory cells, reduction of inflammatory cytokine IL-12 in the serum, and upregulation of IL-10 and TGF- β in the serum. Overexpressing CircSnx5-DCs were injected in mice with autoimmune myocarditis and these mice exhibited lower cardiac inflammation, lower levels of serum troponin I, increased ejection fraction, and smaller heart size (159). Another circRNA involved in immune tolerance in DCs and rejection after heart transplantation is circMalat-1. Recombinant human growth differentiation factor 15 (rhGDF15), known to play a role in DC maturation, inhibits circMalat1 to induce immune tolerance, preventing allograft rejection after heart transplantation in mice (160). Additionally, a study generated immunosuppressive DCs via knockdown of circMAP2K2 with siRNA to induce donor specific immunosuppression and attenuate allograft immune rejection in a mouse heart transplant model. Knockdown of circMAP2K2 reduced the ability of DCs to activate allogeneic naïve T cells and promoted regulatory T cell activation (161). These studies highlight the potential therapeutic approach of targeting circRNA.

A recent study investigated the capacity for circRNA to be used as a therapeutic. This study engineered synthetic circRNA encoding an antigenic protein encapsulated in a charge-altering release transporter. The uptake of circRNA by antigen presenting cells was sufficient to induce dendritic cell activation and maturation that enabled them to interact with antigen-specific T cells. Moreover, circRNA delivery effectively induced a potent innate and adaptive immune response to facilitate tumor clearance (162). The results of this study indicated that circRNA immunization could serve as an effective cancer immunotherapy to inhibit tumor growth *in vivo*.

2.3.4 Role of Circular RNAs in Macrophages

Macrophages are crucial players in the immune system and serve multiple essential functions that include phagocytosis, antigen presentation, cytokine production, and homeostasis. Overall, macrophages are versatile cells that play critical roles in immunity, tissue repair, and homeostasis. They can uniquely change phenotype and function depending on environmental cues. Classically polarized M1 macrophages exhibit pro-inflammatory phenotype and promote secretion of pro-inflammatory cytokines. In contrast M2 macrophages work to alleviate inflammation and promote secretion of anti-inflammatory cytokines. One study profiling circRNA expression in macrophages stimulated with Lipopolysaccharide (LPS) found induction of nearly 2,000 circular RNAs. LPS is a major component of the outer membrane of Gram-negative bacteria that will bind to Toll-like receptor 4 (TLR4), activating macrophages to induce the innate immune response, secrete pro-inflammatory cytokines, and recruit of NKs and T-cells. The authors found that circRNA mcircRasGEF1b is stably expressed, dependent on NF- κ B, and needed for proper activation of macrophages in response to lipopolysaccharide. Knockdown of mcircRasGEF1b in lipopolysaccharide stimulated macrophages resulted in a decrease in the abundance of mRNA and protein of inflammatory adhesion molecule ICAM-1, an adhesion molecule that facilitates the binding of leukocytes to endothelium cells and subsequent transmigration to site of injury (53,54). Another study compared circRNA expression in bone marrow derived macrophages (BMDMs) polarized to M1 (induced by LPS and IFN- γ) or M2 (induced by IL-4) and reported 189 differentially expressed macrophages (163).

Macrophages contribute to the pathological progression of atherosclerosis by releasing inflammatory factors, inducing cell apoptosis and necrosis, and subsequently facilitate plaque formation. Macrophages in the plaque engulf oxidized low-density lipoprotein (LDL) particles, forming foam cells. These foam cells are a hallmark feature of early atherosclerotic lesions. Macrophages can influence the stability of this cap through their secretion of matrix metalloproteinases (MMPs), which can weaken the fibrous cap. A study identified circTM7SF3 to be significantly upregulated in the serum of atherosclerosis patients and in ox-LDL-induced THP-1 derived macrophages. Mechanistically, circTM7SF3 sequesters miR-206 to promote THP-1 apoptosis (164). Meanwhile, circSCAP knockout inhibited ox-LDL-induced lipid deposition and oxidative stress in THP-1 cells by sponging miR-221 and preventing inhibition of miRNA target PDE3B (165). In addition to this, Circular antisense non-coding RNA in the INK4 locus (circANRIL) was reported to modulate ribosomal RNA maturation and atherogenesis. CircANRIL binds PES1, essential pre-ribosomal assembly factor, to impede the generation of pre-rRNA and inhibit ribosome biogenesis in VSMCs and macrophages (46). Overall, these findings suggest the potential for circRNAs to affect macrophage function by controlling activation, phenotype, ribosome biogenesis, and modulating atheroprotection through macrophages.

2.3.5 Circular RNAs in the Adaptive Immune Response

The adaptive immune response provides long term protection against specific pathogens. Initially, lymphocytes B cells and T cells recognize specific antigens present on the surface of pathogens or foreign substances. B cells are activated to produce antibodies and T cells may directly kill infected cells or release signals to activate other immune cells.

Following the clearance of the pathogen, a pool of long-lived memory cells is established. These memory cells persist in the body and provide rapid and robust responses upon re-exposure to the same antigen (166). Circular RNA profiling on CD4⁺ T cells isolated from systemic lupus erythematosus patients and healthy patients, identified 12 circRNAs that are upregulated and two circRNAs that are downregulated. Downregulation of circ_0012919 increased expression of DNMT1, decreased the expressions of CD70 and CD11a, and reversed the DNA hypomethylation of CD11a and CD70 in CD4⁺ T cells of systemic lupus erythematosus (167). Additionally, circRNA profiling was also conducted on CD4⁺ cells in patients with asthma. Hsa_circ_0005519 was up-regulated and negatively correlated with hsa-let-7a-5p expression in CD4⁺ T cells of asthmatic patients. Mechanistically, hsa_circ_0005519 may induce IL-13 and IL-6 expression by inhibiting hsa-let-7a-5p in CD4⁺ T cells, thereby promoting airway inflammation (168).

2.3.6 Circular RNAs in Infectious Diseases

In response to infection, gene expression shifts to prime cells to respond. Consequently, both viral and bacterial infections trigger changes in the expression patterns of host circRNAs. Notably, Kaposi's Sarcoma Herpesvirus (KSHV) encoded numerous circRNAs, specifically expressed in KSHV-infected primary endothelial cells and primary effusion lymphoma cells. Viral circRNAs were also detected in lymph nodes from patients of KSHV-driven diseases such as PEL, Kaposi's sarcoma, and multicentric Castleman's disease. Upon KSHV infection, primary ECs produce hsa_circ_0001400, to work as an antiviral molecule to suppress expression of crucial viral genes, and hsa_circ_0001400 inhibits expression of KSHV encoded genes, latency-associated nuclear antigen and replication and transcription activator, to regulate latent and lytic infection (169).

Conversely, viruses and bacteria can rely on host cell machinery to support pathogenesis. One study reported that human hepatocarcinoma cell lines infected with hepatitis C virus (HCV) will promote biogenesis of circPSD3 and inhibit the antiviral cellular nonsense-mediated decay pathway to enhance pathogenesis (170). A comprehensive study of circular RNA, miRNA, and mRNA regulatory networks in endothelial cells infected with hantaan virus, known to cause hemorrhagic fever, hantavirus pulmonary syndrome, and cardiopulmonary syndrome by targeting vascular endothelial cells causing destruction of capillary integrity and altering vascular permeability, indicated that circ_0000479 indirectly regulated RIG-I expression by sponging miR-149-5p, hampering viral replication (171). In conclusion, the precise functions of these circRNAs during infection remain subjects of ongoing research. However, these studies suggest that certain circRNAs might contribute to pathogenesis, while others could potentially boost innate immune responses.

2.3.7 Circular RNAs in Autoimmune Diseases

Typically, autoimmune conditions arise when multiple regulatory pathways fail resulting in the body's immune system mistakenly attacking itself. The disruption of tolerance to autoantigens is attributed to genetic and environmental factors. In autoimmune diseases, the immune system cannot distinguish between healthy cells and potentially harmful invaders, leading to inflammation, tissue damage, and dysfunction in various parts of the body. However, the precise processes underlying the development of autoimmune diseases remain incompletely understood. Therefore, efforts have been made to try and understand the role of circular RNA in autoimmune diseases. Some reports have suggested the use of circRNA levels as diagnostic biomarkers for rheumatoid arthritis (RA) (172).

Microarray analysis of circRNAs in PBMCs from 5 RA patients and 5 healthy patients identified circular RNAs that were significantly upregulated in RA patients(173). Another study identified Circ_0005008 and circ_0005198 were upregulated in the plasma of RA, and their expression levels are positively correlated with the severity of RA (174). Macrophages are key cells that participate in inflammatory and immune reactions. Elevated level of macrophages can infiltrate in the inflamed tissue causing inflammatory lesions and joint damage in RA. CircRNA_09505 was found to promote proliferation in macrophage-like cell lines THP-1 and RAW264.7 by sequestering miR-6089 resulting in the upregulation of TNF α , IL-6, and IL12. Knockdown of circRNA_09505 in vivo reduced inflammation in collagen induced arthritis mouse model (175).

Additionally, two circRNAs originating from ANXA2, hsa_circ_0005402 and hsa_circ_0003452_2, were downregulated in the PBMCs of patients with multiple sclerosis (MS). CircRNA-miRNA-mRNA analysis indicated hsa_circ_0005402 may bind to miR-155, a miRNA that is upregulated in PBMCs of patients with MS and is positively correlated with severity of the disease. Overall, these studies indicate possible involvement of circRNAs in the pathogenesis and development of autoimmune disease (176).

2.3.8 Circular RNAs in Cancer Immunology

The tumor immune microenvironment (TIME) regulates interactions between tumor cells, fibroblast, endothelial cells, and immune cells. TIME involves the innate and adaptive immune response. Firstly, immune cells recognize and develop mechanisms for inducing tumor cell death. Secondly, tumor variants combat this and become resistant to the immune response (177). Emerging evidence indicates circRNAs association with numerous cancers. CircRNAs may be involved in multiple processes of cancer cells

including proliferation, migration, invasion, alterations of immune cells involved, and survival (178). A recent study indicated that high expression circARSP91 in hepatocellular carcinoma cells increase the cytotoxicity activity of NK cells by upregulating UL-16 binding protein. However, the exact mechanism remains unknown (179).

In lung cancer, intratumoral heterogeneity plays a crucial role in enabling tumor cells to evade immune surveillance and establish immunosuppression. Kras-driven circRNA signaling promotes infiltration of myeloid-associated tumor macrophages leading to immune deregulation and immunosuppression. Kras-driven signaling drives intratumoral heterogeneity by upregulating circHIPK3/PTK2 expression to promote infiltration of tumor associated macrophages that polarize to an M2 phenotype leading to immunosuppressive chemoresistance. Consequently, co-inhibition of circPTK2/M2 macrophage signaling suppresses lung tumor growth, reduces metastatic potential, and prolongs survival *in vivo* (180).

Gene ontology (GO), Kyoto Encyclopedia of Genes and Genomes (KEGG), gene set enrichment analysis (GSEA), CIBERSORT, Estimating the Proportion of Immune and Cancer cells (EPIC), and the Malignant Tumors using Expression data (ESTIMATE) algorithms were utilized to investigate the functional role of circ-cdr1as in cancer. The findings suggest it plays a role in immune and stromal cell infiltration within the tumor tissue, specifically CD8⁺ T cells, activated NK cells, M2 macrophages, cancer-associated fibroblasts (CAFs) and ECs. Tissues with high circ-CDR1as expression had a higher ratio of M2 macrophages and circ-CDR1as expression was negatively correlated with CD8⁺ T cells. Circ-CDR1as may also regulate the TGF- β signaling pathway and ECM-receptor interaction to serve as a mediator in reshaping the tumor microenvironment (181).

Inhibition of T-cell activation is crucial for tumor progression resulting in reduced patient survival. In lung cancer, one study identified high expression of circCPD4 and PD-L1 and low miR-let-7 expression in non-small cell lung cancer. High expression of circCPA4 sequestered miR-let-7 to upregulate PD-L1 resulting in CD8+ T cell inactivation and suppressed T cell growth, leading to tumoral immune escape and increased drug resistance (182).

In conclusion, Circular RNAs (circRNAs) orchestrate the dynamics of the tumor microenvironment by influencing interactions. Dysregulation of circRNAs may impact immune cell responses across various cancer types, consequently altering the composition of the tumor microenvironment (Figure 2.4).

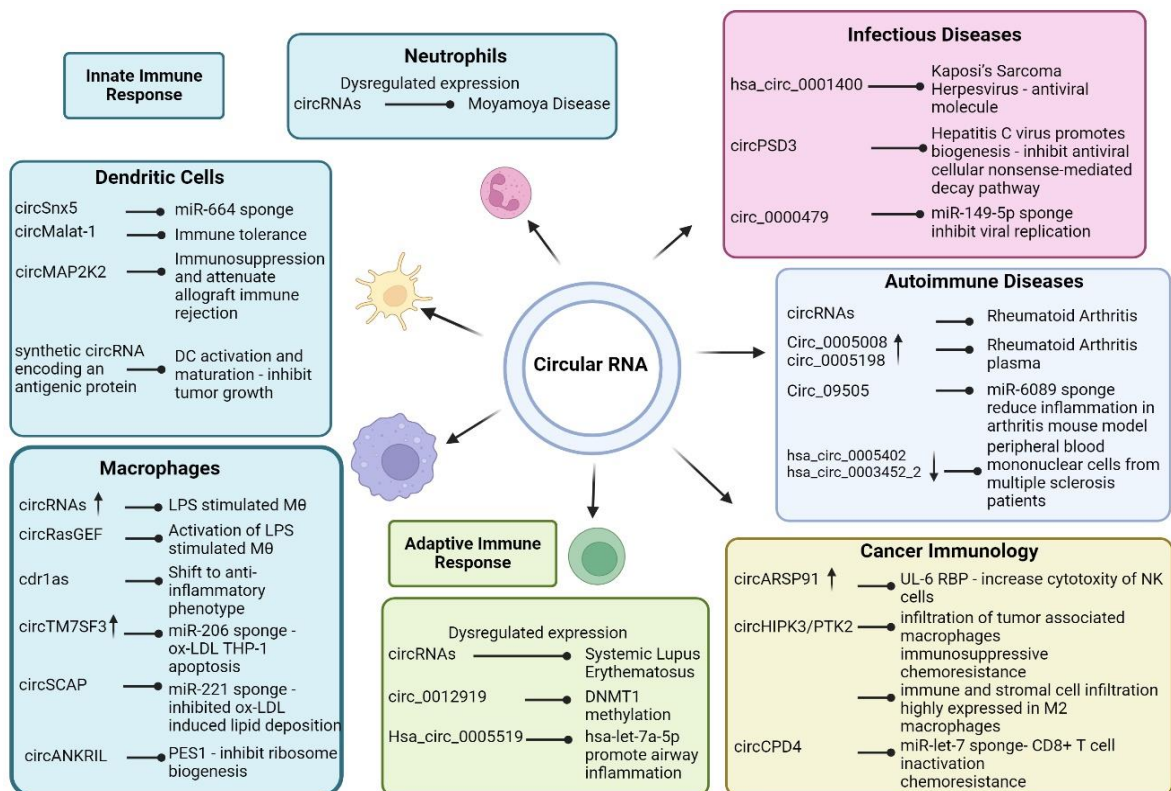


Figure 2.4. Circular RNAs in immune regulation. Circular RNAs are involved in innate immunity, adaptive immunity, infectious diseases, autoimmune diseases, and cancer immunology. (Illustration created in Biorender)

2.4 Summary and Objectives

In response to cardiac injury, blood-derived and tissue-resident macrophages accumulate in the infarcted myocardium and exhibit both pro-(M1) and anti-inflammatory (M2) phenotypes, essential for removing injured tissue and facilitating repair. However, sustained activation of pro-inflammatory macrophages increases adverse remodeling of cardiac tissue that leads to deterioration of cardiac function and heart failure. The molecular mechanism underlying the functional polarization of macrophages into M1 or M2 phenotypes has yet to be fully understood. Circular RNAs (circRNA) are newly discovered non-coding RNA generated from protein-coding genes that are highly abundant, evolutionary conserved, and differentially expressed in cardiovascular disease. They are proposed to regulate transcription and translation, and to act as microRNA (miRNA) sponges, RNA-binding protein (RBP) sponge to regulate cellular functions. Studies have shown that circRNAs are expressed in the heart and are differentially expressed following myocardial infarction (MI). They may also play a role in immunity by contributing to the process of macrophage polarization, maintenance of activation of macrophages when exposed to LPS, and inhibiting the biogenesis of macrophages. **However, there are currently no published studies into the role of circular RNAs in the regulation of macrophage plasticity during cardiac injury.** Given the importance of macrophages in cardiovascular disease, there have been attempts to develop therapeutics that reduce or deplete monocytes post-MI or impair monocyte function and mobilization. However, the unintended consequences were increased risk of prolonging cardiac inflammation due to insufficient clearance of tissue debris and impaired tissue remodeling. Therefore, targeting macrophage phenotypic switching to promote an anti-inflammatory M2 phenotype at an

earlier stage in cardiac injury could promote improved repair and regeneration without these unintended consequences. Circular RNAs are promising therapeutic targets due to their high stability, tissue specificity that can allow for precise modulation of gene expression in specific tissues, and various functional roles in gene regulation, protein interaction, and signaling.

In this dissertation we aim to address 1) the role of circ-cdr1as in bone marrow-derived macrophages phenotypic switching *in vitro* 2) the role of circ-cdr1as after cardiac injury *in vivo* and 3) the molecular mechanism by which circ-cdr1as regulates macrophage phenotype.

In chapter 3 of this study, we investigate the differential expression of circular RNA in macrophages. We identify circular RNAs differentially expressed in macrophages, examine the expression levels of circ-cdr1as in naïve, pro-inflammatory, and anti-inflammatory macrophages, and investigate how loss/gain of function of circ-cdr1as affect phenotype.

In chapter 4 of this study, we investigate the expression of circ-cdr1as in the heart following MI in mice. We determine how overexpression of circ-cdr1as *in vivo* or delivery of circ-cdr1as overexpressing macrophages into the ischemic myocardium affects cardiac function, remodeling, and inflammation. Lastly, we identify circ-cdr1as role as a miRNA sponge to alter macrophage phenotype. Collectively, our goal is to identify and establish the role of circ-cdr1as as a potential therapeutic for the resolution of inflammation after cardiac injury to promote cardiac healing and remodeling.

CHAPTER 3

THE ROLE OF CIRCULAR RNA CDRIAS IN MODULATION OF MACROPHAGE PHENOTYPE

Gonzalez C et al. Life Sci. 2022 Nov 15; 309:121003. doi: 10.1016/j.lfs.2022.121003.

3.1 Introduction

An exacerbated and chronic inflammatory response is implicated in various pathological conditions, including cancer, cardiovascular disease, type 2 diabetes, and autoimmune diseases (52,172,183,184). Macrophages play pivotal roles in the progression of inflammatory diseases by controlling the initiation, maintenance, and resolution of inflammatory responses. Both bone marrow and tissue-resident macrophages exhibit the unique characteristic to phenotypically switch between pro-inflammatory and anti-inflammatory phenotypes, producing a spectrum of cytokines, chemokines, and growth factors with both pro- and anti-inflammatory effects. Pro-inflammatory macrophages, often termed classically activated M1 macrophages, are induced by stimuli like IFN γ , LPS, or TNF α (185). Upon activation, they initiate pro-inflammatory responses and release high levels of pro-inflammatory cytokines such as TNF α and interleukins (IL) IL-12, IL-23, IL-1, and IL-6. Subsequently, during the wound healing phase, they transition to an anti-inflammatory M2, pro-reparative phenotype, secreting high levels of anti-inflammatory cytokines such as IL-10 and growth factors like vascular endothelial growth factor (VEGF) (11,17,186). However, the mechanisms involved in the regulation of macrophage differentiation, polarization, re-polarization, and activation remain unclear.

Given the significance of macrophages in pathological conditions, efforts have been made to develop therapeutics targeting monocyte depletion, impairment of monocyte function, or mobilization. However, studies reported that this had unintended

consequences, such as increased infection risk and prolonged inflammation due to inadequate clearance of tissue debris and impaired tissue remodeling (10,11,187). Consequently, targeting macrophage phenotypic switching to promote an anti-inflammatory phenotype could enhance tissue remodeling and regeneration without these adverse effects. Recent advancements in high-throughput RNA sequencing (RNA-seq) have facilitated the discovery of novel non-coding transcripts, including microRNAs (miRNAs), long non-coding RNAs (lncRNAs), and circular RNAs (circRNAs). Several studies have identified circRNAs as regulators of biological processes, disease initiation, and progression. They have also been implicated in immunity by influencing macrophage polarization, appropriate activation in response to stimuli like LPS, and inhibition of macrophage biogenesis (46,53,54). CircRNAs are generated from pre-mRNA through back-splicing, forming circular RNA molecules with a 3'-5' phosphodiester bond at the junction site (48). Their lack of free ends renders circRNAs resistant to degradation by RNase R exoribonuclease, enabling their enrichment through RNase R treatment (52,55). Previous studies have suggested potential roles for circRNAs to elicit an immune response by regulating genes encoding inflammatory molecules. For instance, one study demonstrated that purified exogenous circRNA elicits a stronger innate immune response compared to linear RNA with the same sequence (45). Another investigation implicated the role of circRNAs in macrophage activation. The authors identified nearly 2000 circular RNAs induced following TLR4 stimulation. They found that circRNA circRasGEF1b, which is dependent on NF- κ B, is essential for macrophage activation in response to LPS (53,54). Although these studies implicate circRNA in the involvement of macrophage activation, the role of circRNAs in phenotypic switching remains unclear.

In this study, we investigate the role of circular RNAs in macrophage phenotypic switching. We provide a comprehensive profile of differentially expressed circular RNAs between pro- or anti-inflammatory macrophages and identify circular RNA *cdrlas* as a key promoter of macrophage polarization towards an anti-inflammatory phenotype.

3.2 Methods

3.2.1 Bone Marrow Cell Isolation and Monocyte Culture

Bone marrow (BM) monocytes are isolated from bone marrow mononuclear cells of C57BL/6 male mice at approximately 8–10-weeks of age by density-gradient centrifugation with histopaque-1083 (Sigma). Red blood cells are removed with NH₄Cl (Stemcell Technologies Cat #07800) as described previously (188,189). After isolation, the monocyte population is cultured in RPMI 1640 1× (Gibco) with 20% FBS, 1% penicillin-streptomycin solution, and 20% of L929-conditioned medium. The media is changed the day after culture, on day 3, and on day 5–7. By day 5–7, high purity of macrophages can be observed as noted previously (190).

The L929 cell conditioned medium was collected as previously described (191). Briefly, 2×10^6 L929 cells are seeded in T75 flask for 3–4 days until reaching confluency of 90% and the conditioned media is collected and centrifuged at 3000 rpm, 4°C. The media is then filtered through a 0.45 µm filter and frozen at –80°C in 50 mL aliquots. All animal experiments are complied with approved protocols of Temple University animal care and use guidelines.

3.2.2 Polarization of BMDMs

On day 5–7, fresh media is added to cultured cells with specific stimulation for the desired phenotype: for pro-inflammatory activation [6], 100 ng/mL IFN γ (R&D systems

Cat# 485-MI-100) and 100 ng/mL TNF α (PromoKine Cat# D-63720); for anti-inflammatory activation [20], 10 ng/mL IL-4 (R&D systems Cat# 404-ML-010), 10 ng/mL IL-10 (R&D systems Cat# 217-IL-005), and 20 ng/mL TGF- β (R&D systems Cat#7666-MB-005) for a period of 24 h.

3.2.3 RNA Isolation

Total RNA was isolated from cells using miRNeasy Mini Kit (Qiagen). For RNase R treatment, 500 ng of RNA is incubated for 30 mins at 37°C with or without 2.5 U of Rnase R (Epicentre Technologies Cat# RNR07250).

3.2.4 Circular RNA Microarray and Microarray Data Analysis

CircRNA expression analysis was conducted on total RNA extracted from naïve, pro-inflammatory, and anti-inflammatory macrophages 24 h after polarization (n = 3). Total RNA from each sample was measured using the NanoDrop ND-1000. Sample preparation and microarray hybridization followed Arraystar's standard protocols (Arraystar MD, USA). In summary, total RNA underwent digestion with Rnase R (Epicentre, Inc.) to remove linear RNAs and enrich circular RNAs. The enriched circular RNAs samples were then amplified and transcribed into fluorescent cRNA utilizing a random priming method (Arraystar Super RNA Labeling Kit; Arraystar) and subsequently hybridized onto the Arraystar Mouse circRNA Array V2 (8 \times 15K, Arraystar). Following washing of the slides, arrays were scanned by the Agilent Scanner G2505C.

To analyze the acquired array images, Agilent Feature Extraction software (version 11.0.1.1) was used. Quantile normalization and data processing were conducted using the limma package from the R software package. Differentially expressed circRNAs with statistical significance between two groups were determined through Volcano Plot.

Hierarchical Clustering was utilized to visualize the distinct circRNA expression patterns among samples. Differentially expressed circRNAs between two samples were identified through Fold Change filtering and differential analysis between two groups was analyzed by t-test. The criteria for significant were set at $FC \geq 1.5$ and $p \leq 0.05$. The circRNAs identified as differentially expressed by microarray analysis were uploaded into Qiagen's IPA system for core analysis and then overlaid with the global molecular network in the Ingenuity Pathway Knowledge Base (IPKB). IPA was employed to identify canonical pathways, diseases, and gene networks that are most significant to microarray outcomes. The top 10 circular RNA were ranked by fold change. Conservation between human and mice was determined by pairwise alignment between human and murine circular RNA by blast NCBI. The database www.circbase.org was used for identification of human circular RNA sequences. .

3.2.5 Generation of Circ-cdr1as Overexpression Plasmid and in vitro Overexpression in BMDMs

To generate a circRNA circ-cdr1as expression plasmid, we utilized the previously described pcDNA3.1 (+) Lacasse2 MCS exon vector (Addgene plasmid # 69893; <http://n2t.net/addgene:69893>; RRID:Addgene_69893) (192). This plasmid contains bacterial resistance to ampicillin and G418/neomycin resistance in eukaryotes. Expression of the circRNA is driven by a CMV promoter. Circ-cdr1as sequence (1263bp) gene fragment could not be synthesized as a double stranded DNA fragment due to its high complexity and so, it was cloned in pUC57 by EcoRV between EcoRI and HindIII sites (Genescript Project ID U8508GC140-2). Then the plasmid was digested, the mature sequence fragment was purified by gel purification and subcloned into the above vector. Fragment insertion was verified by gel electrophoresis and sanger sequencing.

The following sequence was inserted between PacI and SacII sites of pcDNA3.1

(+) Lacasse2 MCS exon vector (restriction enzyme sites are in lowercase):

tatgcagaaattaattaaGGTTTCCAGTGGTGCCAGTACCAAGGTCTTCCAACATCTCCA
GGTCTTCCAGCAACTGCAAGTCTTCCAACACTGTCAAGGTCTTCCAGACAATC
GTGATCTTCCAGAAAATATGTCTTCCAGATGATATATGTCTTCCAACAACCTC
AGAGTCTTCCAGTAAATTCAGTCTTCCATGGTATCTAGATCTTCCGTGATATC
TAGATCTTCTAGGAAAATCTGTGTCTTCCAGGAAAATCTTTGTCTTCCAAGGG
ATCCATGTCTTCCAGAAAAAATCCACGTCTTCCAGAAAATTCATGTCTTCC
AGGAAAATCCATGTCTTCCAGAAAATCCAAGTCTTCCAGAAGAATCTAAGT
CTTCCTGAAAAATCCATGTCTTCCATAACAATCTACATCTTCCAGAATAATCA
ACGTCTTCCACAAAATTCAGGTCTTCCAGAAAATATCCAGGTCTTCCAACCA
GTCTATGTCTTCCAGAAAATCCAGGTCTTCCAGCTCATCTATGTCTTCCATC
AGTTCAAGTCTTCCAGATACCCATGTCTTCCATTAAATCTAGCCATGTCTTCCCT
GAAAATCCATGACTTCCCAAAAATCCAATCTTCCTGAAAAATCCATATCTTC
CCAAAATCCACGACTTCCCAAAAATCCATGTCTTCGTGAATATCCACGTCTT
CCTGAAAATCCAAGTCTTCCAGAAATCCATGTCCTTCCAAAATCCATGTCT
TCCTGAAAATCTATGCCTTCCATAAATCTACATCTTCCTGAAAATCCACATCT
TCCTGAAAATCTACATCTTCCTGAAAATCCACATCTTCCATAAATCCCAGTCT
TCCAGAAATCCAAGTCTTCTGGAAAATCCATGTCTTCCTGAAAATCTATGCC
TTCCACAAATCCATGTCCTCCTAACAATCCAAGTCTTCCATAAAAATCTACGCC
TTCCACAAATCTACATCTTCCTGAAAATCCACATCTTCCCAAAAATCCATGTCT
TCGGAAAAAATCCATGTCTTCCAAGGAGTACATGTGTCTTCCTTCACCTCCAA
GTCTTCCAGCATCTCCAGGGCTTCCAGCATCTGCCTGTCTTCCAACATCTCCA

CATCTTCCAGCATCTTTATGTCTTCCAACAACACTGCGCAGTGTCTCCAGTGTAT
CGGCGTTTTGACATTCAGGTTTTCTGGTGTCTGCCGTATCCAGccgcgaggcgtaagta
t.

Prior to transfection, BMDMs were polarized for 24 h for the desired phenotype as described in section 3.2.2. For overexpression of circ-cdr1as in BMDMs *in vitro*, the cells were transfected with 100 nM of control or circ-cdr1as overexpression plasmid for 24 h. The plasmid was added in 500 uL of Opti-MEM and in another 1.5 mL Eppendorf tube 5 uL of Lipofectamine RNAiMAX was added in 500 uL of Opti-MEM and incubated for 5 min. The two mixtures were then pooled and incubated for 15 min at room temperature (RT). The solution mixture was added to the plate and incubated for 24 h. The following day, the media was changed to media containing 3 µg/mL of G418 antibiotic. Cells were harvested and changes in the expression or transcription of macrophage markers were measured by FACS or RT-qPCR, respectively.

3.2.6 Lentiviral Short Hairpin RNA Construction and in vitro Knockdown of circ-cdr1as in BMDMs

To generate a knockdown circ-cdr1as plasmid, a custom shRNA plasmid was constructed using Vector TR30023 pGFP-C-shLenti containing a TCAAGAG loop targeting the splicing junction sequence of circ-cdr1as. This plasmid contains resistance to chloramphenicol in bacteria and puromycin in eukaryotes. The shRNA circ-cdr1as plasmid and sh-scrambled control plasmid were expanded and packaged into Lentivirus. All viruses were produced using the third-generation lentivirus system. Briefly, HEK293 cells were plated at 1×10^7 cells/15 cm plate one day prior to transfection. Production of 3rd generation lentivirus was performed using the combined ratio of transfer plasmid (Custom shRNA plasmid from Origene, Inc.). Plasmid is TR30023 Lenti GFP-C-sh-9B with the following

Sequence: TTCCAACAACACTGCGCAGTGTCTCCAGTGT; packaging plasmid, Env plasmid and pRSV-Rev plasmid at 2:1:1:1, respectively. Polyethylenimine HCl MAX, MW 40000, Transfection Grade (Polysciences, Inc) was used as the transfection reagent at a ratio of 1:2 μg DNA: μg PEI-Max. Without changing the media on the 15 cm plates, the DNA-PEI reagent was added to the cells drop-wise. At 72 h post transfection, supernatant of 293 T cell cultures were PEG precipitated (1 volume of 40 % PEG to 3 volumes of supernatant) for overnight at 4 °C and the samples were centrifuged at 1600 $\times g$ for 45 min at 4 °C and the pellets were gently re-suspended in 15 mL 1 \times PBS containing 0.001 % Pluronic F68 and 5 % Glycerol, buffer exchanged two times and concentrated down to 1 mL using Amicon Ultra-15 100 K filter. The purified virus was then recovered and filtered through a 0.45 μm PES filter and quantified using Lenti-X™ qRT-PCR Titration Kit (Takara Bio, USA). The viruses were aliquoted and stored at -80 °C (193-195).

For circ-cdr1as knockdown in BMDMs *in vitro*, the cells were transfected with MOI 15 lentiviral shRNA (titer concentration for shRNA scrambled: 2.9×10^9 ; shRNA Circ-cdr1as: 3.67×10^9 vp/mL). The cells were transfected with lentivirus shRNA and viral enhancer (ABM Cat# G515) for 48 h. The media was then changed to media containing 3 $\mu\text{g}/\text{mL}$ of puromycin antibiotic for selection of stably transfected cells. The cells were polarized for 24 h. Cells were harvested and changes in the expression or transcription of macrophage markers were measured by FACS or RT-qPCR, respectively.

3.2.7 FACS Analysis and Cell Sorting

BMDMs were harvested and washed with PBS staining buffer containing 2 % FBS and 0.05 % EDTA. The cells were pre-incubated with 0.25 μg of TrueStain FcX PLUS

(anti-mouse CD16/32) antibody (Biolegend Cat# 156603) in 100 uL volume for 10 mins on ice. The cells were then washed with staining buffer and incubated with the following antibodies at 4 °C for 30 min then washed with staining buffer 3× and resuspended in 1 mL of staining buffer. The BDMD were then sorted using BD FACS Aria IIµ based on the following markers: pro-inflammatory- F4/80+, CD86+, CD11c+, CD206–; anti-inflammatory- F4/80+, CD86–, CD11c–, CD206+. BD LSR II was used for FACS analysis, 1.5×10^6 cells were collected, and the cells were stained with the following markers: F4/80, CD86, and CD206. Gating strategies were based on fluorescence minus one (FMO).

3.2.8 Reverse Transcription and RT-qPCR

Reverse Transcription (RT) was performed using High-Capacity cDNA RT kit (Invitrogen Cat# 4368813) to obtain cDNA and quantitative Polymerase Chain Reaction (qPCR) was performed using SYBR Green master mix (Applied Biosystems). To quantify expression of circRNA transcripts, divergent primers are designed to amplify across the backsplicing junction. To quantify linear transcripts, convergent primers were designed to amplify exonic sequences not present in the circular RNA. Reverse Transcription Quantitative Polymerase Chain Reaction (RT-qPCR) was performed on an Applied Biosystems 770 StepOnePlus system using the Fast SYBR™ Green Master Mix (Applied Biosystems) according to the manufacturer's instructions. Expression was quantified using fold change of $2^{\Delta\Delta ct}$ compared to naïve control, normalized to 18S rRNA used as a reference gene.

3.2.9 CircRNA-miRNA-mRNA Interaction Network

Circular RNA-miRNA-mRNA interactions were predicted by Arraystar's

miRNA target prediction software based on TargetScan and miRanda, and the differentially expressed circRNAs within all the comparisons annotated in detail including 2D structure, local AU, position, conservation.

3.2.10 TargetScan and Gene Ontology Analysis

The miRNA targets were uploaded into TargetScan software (release 8.0) to determine microRNA targets and presence of conserved 8mer, 7mer, and 6mer sites that match the seed region of each miRNA. The Gene Ontology (GO) enrichment analysis of the miRNA target genes was determined using Consortium's online tool (<http://www.geneontology.org/>) that identified several significantly enriched GO terms (False Discovery Rate: FDR, p-value <0.05), including associated biological processes, molecular function, PANTHER pathways.

3.2.11 Statistical Analysis

All data were represented as Mean \pm SEM. Analyses were performed using Prism (GraphPad Software Inc). Mean of the groups were compared using unpaired two tail t-test (for two groups) and One-way ANOVA (more than two groups). P values of <0.05 indicate statistical significance. GraphPad Prism version 9.4.0 was used for making data visualization and for statistical analysis. Data are expressed as mean \pm standard error of the mean (S.E.M.), and P < 0.05 was accepted as statistically significant.

3.3 Results

3.3.1 Circular RNA Profiling in Pro- and Anti-Inflammatory Macrophages

To investigate circRNA transcriptome changes between naïve, pro-, and anti-inflammatory macrophages, we initially established and characterized BMDMs stimulated to pro-inflammatory or anti-inflammatory phenotype compared to naïve unpolarized

macrophages (Fig 3.1A). The BDMDs were sorted based on the following markers: pro-inflammatory- F4/80+, CD86+, CD11c+, CD206–; anti-inflammatory- F4/80+, CD86–, CD11c–, CD206+ (Fig 3.1B). Additionally, RT-qPCR analysis was performed for further validation of BMDM polarization based on pro- or anti-macrophage markers (Fig 3.1C) (17,196,197).

We then performed circRNA microarray expression profile from the RNA isolated from BMDMs polarized to a pro-inflammatory phenotype (stimulated with INF γ and TNF α , 24 h) or an anti-inflammatory phenotype (stimulated with IL-10, IL-4, and TGF- β , 24 h). We found differential expressions of circRNAs in all experimental groups as depicted in the heat map (Fig 3.2A). Circular RNAs were then selected based on a log fold change of >1.5 and a p-value of <0.05.

A total of 419 circRNAs were differently expressed in pro-inflammatory macrophages compared with anti-inflammatory macrophages. Among these, 218 circRNAs were upregulated and 201 were downregulated (Fig 3.2B). Moreover, the scatter plot demonstrates the aberrantly expressed circRNAs between pro- and anti-inflammatory macrophages (Fig 3.2C). Lastly, Among the circular RNA found to be differentially expressed between pro-inflammatory vs naïve and anti-inflammatory vs naïve, 932 circular RNA were present in pro-inflammatory macrophages, 136 circular RNA present in anti-inflammatory macrophages, and 78 circular RNA found in all three phenotypes (Fig 3.2D).

3.3.2 Gene Interaction Networks and Disease Enrichment Analysis

Ingenuity Pathway Analysis (IPA) generated gene interaction networks that span across all datasets, indicating predicted activated and inhibited genes associated with cell death and survival, cell-to cell signaling, cardiovascular system development and function,

and cell-mediated immune response. Noteworthy activated predicted genes include crucial inflammatory regulators nuclear factor- κ B (NF κ B), interferon α (INF α), and IL-10 (Fig 3.3A). These genes are associated with the top enriched canonical pathways between all data sets including senescence, and B cell receptor signaling (Figure 3.3B).

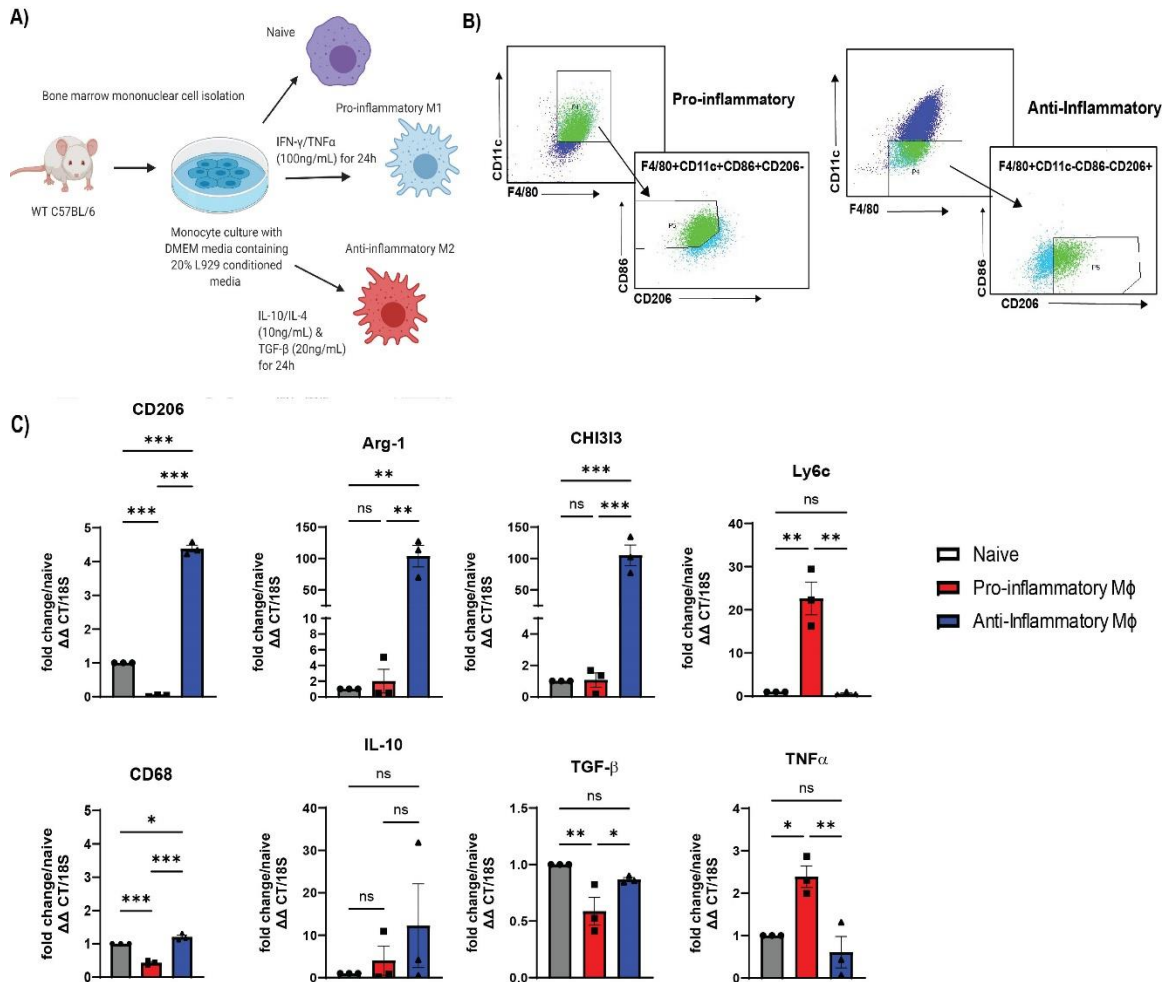


Figure 3.1. Characterization of bone marrow derived macrophages (BMDM) stimulated to pro-inflammatory or anti-inflammatory phenotype compared to naïve macrophages. (A) Schematic of experimental outline for the polarization to a pro-inflammatory phenotype by INF γ (100ng/mL) and TNF α (100ng/mL) or an anti-inflammatory phenotype by IL-10(10ng/mL), IL-4(10ng/mL), and TGF- β (20ng/mL). (B) The BMDMs were sorted based on the following cell surface markers: pro-inflammatory- F4/80+, CD86+, CD11c+, CD206-; anti-inflammatory- F4/80+, CD86-, CD11c-, CD206+. Total RNA was isolated. (C) RT-qPCR analysis of transcriptional changes of pro or anti-inflammatory macrophage markers compared to naïve macrophages, normalized to 18S. n= 3. Data are Mean \pm SEM. * p<0.05, ** p<0.01, *** p<0.001, ns non-significant vs naïve BMDM (one-way ANOVA).

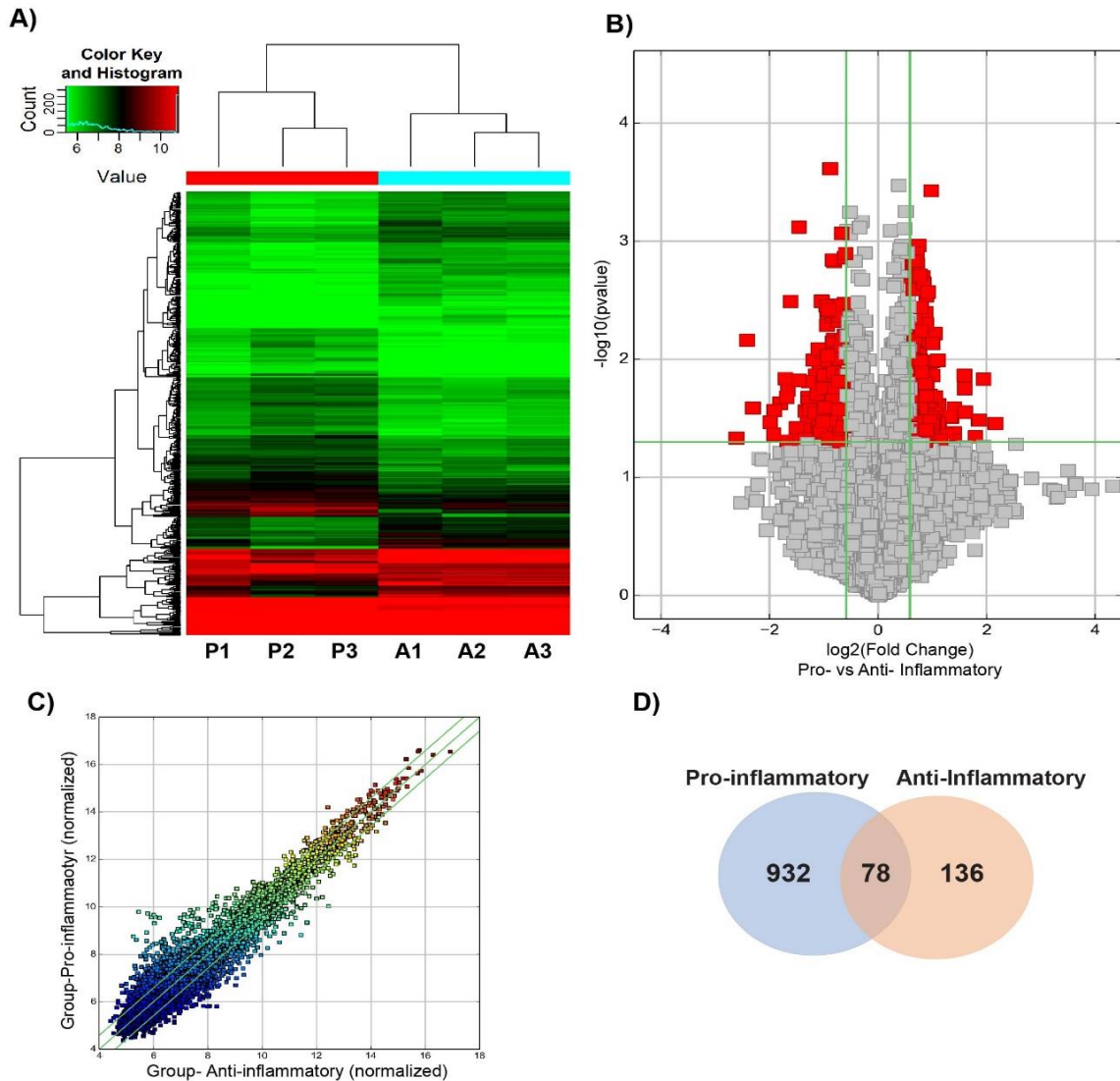


Figure 3.2. Microarray analysis of differentially expressed circular RNAs in bone marrow derived macrophages. (A) Heat map revealing differential circular RNA expression profiles between pro-inflammatory and anti-inflammatory macrophages. The red color indicates a higher FC value; green indicates a smaller FC value. (B) Volcano plot comparing significantly expressed circular RNA between pro-inflammatory and anti-inflammatory macrophages. The circular RNA expression log 2- transformed FC values (x-axis) were plotted against the log10 P values (on the y-axis). The red dots represent the circular RNAs having an FC value ≥ 1.5 and $P < 0.05$ comparing between pro-inflammatory and anti-inflammatory macrophages. (C) Scatter plot demonstrating the distributions of circular RNAs that are differentially expressed between pro-inflammatory and anti-inflammatory macrophages. The values of the x- and y-axes in the scatter plot were averaged to the normalized signal values of the group. (D) Venn Diagram illustrating the overlap of circular RNA found between pro-inflammatory vs naïve or anti-inflammatory vs naïve macrophages. FC, fold change; circRNA, circular RNA; N, naïve; P, pro-inflammatory; A-anti-inflammatory macrophages.

Disease enrichment analysis identified top diseases associated with circular RNA differently expressed between pro- and anti-inflammatory macrophages. Among them, the most common diseases are related to the liver in which macrophages are a key cellular component and essentially for tissue homeostasis (Fig 3.3C) (198). Additionally, cardiac fibrosis and cardiac enlargement are also noted as the top related disease in which macrophages are the predominant leukocyte type after cardiac injury (Fig. 3.3C) (16).

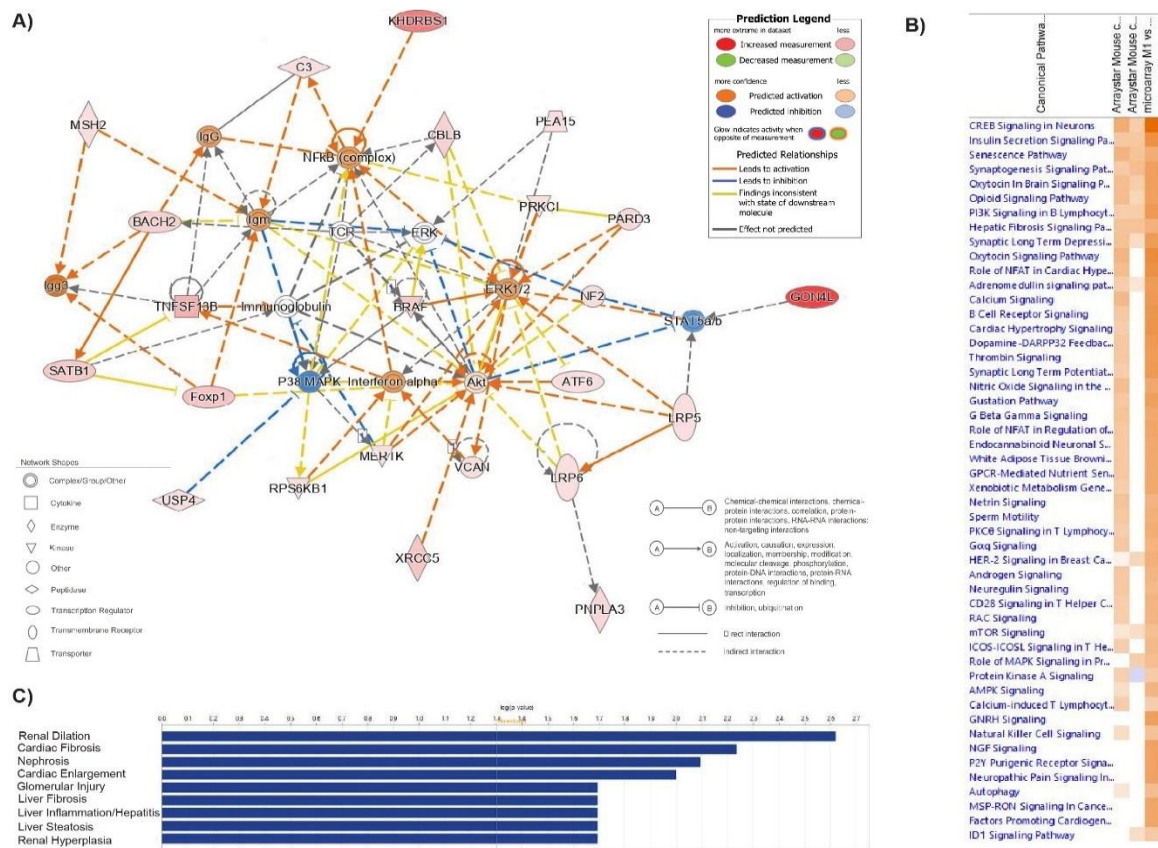


Figure 3.3. Ingenuity pathway analysis for differentially expressed circular RNAs between pro-inflammatory and anti-inflammatory macrophages. (A) Overlapping interaction network analysis regulated by circular RNAs found between all data sets indicating predicted activated and inhibited genes that either directly or indirectly interact. (B) Heatmap of the canonical pathway network construction of circular RNA activation Z-score comparing data sets: naïve vs pro-inflammatory, naïve vs anti-inflammatory, and pro-inflammatory vs anti-inflammatory (orange and blue represent activation and suppression, respectively). (C) Disease enrichment analysis based on $-\log(p\text{-value}) > 4$ threshold on the IPA system.

3.3.3 Validation of the Top Ten Highly Conserved and Differentially Expressed RNAs

Based on the microarray analysis, we determined the top ten differentially expressed circular RNAs that are also conserved between human and mouse, ranked by fold change. Among them, 6 were downregulated (circZfhx3, circCdr1as, circAmotl1, circBnc2, circPtk2, and circSlc30a7) and 3 (circElf2, circGigyf2, and circRsrc1) were upregulated in pro-inflammatory (M1) macrophages; and 1 (circ-Mipol1) was upregulated in anti-inflammatory (M2) macrophages (Fig 3.4A). RT-qPCR confirmation of profile data based on detection of divergent primers showed circZfhx3, circAmotl1, and circBnc2 were downregulated in both phenotypes; circElf2, and circMipol1 were downregulated in anti-inflammatory phenotypes; circGigyf2, circPtk2, and circSlc30a7 were non-significantly expressed between phenotypes; circCdr1as was significantly upregulated in anti-inflammatory macrophages (Fig 3.4B). We selected target circRNA cdr1as for further analysis based on significant downregulation in pro-inflammatory macrophages, significant upregulation in anti-inflammatory macrophages, 74% sequence similarity between human and mouse, and no significant change in parental cdr1 regardless of phenotype (Figure 3.4A, B; Figure 3.5). Additionally, there are currently no reports on the role of circ-cdr1as in macrophage phenotypic switching; however, circ-cdr1as was reported to be involved in the regulation of brain development, diabetes, increase in cardiac infarct size, and cardiomyocyte apoptosis (51,105,106,151).

A)

Top 10 upregulated or downregulated conserved circRNA between human and mouse in bone marrow derived macrophages ranked by fold change.

circRNA ID	circRNA type	Chromosome	Source Gene	Fold Change	P _{adj} Value	% homology of splicing junction (human vs mouse)	Regulation in BMDM
mmu_circRNA_005039	Exonic	Chr3	Elf2	10.4129583	0.031236023	81.1%	Upregulated in M1
mmu_circRNA_005434	Antisense	Chr8	Zfhx3	3.4138622	0.019556071	94.4%	Downregulated in M1
mmu_circRNA_010385	Exonic	Chr1	Gigyf2	2.7595952	0.05860264	92%	Upregulated in M1
mmu_circRNA_001946	antisense	ChrX	Cdr1	2.4249507	0.013344931	74%	Downregulated in M1
mmu_circRNA_43784	Exonic	Chr9	Amot1	1.9046831	0.017305584	84%	Downregulated in M1
mmu_circ_0001136	Intronic	Chr3	Rsrc1	1.8513597	0.013099638	84.8%	Upregulated in M1
mmu_circRNA_014660	Exonic	Chr4	Bnc2	1.7290235	0.037834294	90.7%	Downregulated in M1
mmu_circ_0000612	Sense overlapping	Chr15	Plk2	1.673395	0.037898566	45.1%	Downregulated in M1
mmu_circRNA_25157	Exonic	Chr12	Mipol1	1.5065144	0.04025052	88.7%	Upregulated in M2
mmu_circ_0001160	Exonic	Chr3	Slc30a7	1.1896273	0.118923222	89.5%	Downregulated in M1

B)

Naive
 Pro-inflammatory M1
 Anti-inflammatory M2

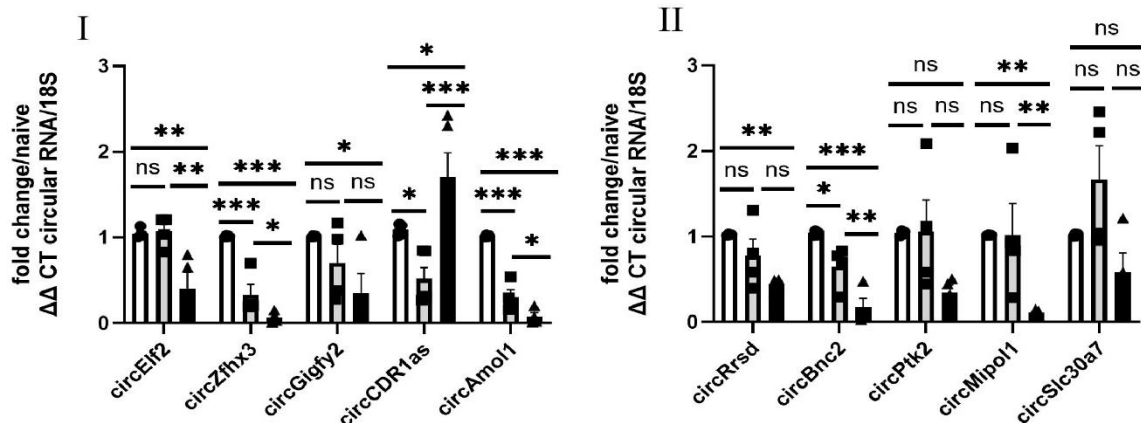


Figure 3.4. Top 10 Differentially expressed and conserved circRNAs in BMDMs. (A) The top 10 circular RNA were ranked by fold change and www.circbase.org was used for identification of human circular RNA sequences followed by pairwise alignment between human and murine circular RNA by blast NCBI as indicated in Table 1. (B) Validation of the top 10 differentially expressed circRNAs by RT-qPCR analysis (CT value <31) of bone marrow derived macrophages polarized to pro-inflammatory or anti-inflammatory phenotype compared to naïve macrophages, normalized to 18S. n = 4–5. Data are Mean ± SEM. * p < 0.05, ** p < 0.01, *** p < 0.001, ns non-significant vs naïve BMDM (one-way ANOVA).

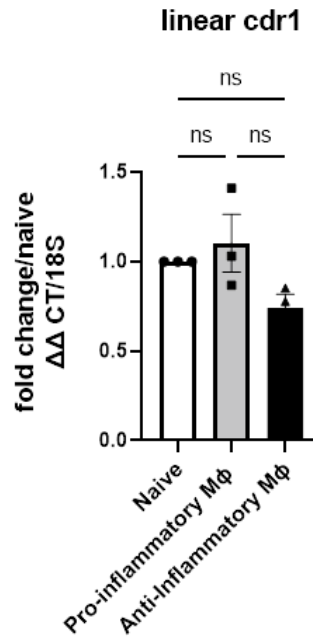


Figure 3.5. Parent Gene Cdr1 is unaffected in polarized BMDMs. RT-qPCR analysis of the transcription factor linear cdr1 compared to naïve macrophages, normalized to 18S. $n=3$. Data are Mean \pm SEM. * $p<0.05$, ** $p<0.01$, *** $p<0.001$, ns non-significant vs naïve BMDM (one-way ANOVA).

3.3.4 Overexpression of circ-cdr1as Increases Transcription of Anti-inflammatory markers and Percentage of CD206+ cells in vitro

Based on mentioned data indicating circ-cdr1as upregulation in anti-inflammatory macrophages, we sought to determine if overexpression promotes phenotypic switching to an anti-inflammatory phenotype. We generated circ-cdr1as overexpression plasmid containing laccase2 intronic regions to promote circularization (Figure 3.6A). The overexpression plasmid was then transiently transfected into naïve or pro-inflammatory BMDMs (Figure 3.6B). Overexpression did not significantly change transcription of linear cdr1 (Figure 3.6C); meanwhile, overexpression increased circ-cdr1as levels by >100-fold compared to scrambled plasmid control and un-transfected naïve controls, confirming successful transfection of plasmid. in all phenotypes (Figure 3.6D).

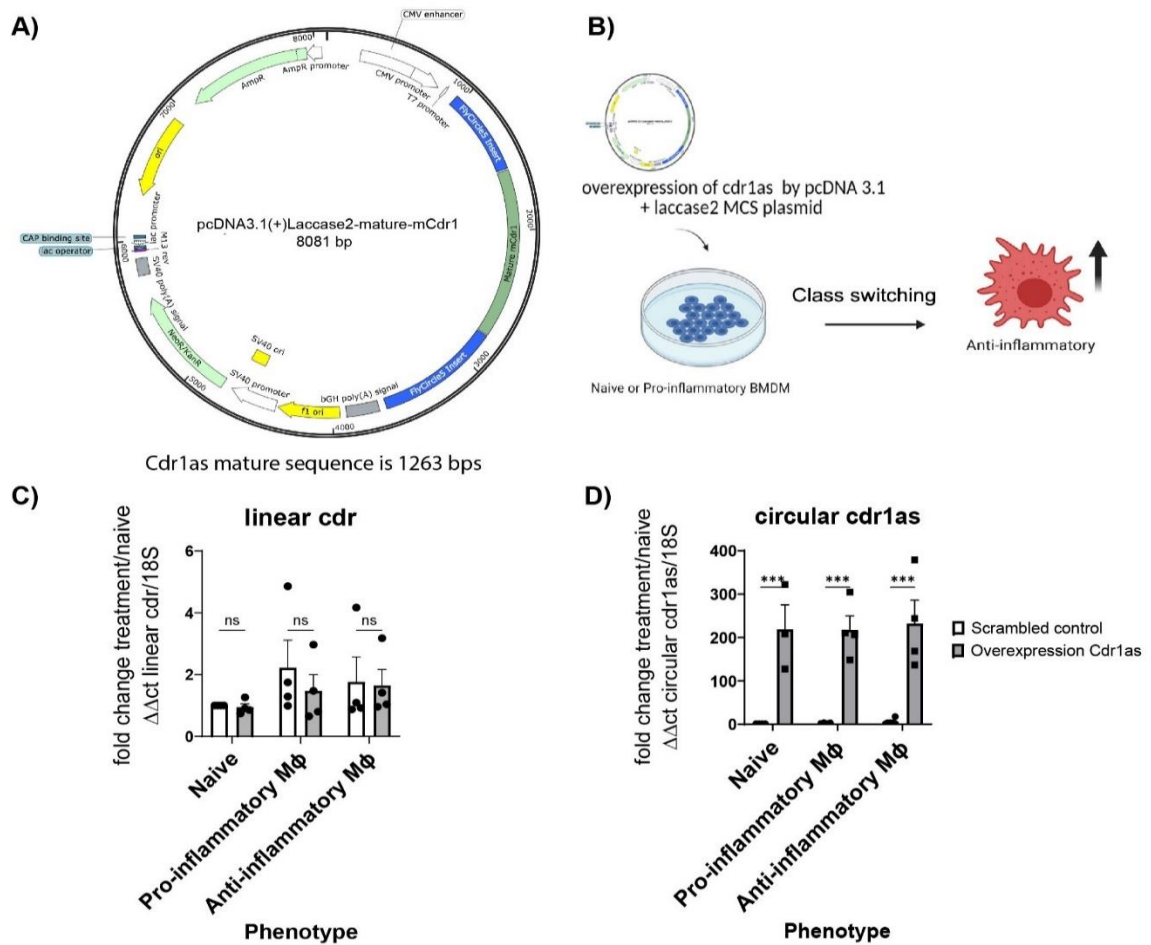


Figure 3.6. Transcriptional changes in naïve, pro-inflammatory, and anti-inflammatory macrophages treated with scrambled control or overexpression plasmid. (A) Vector map for pcDNA3.1 (+) Laccase2 MCS-CDR1as plasmid containing laccase2 flanking introns to promote circularization of circ-cdr1as. (B) Schematic of the experimental outline for determining if overexpression of circ-cdr1as in naïve or pro-inflammatory macrophages promotes class switching to an anti-inflammatory phenotype. (C, D) RT-qPCR analysis of linear cdr1 (C) or circular cdr1as (D) in naïve, pro-inflammatory, and anti-inflammatory macrophages treated with scrambled control or overexpression plasmid, compared to naïve macrophages, normalized to 18S. n= 3-4 Data are Mean ± SEM. * p<0.05, ** p<0.01, *** p<0.001, ns non-significant vs naïve BMDM (one-way ANOVA for figures C-D)

FACS analysis and density plots demonstrated a shift in the distribution of cells indicating an increase in CD206 (anti-inflammatory macrophage marker) in naïve (Figure 3.7A) and pro-inflammatory macrophages (Figure 3.7B) overexpressing circ-cdr1as compared to scrambled control. The transcriptional levels of anti-inflammatory

macrophage markers such as chitinase-3-like protein 1 (CHI3I3), arginase 1 (Arg-1), CD206 were increased in naïve and pro-inflammatory macrophages overexpressing circ-cdr1as compared to scrambled control. IL-10 and TGF β mRNA levels were also increased in both phenotypes (Figure 3.7C, D). Pro-inflammatory marker Ly6c was significantly downregulated in pro-inflammatory macrophages overexpressing circ-cdr1as compared to scrambled control (Figure 3.7D). In conclusion, this data suggests that overexpression of circ-cdr1as not only drives naïve macrophages to M2/anti-inflammatory phenotype, but it has a similar effect in polarized pro-inflammatory macrophages.

3.3.5 Knockdown of circ-cdr1as Decreases Transcription of Anti-inflammatory markers and Increases Percentage of CD86+ cells in vitro

To determine if circular cdr1as downregulation has the opposite effect of gain of function experiments, we used lentiviral small hairpin RNA (shRNA) targeting the splicing junction specific to circular RNA (Figure 3.8A, B). It was stably transduced into naïve and BMDMs prior to polarization. Knockdown significantly reduced circ-cdr1as transcription across all phenotypes (Figure 3.8D). Importantly, circ-cdr1as knockdown did not significantly change the expression of linear cdr1 (Figure 3.8C). FACS analysis showed an increase of CD86 (pro-inflammatory macrophage marker) in both naïve and anti-inflammatory macrophages overexpressing circ-cdr1as compared to the scrambled control. Furthermore, density plots displayed a shift in cell distribution compared to the scrambled control (Fig 3.9A, B). Transcriptional levels of anti-inflammatory lineage markers Arg-1 and CD206 were diminished in shRNA-treated naïve and anti-inflammatory macrophages compared to controls. Similarly, the mRNA levels of IL-10 and TGF β were reduced in both phenotypes (Fig 3.9C, D). These findings suggest that cirRNA cdr1as plays a role in promoting an anti-inflammatory phenotype in naïve and polarized macrophages.

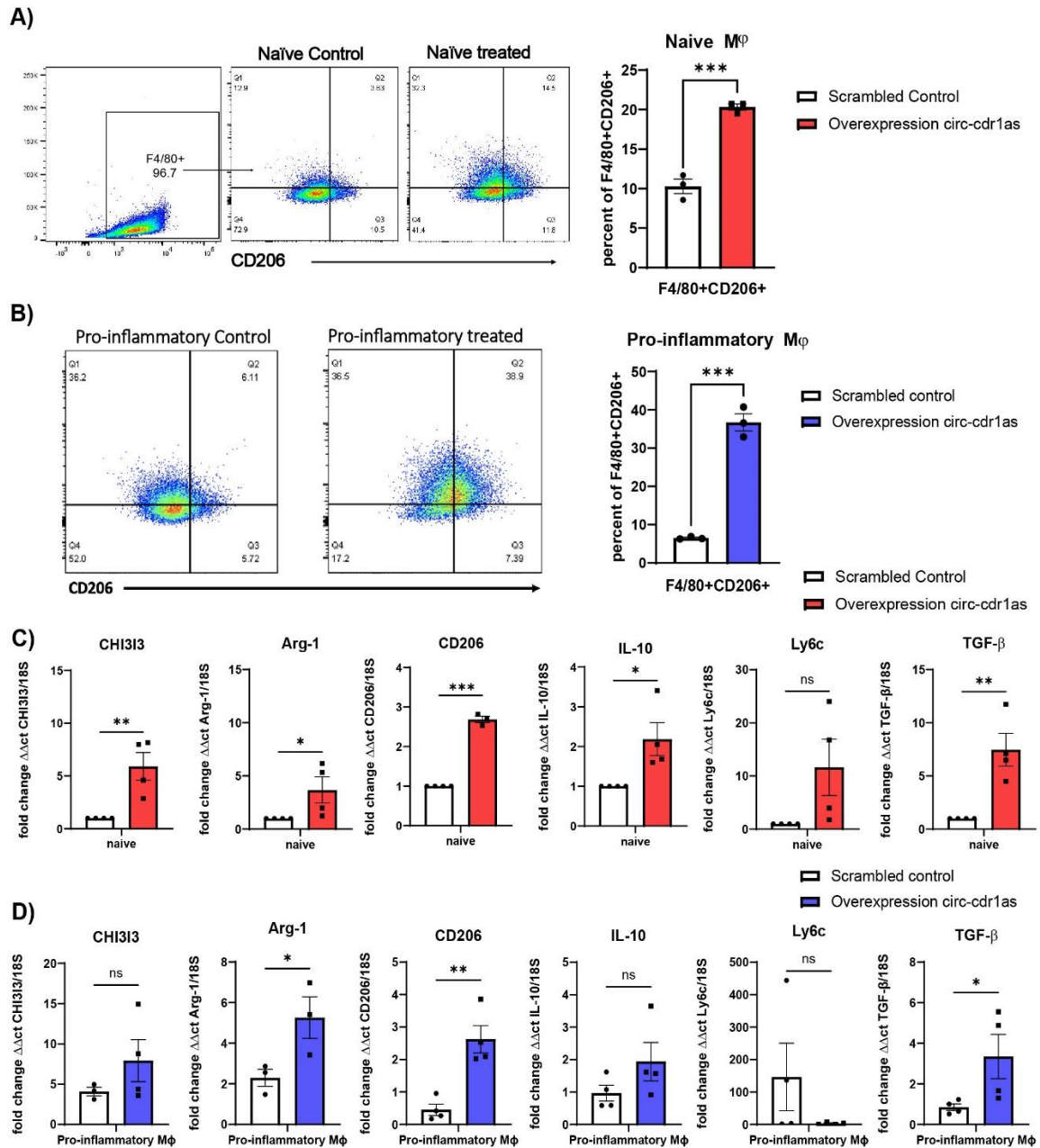


Figure 3.7. Overexpression of circ-cdr1as upregulates expression of anti-inflammatory markers in naïve macrophages and pro-inflammatory macrophages. (A, B) FACS analysis of F4/80 + CD206+ cells in naïve (A) or pro-inflammatory (B) macrophages treated with overexpression plasmid compared to scrambled control, normalized to 18S. (C,D) qRT-qPCR analysis of transcriptional changes of macrophage markers and cytokines in naïve (C) or pro-inflammatory (D) macrophages compared to scrambled control, normalized to 18S. n = 3–4. Data are Mean ± SEM. * p < 0.05, ** p < 0.01, *** p < 0.001, ns (non-significant) vs control (unpaired two tail t-test). CHI3I3, chitinase-3-like protein 1; Arg-1, arginase 1; IL-10, Interleukin 10; TGFb-Tumor grow factor-b.

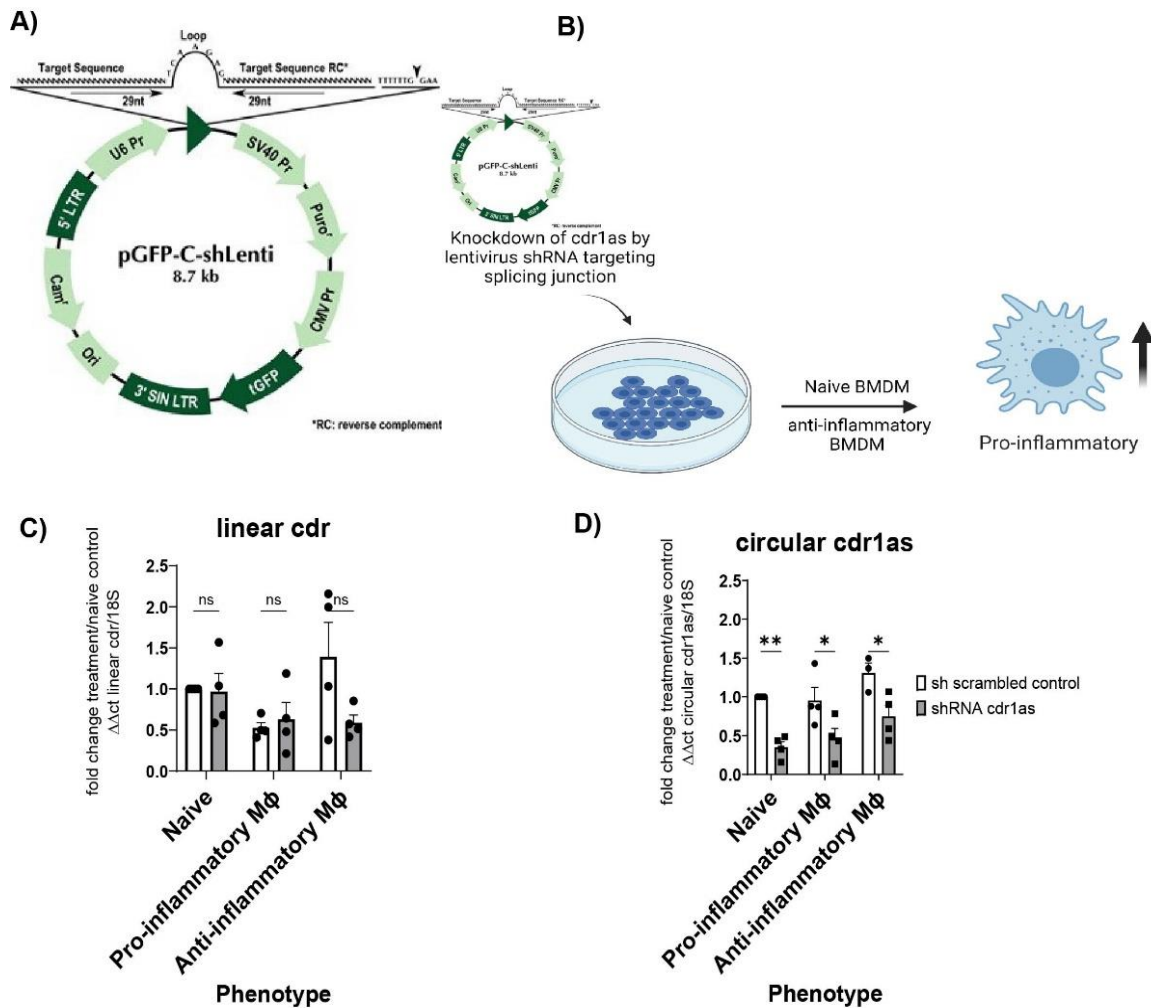


Figure 3.8. Transcriptional changes in naïve, pro-inflammatory, and anti-inflammatory macrophages treated with scrambled control or lentivirus circ-cdr1as shRNA. (A) Vector map of small hairpin (sh) RNA lentiviral vector targeting the splicing junction specific to circ-cdr1as. (B) Schematic of experimental outline for determining if knockdown of circ-cdr1as promotes class switching to an anti-inflammatory phenotype. (C-D) RT-qPCR analysis of linear cdr1 (C) or circular cdr1as (D) in naïve, pro-inflammatory, and anti-inflammatory macrophages treated with lentivirus scrambled control or lentivirus shRNA circ-cdr1as, compared to naïve macrophages, normalized to 18S. n=3-4 Data are Mean \pm SEM. * p<0.05, ** p<0.01, *** p<0.001, ns non-significant vs naïve BMDM (one-way ANOVA for figures C-D).

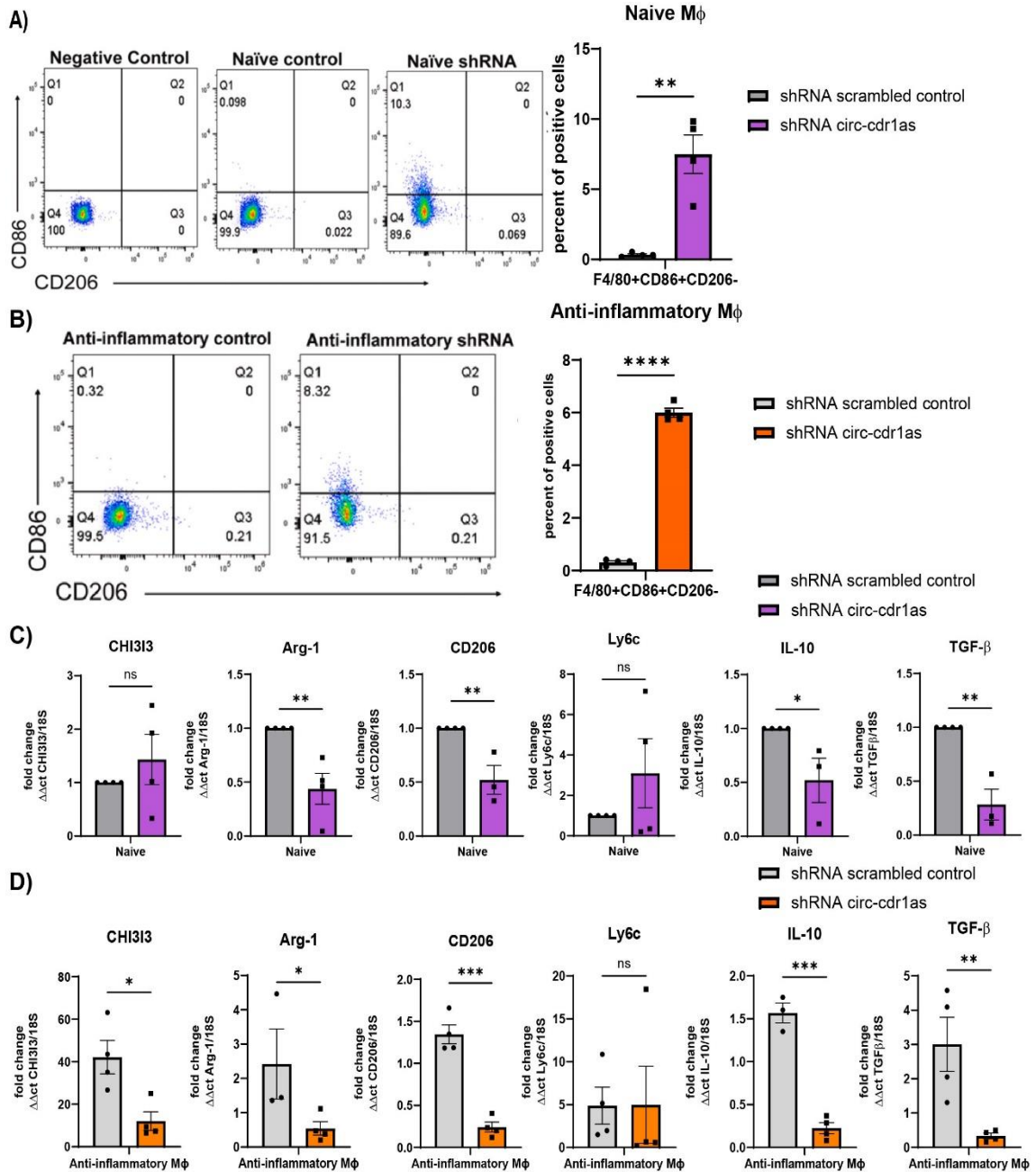


Figure 3.9. Knockdown of circular *cdr1as* downregulates expression of anti-inflammatory markers in naïve or polarized anti-inflammatory macrophages. (A,B) FACS analysis of F4/80+CD86+CD206⁻ cells in naïve (A) or anti-inflammatory (B) macrophages treated with lentiviral shRNA circ-*cdr1as* compared to lentivirus scrambled control, normalized to 18S. (C,D) qRT-qPCR analysis of transcriptional changes of cytokines and macrophage markers in naïve (C) or anti-inflammatory (D) macrophages compared to lentivirus scrambled control, normalized to 18S. n=3-4. Data are Mean \pm SEM. * p<0.05, ** p<0.01, *** p<0.001, ns (non-significant) vs control (unpaired T-test). CHI3I3, chitinase-3-like protein 1; Arg-1, arginase 1; IL-10, Interleukin 10; TGF β -Tumor grow factor-b.

3.3.6 CircRNA Cdr1as-miRNA-mRNA Network and GO Enrichment Analysis

Recent studies demonstrate that circular RNAs play a crucial role in fine tuning the level of miRNA mediated regulation of gene expression by sequestering the target miRNAs (49,51,87,106,132,133,199-202). Therefore, we sought to identify possible miRNA targets. CircRNAs and miRNAs were predicted with Arrays miRNA target prediction software based on TargetScan and miRanda according to the complementary miRNA matching sequence. A total of 4 miRNAs (miR-7a/b-5p, miR-450b-3p, miR-7685-3p, miR-7074-5p) were predicted to have an interaction with circ-cdr1as (Figure 3.10). The highest conserved miRNA based on TargetScan and miRanda analysis is miR-7-5p. To determine functional significance of the downstream target genes in the circRNA-miRNA-mRNA regulatory network, we performed GO enrichment analysis for the biological process, molecular function, and pathways involved (Figure 3.10).

3.4 Discussion

Macrophages play crucial roles in both physical and pathological conditions, mediating tissue damage and inflammatory responses (186,198). Particularly, macrophages are vital immune cells in the inflammatory response and are key cellular elements in chronic inflammatory diseases such as CVD and cancer (183,196). These versatile leukocytes can adapt their phenotypes in response to environmental cues and signals, with two primary subpopulations: classically activated pro-inflammatory macrophages and anti-inflammatory macrophages (185,203,204). Understanding the mechanisms governing macrophage polarization could offer insights into developing therapies that modulate the balance between pro- and anti-inflammatory phenotypes without impairing monocyte function and recruitment (187,205).

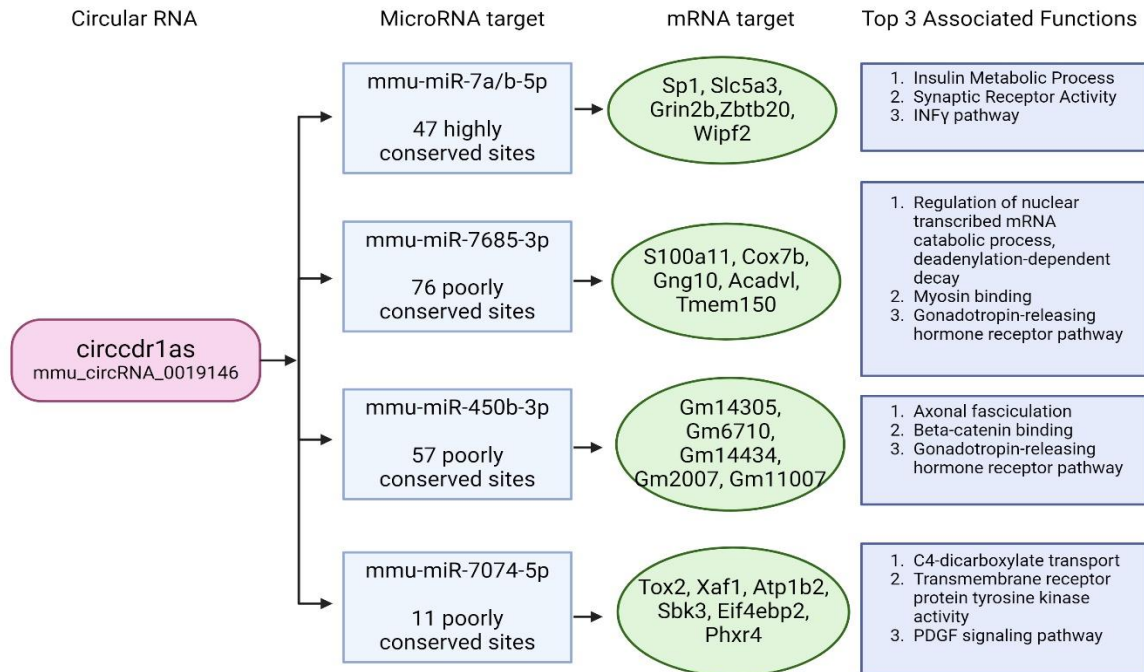


Figure 3.10. Predicted circular RNA cdr1as-miRNA-mRNA targets and top 3 associated functions. The microRNA targets were identified using Arraystar’s miRNA target prediction software based on TargetScan and miRanda from all the differentially expressed circRNAs between naïve, pro-, and anti-inflammatory macrophages. Predicted miRNA targets (only top 5 included) were determined using TargetScan and sorted by cumulative weighted context ++ score that is the sum of the contribution of 14 features, previously described (206). GO enrichment Analysis identified top biological processes, molecular functions, and pathways involved for the circular RNA-miRNA networks (Illustration created with Biorender.com).

Advances in high-throughput RNA sequencing with depletion of ribosomal RNA to enhance sequencing of non-polyadenylated RNA species have identified a new class of non-coding RNAs called circular RNAs. Circular RNAs form covalently closed transcripts generated when the pre-mRNA splicing machinery back splices to join a downstream 5’ splice site to an upstream 3’ splice site (68). They are derived from exonic, intronic sequences, or both. These circular RNAs exhibit high conservation across species and have a high degree of stability in mammalian cells, rendering them potential therapeutic targets (85,86,88).

Whether circRNAs are involved in macrophage polarity and phenotype is not yet established. Therefore, this study sought to investigate expression patterns of circular RNAs in pro- and anti-inflammatory macrophages. Our findings revealed significant differences in 419 circular RNAs between these two phenotypes, with 218 circRNAs upregulated and 201 circRNAs downregulated in pro-inflammatory macrophages. Additionally, 78 circRNAs were found across naive, pro-, and anti-inflammatory macrophages. It should be noted that macrophage activation deregulates expression of other potential circular RNAs that are not annotated by microarray chip.

Several studies have implicated circRNAs in regulating various physiological conditions and disease progression (128,132,172). Ingenuity Pathway analysis of differentially expressed circular RNAs between pro- and anti-inflammatory macrophages revealed gene interaction networks associated with critical processes like cell death and survival, cell signaling, cardiovascular system development and function, and cell-mediated immune response. Notably, master inflammatory regulators like NF- κ B, INF α , and IL-10 were predicted to be activated within these networks as well. These master regulators are vital to many of the roles that macrophages play in orchestrating an inflammatory response (204,207,208). How we may utilize circRNAs to modulate the inflammatory response is an important field of future research.

Disease enrichment analysis identified top diseases associated with circular RNA differently expressed between pro- and anti-inflammatory macrophages. The top two targeted organs were the liver and the heart, in which macrophages play a major role in the initiation and resolution of inflammation after injury (16,198). Currently, circular RNAs have been implicated to play a role in cardiovascular diseases such as cardiac hypertrophy,

coronary artery disease, cardiac fibrosis, rheumatic heart disease, and myocardial infarction (34,52,123,127,128,209). One of the most characterized circular RNA, heart-related circular RNA (HRCR), is repressed in hypertrophic and failing hearts. HRCR sequesters miR-223 to attenuate cardiac hypertrophy by preventing the inhibition of the protein apoptosis inhibitor *in vitro* and *in vivo* (138). Additionally, our lab found that circular RNA circFndc3b modulates cardiac repair after MI. This circular RNA is down regulated in post-MI murine hearts and in ischemic cardiomyopathy patients. CircFndc3b interacts with RNA binding protein FUS to regulate VEGF expression. Overexpression of circFndc3b in MI mouse model reduced endothelial apoptosis, cardiomyocyte apoptosis, and enhanced angiogenesis after cardiac injury (39). These studies highlight the potential of therapeutically targeting circRNA promote cardiac function and remodeling post-MI. Therefore, our future studies focused on translational functionality of circular RNA cdr1as following myocardial injury.

Based on the microarray analysis and pairwise comparison analysis between human and mouse circRNA sequences, we selected the top 10 differentially expressed and highly conserved circRNAs. Validation by RT-qPCR demonstrated discrepancies between the microarray data and RT-qPCR analyses. Therefore, validation of circRNA targets is an essential step of screening. Furthermore, we chose circular RNA cdr1as for investigation as both analyses indicated a downregulation in pro-inflammatory macrophages, conservation, and RT-qPCR analysis showed a significant upregulation in anti-inflammatory macrophages. Ingenuity Pathway analysis highlighted gene interaction networks associated with macrophage biology and inflammation, specifically involving master inflammatory regulators and inflammatory disease-associated pathways.

Although there are limited studies on the role of circRNAs in immunity, there are circular RNAs previously found to be involved in T cell and macrophage biology. One study found significant induction of over 2,000 circular RNAs in macrophages stimulated with LPS, a major component of the outer membrane of Gram-negative bacteria that will activate macrophages. The authors found that circRNA mcircRasGEF1b is needed for proper activation of macrophages in response to LPS (53, 54). In addition to this, one study found that high expression of circ-CPA4 sequestered miR-let-7. This led to upregulation PD-L1 resulting in CD8⁺ T cell inactivation, suppressed T cell growth, tumor immune escape, and increased drug resistance (182).

A bioinformatics study on functional roles of circular CDR1as in cancer, analyzed over 868 cancer samples using Gene ontology (GO), Kyoto Encyclopedia of Genes and Genomes (KEGG), gene set enrichment analysis (GSEA), CIBERSORT, Estimating the Proportion of Immune and Cancer cells (EPIC), and the Malignant Tumors using Expression data (ESTIMATE) algorithms. They suggest circ-CDR1as involvement in immune and stromal cell infiltration including immune cells CD8⁺ T cells, NK cells, and anti-inflammatory macrophages. Interestingly, tissues with the highest circ-CDR1as expression had a higher ratio of anti-inflammatory to pro-inflammatory macrophages (181). However, there are no reports on circular RNA cdr1as in the regulation of macrophage biology and function. Our data, for the first time, reports that overexpression of circ-cdr1as promotes phenotypic switching to an anti-inflammatory phenotype in naïve and pro-inflammatory macrophages. Meanwhile, knockdown of circ-cdr1as induces a pro-inflammatory phenotype in naïve and anti-inflammatory macrophages. Loss or gain of function experiments did not significantly alter the linear counterpart.

Numerous reports have identified the role of circ-cdr1as as a miRNA sponge (51,106,181,200,202,210). Therefore, we investigated the potential relationship between circ-cdr1as and miRNAs. This present study identified 4 miRNA and subsequent mRNA targets that are associated with circ-cdr1as. Among them, circ-cdr1as contains >70 binding sites for miR-7 acting as a miRNA sponge to inhibit miRNA-7 function. Previously, functional studies suggested that overexpression of circ-cdr1as resulted in development defects in the midbrain of embryonic zebrafish; meanwhile, overexpression of miR-7 reduced these effects (210). However more investigation into the molecular mechanisms underlying circRNA-miRNA-mRNA interactions related to phenotypic switching in macrophages is needed. Although there are some reports describing that dysregulation of miR-7 is associated with aberrant NFkB activation in cancer and respiratory diseases, there is currently limited research on whether circ-cdr1as indirectly targets key inflammatory regulators via miR-7 inhibition (211,212). Overall, this current study identified miR-7 as a target for circ-cdr1as in BMDMs and GO enrichment analysis provided insight into the possible biological process, molecular functions, and pathways involved including inflammatory pathways such as interferon-gamma signaling and interleukin signaling pathways. Therefore, this study sheds light on the regulatory roles of circRNAs, particularly circ-cdr1as, in modulating macrophage phenotype and function, offering potential avenues for therapeutic intervention in inflammatory diseases.

3.5 Conclusion

In conclusion, this study demonstrates the differential transcriptional changes of circRNAs in naïve, pro-/anti- inflammatory macrophages. Our findings highlight circ-cdr1as as significantly downregulated in pro-inflammatory macrophages and upregulated

in anti-inflammatory macrophages. Through loss or gain of function studies, we demonstrated that overexpression of circ-cdr1as promotes phenotypic switching to an anti-inflammatory phenotype, while knockdown has the opposite effect. Further investigation into the detailed molecular mechanisms underlying circ-cdr1as's role in regulating macrophage polarization is warranted. Given the relevance of circRNAs in cardiovascular disease and our IPA disease enrichment analysis of the circRNAs, further investigation is needed on whether circ-cdr1as could modulate macrophage biology during cardiac injury and potentially regulate post-injury cardiac inflammation.

CHAPTER 4

CIRCULAR RNA CDR1AS MODULATES MACROPHAGE PHENOTYPE AND CARDIAC REPARATIVE FUNCTION AND IMPROVES POST-INJURY CARDIAC REPAIR

4.1 Introduction

Cardiovascular disease (CVD) is the leading cause of morbidity and mortality, accounting for more than 900,000 deaths in the United States annually. It is estimated that roughly 48.6% of Americans suffer from at least one form of cardiovascular disease. Overall, CVD estimated annual economic burden is 254.3 billion, constituting 15% of national medical expenditure. Despite advances in treatment and care, the total case numbers and long-term prognosis remain poor (1). Myocardial infarction (MI) is one of the most common forms of acute cardiac injury, defined as partial or complete obstruction of blood flow resulting in sudden ischemic death of myocardial tissue and persistent inflammation (3). These staggering figures highlight the urgent need to further understand the underlying mechanisms to identify therapeutic targets for pharmacological intervention for patients with heart disease.

In the initial stages of cardiac injury, dying cardiomyocytes release damage associated molecular patterns and pro-inflammatory cytokines to recruit leukocytes and initiate an inflammatory response. Neutrophils are the first leukocyte to be recruited, they release matrix degrading enzymes and reactive oxygen species. Macrophages are then recruited in high numbers to the infarcted myocardium and undergo phenotypic switching from pro-inflammatory phenotype in the early stage to anti-inflammatory phenotype in the later stage to control the initiation and resolution of the inflammatory response.(4,11,15). As a result of macrophages being central regulators for the immune system, there have

been attempts to target them via reduction, depletion, or impairment of mobilization and function. However, these strategies prolonged cardiac inflammation leading to insufficient clearance of dead cells and impaired tissue remodeling (16,27,29). Therefore, further investigation is needed to identify mechanisms involved in the modulation of the inflammatory response and their potential for therapeutic intervention. In recent years, non-coding RNAs (ncRNAs) have been investigated as regulatory RNAs involved in pathological process in CVD (31). In particular, circular RNAs have begun to garner interest as potential biomarkers and regulators of cardiac dysfunction (52,57,127,128) and immune response in infections, auto-immune diseases, and cancer (169,172,177,178).

Circular RNAs are newly discovered non-coding RNA generated from protein-coding genes with covalently closed loop generated by the pre-mRNA splicing machinery that backsplices to join a downstream 5' splice site to an upstream 3' splice site (48,55). The unique characteristic of circRNAs to lack free terminals allow circRNAs to be resistant to exonuclease degradation resulting in high stability. Studies have reported that circRNAs exhibit biological functions, including transcriptional and translational regulation, sequesters of miRNA and RBPs, and cell-to-cell communication (52,80,82,112,213). Circular RNAs are abundant in the eukaryotic transcriptome and have been identified to be differentially expressed during cardiovascular development and disease (127,128). For example, a study found that in failing mouse, rat, and human hearts, there is an overall increase in circRNA expression arising from the titin (Ttn) gene across all species (47). Later studies have implicated circRNAs to play a role in cardiac hypertrophy, coronary artery disease, cardiac fibrosis, and myocardial infarction (52,127). Additionally, circRNAs have also been implicated in immune regulation. One study has shown that the

delivery of purified exogenous circRNAs stimulates a more prominent innate immune response compared to their linear counterpart (45). Circular RNA *cdrlas*, has been implicated to play a role in the regulation of brain development (105), diabetes (106), cardiomyocyte apoptosis 24 hours after cardiac injury (51), and immune and stromal cell infiltration within tumor tissue (181). Notably, our previous findings identified circ-*cdrlas* to modulate phenotypic switching of macrophages to a more anti-inflammatory phenotype and overexpression of circ-*cdrlas* increased the transcription of anti-inflammatory markers in both pro- and anti-inflammatory macrophages *in vitro* (40). However, there are currently no reports on the role of circRNAs in macrophage biology and function during cardiac ischemia. Therefore, we aim to understand the role of circ-*cdrlas* in macrophage function post-cardiac injury. In this current study, we provide evidence that cardiac overexpression of circ-*cdrlas* *in vivo* and *ex vivo* overexpression of circ-*cdrlas* in fluorescently labeled bone marrow derived macrophages directly injected into the ischemic myocardium can increase anti-inflammatory macrophages in the injured myocardium, enhance angiogenesis and attenuate LV dysfunction post-MI. Mechanistically, we provide supporting evidence that circ-*cdrlas* may invokes physiological changes in macrophages in both the steady-state and in the injured heart by acting as a sponge for miRNA-7 to inhibit its function.

4.2 Methods

4.2.1 Animal Models

All animal procedures were performed following the approved protocols of the Institutional Animal Care and Use Committee (IACUC) of Temple University and conforms to the Guide for the Care and Use of the laboratory animals published by the US National Institutes of Health. Eight weeks old wild type (WT) male mice of C57BL/6

background and C57BL/6-Tg (UBC-GFP)^{30Scha/J} with a C57BL/6 background (JAX stock #004353) were procured from Jackson Research Laboratory (Bar Harbor, ME). Briefly, UBC-GFP transgenic mice express green fluorescent protein (GFP) directed by the human ubiquitin C promoter and allows *in vivo* leukocyte tracking based on distinct expression levels of GFP (214,215).

4.2.2 Myocardial Infarction Surgery

Animals are acclimated to the house environment for at least a week prior to surgery. Mice were anesthetized with 2% isoflurane and orally intubated with an intubated with a 22 G i.v. catheter, and artificially ventilated with a respirator (Harvard Apparatus). To provide analgesia, buprenorphine (0.5 mg/kg) was injected subcutaneously before the operation. A left intercostal thoracotomy was performed, and the ribs were retracted with 5-0 polypropylene sutures to open the chest. After the pericardium was opened, the left anterior descending artery (LAD) was ligated distal to the bifurcation between the LAD and diagonal branch using 8-0 polypropylene sutures through a dissecting microscope. After positive end-expiratory pressure was applied to inflate the lung fully, the chest was closed with 7-0 polypropylene sutures. A 22 G syringe was used to evacuate air from the chest cavity. The mice in the sham group underwent the same procedure except for the LAD ligation.

For the first *in vivo* study, immediately after LAD ligation, each mouse received intramyocardial injection of ~500,000 AAV2 circ-cdrlas macrophages (N=17) or AAV2 vehicle macrophages (N=17) or saline (N=17) in a total volume of 25 μ l at 5 different sites (basal anterior, mid anterior, mid lateral, apical anterior, and apical lateral).

For the second *in vivo* study, mice received 1×10^{11} vp/mL of AAV9 circ-cdr1as (N=15) or AAV9 vehicle (N=15) by tail vein injection in a total volume of 200 μ L 14 days prior to MI as previously described (216-219). Briefly, prior to injection animals were warmed for 5-10 minutes to dilate the veins by placing a heating pad under the cage. Then each mouse was placed in a restraint device and injected slowly with either AAV9 circ-cdr1as or AAV9 vehicle and the device was cleaned between each mouse. Following injection, we applied a firm compression on the injection site with a clean gauze to minimize bleeding and then returned them to their cage. The mice were then monitored until they resumed normal activity.

The survival rate of MI surgery was 83.6%. At the endpoint, body weight, heart tissue weight, and tibia length were measured and heart tissues were collected under anesthesia with Avertin® (222-Tribromoethanol; T48402; MilliporeSigma, USA). The animals were then euthanized following the procedure from our approved IACUC protocol.

4.2.3 Circ-cdr1as Expression Plasmid and AAV Construction

Our circ-cdr1as expression plasmid was generated as previously described (40). Briefly, we used pcDNA3.1 (+) Lacasse2 MCS exon vector (Addgene plasmid # 69893; <http://n2t.net/addgene:69893>; RRID:Addgene_69893) (192) with fragment insertion in *PacI* and *SacII* sites of pcDNA3.1 (+) Lacasse2 MCS exon vector.

For *in vivo* expression, the sequence was cloned into a self-complementary AAV backbone plasmid (pTRUFR) and expression of the circRNA is driven by a CMV promoter and flanked by AAV9 ITRs (*in vivo* tail vein injections) or AAV2 (*ex vivo* overexpression in macrophages). AAV9-GFP and AAV2-empty vector were used as controls. All viruses were produced using the triple transfection technique (220). In brief, HEK293 cells were

plated at 1×10^7 cells/15 cm plate one day prior to transfection and polyethyleneimine (Linear PEI, MW 25 kDa, Sigma-Aldrich) was used as the transfection reagent. For each 15 cm plate, the following reagents were added: 12 μ g XX6-80 (221), 10 μ g pXR9 (222), and 6 μ g pTRUFR WT-circ-cdr1as. These plasmids were combined in 500 μ l of DMEM without serum or antibiotics and 100 μ l of PEI reagent (1 mg/ml pH5.0) was added, mixed, and set aside for 5–10 min. Without changing the media on the 15 cm plates, the DNA-PEI reagent was added to the cells drop-wise. Cells were then harvested 48–72 h after transfection, collected by centrifugation and the cell pellets were re-suspended in water and freeze-thawed once prior to sonication (Branson Sonifier 250, VWR Scientific). DNase I (Sigma, MO) and MgCl₂ were then added before incubating at 37 °C for 60 min. The viruses were purified by Iodixanol step gradient centrifugation⁵ followed by FPLC using HiTrap Q HP anion exchange chromatography column and AKTA Pure FPLC system (GE Healthcare Life Sciences). The purified virus particles were recovered and filtered through a 0.22 μ m filter and quantified by OD 260. The viruses were aliquoted and stored at –80 °C in phosphate buffered saline (PBS) containing 5% sorbitol. AAV titers were determined by real-time PCR on plasmid genomes using the SYBR Green Master Mix (Roche).

4.2.4 Left Ventricle Heart Tissue Collection and Cardiac Cell Isolations

To isolate RNA from the LV tissue, the heart was quickly removed from the chest and perfused with phosphate buffered saline (PBS) 3x. The LV tissue was excised and minced prior to RNA extraction. Adult mouse cardiomyocytes, endothelial cells, and fibroblast were isolated as previously described (223). Once cardiomyocytes are isolated, non-myocyte supernatant fractions of LV digestion was centrifuged (300g for 5 mins), and cardiac endothelial cells were isolated by magnetic bead separation using CD31⁺ beads.

Afterwards, fibroblasts were isolated according to the previously described protocol. To obtain macrophages from the heart, the LV was excised, weighed, and minced with a fine scissor prior to digestion with collagenase type 2 (250 U/mL; Worthington LS004196), collagenase type XI (125 U/mL; Worthington LS004188), deoxyribonuclease I (60 U/mL Worthington LS002060), and hyaluronidase (60 U/mL; Worthington 101215) for 10 minutes at 37 °C. The tissue was then allowed to settle to the bottom, the supernatant was collected and passed through a 40µm mesh filter into a 50mL conical tube. Then 2 ml of stopping buffer (10% FBS in PBS) was added to the collected supernatant. The 15 mL tube with the settled tissue then went through another round of digestion. This process was repeated 4 times and then the collected supernatant was centrifuged at 50G for 5 minutes. The supernatant was then collected into another 50 mL conical tube and centrifuged at 500 g for 10 mins. The supernatant was discarded, and the pellet was resuspended in 1 mL of ACK lysis buffer (Gibco Cat# A10492-01) for 5 mins. Then, 5mL of HEPES stock solution (Gibco Cat #14170-112) was added and centrifuged for 400 g for 5 mins at 4 °C. The cells were then prepared for FACS.

4.2.5 Echocardiography

Transthoracic two-dimensional M-mode echocardiography using the Vevo 2100 equipped with 30 MHz transducers (VisualSonics, Toronto, ON, Canada) was performed before MI (baseline), and at 7, 21, and 28 days after surgery as described previously. Mice were anesthetized with a mixture of 1.5% isoflurane and oxygen (1 L/min) with an isoflurane delivery system (Viking Medical, Medford, NJ).

The internal diameter of the LV was measured in the short-axis view from M-mode recordings; percent ejection fraction (% EF) and fractional shortening (% FS) were calculated using corresponding formulas as previously described (39).

4.2.6 FACS Analysis of Cardiac Cells and Bone Marrow Derived Macrophages

After isolation of macrophages from the heart as described above, the cells were pre-incubated with 0.25 μ g of TrueStain FcX PLUS (anti-mouse CD16/32) antibody (Biolegend Cat# 156603) in 100 μ L volume for 10 minutes on ice. The cells were washed with staining buffer and incubated with F4/80 antibody at 4°C for 30 minutes then subsequently washed with staining buffer 3x and resuspended in 1 mL of staining buffer. The cells were then sorted using BD FACS ARIA II μ based on F4/80+ marker. The sorted cells were then collected for RNA extraction.

Flow cytometry was used to characterize and identify the percentage of GFP+, F4/80+, CD206+, or Ly6c+ cells in cardiac macrophages and bone marrow derived macrophages. Briefly, after isolation of macrophages from the heart as described above or harvested BMDMs, the cells counted and 1.5x10⁶ cells were collected for FACS analysis. The cells were pre-incubated with 0.25 μ g of TrueStain FcX PLUS (anti-mouse CD16/32) antibody (Biolegend Cat# 156603) in 100 μ L volume for 10 minutes on ice. The cells were washed with staining buffer and incubated with the following antibodies at 4°C for 30 minutes then subsequently washed with staining buffer 3x and resuspended in 1 mL of staining buffer. The samples were analyzed using the BD FACS Aria™ (BD Biosciences, USA). Appropriate compensation controls were used to negate spectral overlap and gating strategies were based on fluorescence minus one (FMO).

Table 4.1. Antibodies for FACS analysis

Antibody	Fluorophore	Final Concentration	Company and catalog number
F4/80	FITC	0.5 ug/100 μ L	Thermofisher 11-4801-82
GFP	FITC	1 ug/100 μ L	Biolegend 338008
CD206	APC	0.5 ug/100 μ L	Biolegend 141708
Ly6c	BV421	0.25 ug/100 μ L	Biolegend 128032

4.2.7 Tissue preparation and Immunohistochemistry

Mouse heart tissue samples were fixed in 4% paraformaldehyde (PFA) for at least 48 hours. The tissue was washed with PBS 3x and then placed in 10% sucrose for one hour, washed 3x, then placed in 20% sucrose for hour, washed 3x, and placed in 32% sucrose O/N. The tissue was then dissected and embedded with OCT in a labeled cryomold. The cryomold was frozen in liquid nitrogen then temporarily stored in dry ice and wrapped in foil for long term storage in -80°C. Cardiac tissues were cross-sectioned into 4–5 μ m-thick slides.

Masson Trichrome staining (Sigma Aldrich, USA) was performed following the manufacturer's instructions and percent of fibrotic area was determined by fibrosis area/total area using Image J software. Masson Trichrome staining images were acquired with Nikon stereomicroscope at 1X (scar quantification). For identification of new capillary network, sections were stained with CD31 and α -SMA. For identification of immune cells and anti-inflammatory macrophages, sections were heat-induced for antigen retrieval prior to immunolabeling for CD45 (immune cells), CD163, CD68, and CD206 (anti-inflammatory macrophage markers) were used. For identification of GFP⁺ cells, sections were stained with GFP antibody. To determine AAV9 GFP⁺ cardiomyocytes,

sections were stained with GFP in green and Troponin T in red. To determine cell death in cardiomyocytes, sections were stained with TUNEL in red (Roche, 12156792910) and Troponin T in green. To determine cardiomyocyte hypertrophy, sections were stained with wheat germ agglutinin (WGA). Nuclei were counter-stained with 4,6-diamidino-2-phenylindole (DAPI, 1:10,000, Sigma Aldrich, St Louis, MO). Images were acquired using 4X, 10X, 20X, and 40X using EVOS 7000 (Thermo Fisher Scientific). Quantitative image analysis was performed with NIH ImageJ by scoring random multiple imaging fields.

Table 4.2. Primary antibodies for Immunohistochemistry

1° Antibody	Host Species	Company and catalog number
CD45 (1:200)	Goat	R&D Systems AF114
CD163 (1:30)	Rabbit	Abcam AB182422
CD206 (1:50)	Goat	R&D systems AF2535
CD68 (1:50)	Rabbit	Rockland 600-401-R10
GFP (1:100)	Chicken	Invitrogen A10262
CD31 (1:30)	Goat	R&D systems AF3628
Anti-Actin, α-Smooth Muscle - Cy3™ antibody (1:1000)	Mouse	Sigma C6198
Troponin T (1:200)	Mouse	Invitrogen MA5-12960
Wheat Germ Agglutinin, Alexa Fluor™ 488 Conjugate (1:250)		Thermofisher W11261

Table 4.3. Secondary antibodies for Immunohistochemistry

2° Antibody	Conjugate	Company and catalog number
Donkey anti-rabbit (1:100)	Alexa Fluor 488	ThermoFisher A21206
Donkey anti-mouse (1:100)	Alexa Fluor 488/555	ThermoFisher A21202/ A31570
Donkey anti-goat (1:1000)	Alexa Fluor 488/555	ThermoFisher A11055/ A21432
Goat anti-chicken (1:100)	Alexa Fluor 488	ThermoFisher A11039

4.2.8 Cell Culture and in vitro Studies

Bone marrow (BM) monocytes were isolated from bone marrow mononuclear cells of C57BL/6 male (approximately 8–10-week-old) mice by density-gradient centrifugation with histopaque-1083 (Sigma) and red blood cells were removed with NH₄Cl (Stemcell Technologies Cat #07800) as previously described (40,224). The monocyte population was cultured in RPMI 1640 1× (Gibco) with 20% FBS, 1% penicillin-streptomycin solution, and 20% of L929-conditioned medium. The media was changed the day after culture, on day 3, and on day 5–7. By day 5–7, high purity of macrophages can be observed as previously noted (190). On day 5–7, change to fresh stimulation media: for pro-inflammatory activation (17), 100 ng/mL IFN γ (R&D systems Cat# 485-MI-100) and 100 ng/mL TNF α (PromoKine Cat# D-63720); for anti-inflammatory activation (203), 10 ng/mL IL-4 (R&D systems Cat# 404-ML-010), 10 ng/mL IL-10 (R&D systems Cat# 217-IL-005), and 20 ng/mL TGF- β (R&D systems Cat#7666-MB-005) for a period of 24 h as previously described (40). The Raw 264.7 monocytes were cultured in DMEM-F12 medium (Corning, USA) with 10% fetal bovine serum (FBS) and 1% penicillin-streptomycin solution. Raw 264.7 cells were activated with 100 ng/mL of LPS for 24 hours. BMDMs or RAW 264.7 cells were transfected for 24 hours with 100nM miRNA mimic miR-7b-3p (mirVana mRNA mimic cgr mir-7b Assay ID MC26348, Thermofisher Cat # 4464066) or anti-miR-7b-3p (mmu-miR-7b-5p miR-inhibitor Assay ID: MH26348, Thermofisher Cat #4464084) or corresponding controls (mirVana™ miRNA Inhibitor, Negative Control #1, Thermofisher Cat # 4464076; mirVana™ miRNA Mimic, Negative Control #1, Thermofisher Cat # 4464058). Lipofectamine RNAiMAX (Thermofisher Cat # 13778075) was used to facilitate transfection. The cells were transfected prior to

polarization for 24 hours. For knockdown of circ-cdr1as, BMDMs were transfected with MOI 15 lentiviral shRNA (titer concentration for shRNA scrambled: 2.9×10^9 ; shRNA circ-cdr1as: 3.67×10^9 vp/mL) as previously described (40). Briefly, the cells were transfected with lentivirus shRNA and viral enhancer (ABM Cat# G515) for 48 h. The media was then changed to media containing 3 μ g/mL of puromycin antibiotic for selection of stably transfected cells. The cells were polarized for 24 h. Cells were harvested and changes in the expression or transcription of macrophage markers were measured by FACS or RT-qPCR, respectively.

4.2.9 Ex vivo Overexpression of circ-cdr1as in BMDMs

BMDMs were transfected with 500 MOI of AAV2 circ-cdr1as (titer concentration for AAV2 vehicle and AAV2 circ-cdr1as is 4×10^9 vp/mL). The cells were transfected with AAV2 and viral enhancer (VirallentryTM transduction enhancer ABM Cat # G515). The following day, the media was changed to media containing 3 μ g/mL of G418 antibiotic for selection of stably transfected cells. Cells were harvested and circ-cdr1as overexpression was verified by RT-qPCR.

4.2.10 Pull Down Assay

Circ-cdr1as was captured using magnetic instant capture beads with circ-cdr1as single probe covalently attached to the surface of nanomagnetic particles designed by ElementZero Biolabs to target only the backsplicing junction. This allows the RNA affinity purification with magnetic instant capture beads for the capture of RNA-miRNA or RNA-protein complexes from chemically cross-linked material. The following protocol was used according to manufacturer instructions. MagIC-beads-RNA-enrichment-protocol-proteome-capture (elementzero.bio).

4.2.11 RNaseR Treatment, Reverse transcription, and RT-qPCR

Total RNA was isolated from cells using miRNeasy Mini Kit (Qiagen). NanoDrop-1000 (Thermo Scientific, USA) was used to identify RNA concentration and purity determined by the 260 A/280 A ratio. For RNase R treatment, 500 ng was incubated 30 mins at 37°C with or without 2.5 U of Rnase R (Epicentre Technologies Cat# RNR07250). High-capacity cDNA Reverse Transcription Kit (Applied Biosystems, 4368814) was used to obtain cDNA and quantitative PCR (qPCR) was performed on StepOnePLUS Real-Time PCR system (Applied Biosystems 7000 apparatus) using the Fast SYBR™ Green Master Mix (Applied ThermoFisher, USA) according to the manufacturer's instructions. To quantify expression of circRNA transcripts, divergent primers were designed to amplify across the backsplicing junction. To quantify linear transcripts, convergent primers were designed to amplify exonic sequences that are not present in the circular RNA. Expression was quantified using fold change of $2^{e(\text{delta ct})}$ compared to control, normalized to 18S rRNA used as a reference gene.

For detection of miRNAs, TaqMan™ Advanced miRNA cDNA Synthesis Kit was used (Thermofisher Cat # A28007). Quantitative PCR (qPCR) was performed on StepOnePLUS Real-Time PCR system (Applied Biosystems 7000 apparatus) using the TaqMan™ Fast Advanced Master Mix for qPCR (Thermofisher Cat # 4444557) according to the manufacturer's instructions. To detect miR-7b-3p expression primer mmu-miR-7b-5p (Thermofisher Cat # A25576) was used and expression was quantified using fold change of $2^{e(\text{delta ct})}$ compared to control, normalized to miR-24-3p (Assay ID 477992_mir, Thermofisher Cat # A25576) used as a reference gene.

4.2.12 Statistical Analysis

Data are expressed as mean \pm standard error of the mean (S.E.M.) represent at least 3 independent biological experiments. Data visualization and statistical analyses were performed using GraphPad Prism 10.0 software (GraphPad, La Jolla, CA). Mean of the groups were compared using unpaired two tail t-test (for two groups) and One-way ANOVA (more than two groups) with Tukey's multiple comparisons test. P values of <0.05 indicate statistical significance.

4.3 Results

4.3.1 Circular RNA *cdrlas* is Downregulated in Post-MI Hearts

We previously profiled circRNAs expression in bone marrow-derived macrophages polarized to pro-inflammatory or anti-inflammatory phenotype. Through Ingenuity Pathway Analysis, we identified circular RNAs involved in gene interaction networks associated with cardiovascular system involvement and cardiac fibrosis (40). We compared circRNAs found in BMDMs circRNAs profiling data set with the circRNAs profiling dataset of cardiac tissue 3 days post-MI hearts we published before (39). We identified circ-*cdrlas* as a circular RNA differentially expressed in both BMDMs and MI hearts. Therefore, we investigated circ-*cdrlas* expression at different time points post-MI. Circ-*cdrlas* was significantly downregulated at 3-5 days post-MI, the time during which pro-inflammatory macrophages are most prominent, and upregulation starting at 7 days to 28 days post-MI, the time in which inflammation subsides (Figure 4.1A). We then identified circ-*cdrlas* expression in different cardiac cell types in the left ventricular tissue. Circ-*cdrlas* expression was significantly downregulated in the left ventricular tissue at 3 days post-MI, macrophages (F4/80+ sorted cells), and cardiomyocytes.

However, circ-cdr1as expression was not affected in endothelial cells (CD31+ cells) or fibroblast (Figure 4.1B). These results suggest cell-specific downregulation of circ-cdr1as after MI, particularly in macrophages and cardiomyocytes.

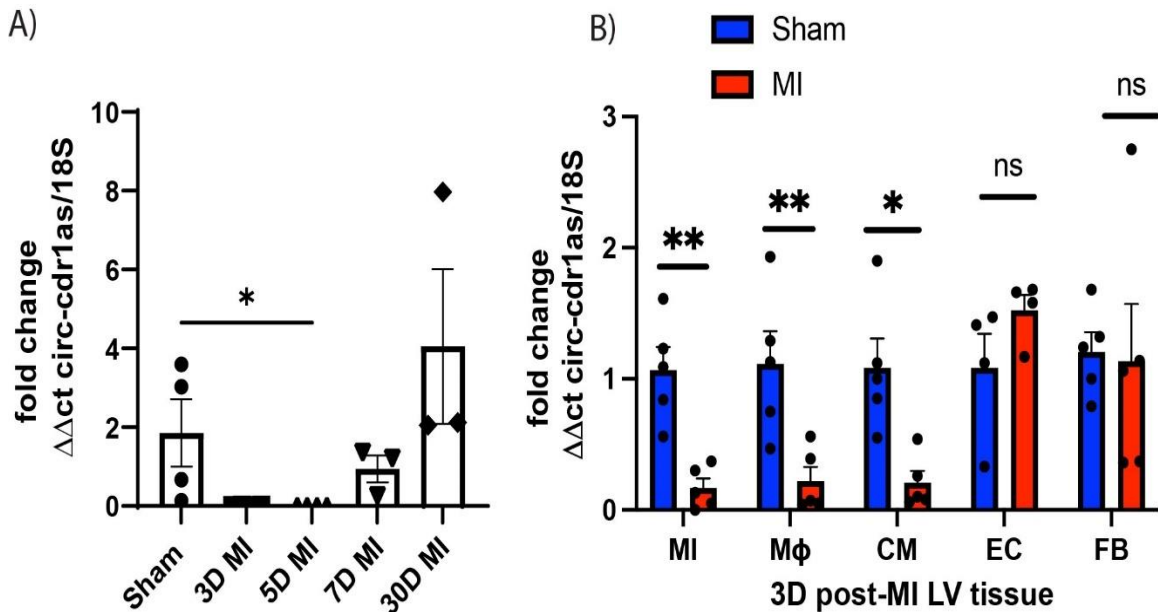


Figure 4.1. Circular RNA cdr1as expression in sham and MI hearts. (A) qRT-qPCR of circ-cdr1as expression at different time points in post-MI hearts compared to sham, normalized to 18S. N=3-4/group. (One-way ANOVA). (B) qRT-PCR analysis of circ-cdr1as expression in 3D post-MI left ventricular (LV) tissue including isolated macrophages (M Φ) (Aria sorted for F4/80+ cells), cardiomyocytes (CM), endothelial cells (EC) (CD31+ cells), and fibroblast (FB) cells isolated from 3D post-MI tissue compared to sham controls, normalized to 18S. (Two-sided unpaired t-test). N=4=5/group. Data are mean \pm SEM. NS, non-significant, *p<0.05, ** p<0.01. M Φ , macrophages; CM, cardiomyocytes; EC, endothelial cells; FB, fibroblast.

4.3.2 *Ex Vivo* Overexpression of circ-cdr1as in Bone Marrow Derived Macrophages Retain their M2 Macrophage Phenotype when Injected in Post-MI Hearts

We utilized C57BL/6-Tg (UBC-GFP)30Scha/J with a C57BL/6 background to isolate GFP+ BMDMs to track macrophages in the myocardium after injection. The isolated macrophages were infected with AAV2 control and AAV2 circ-cdr1as vector and 5×10^5 cells were injected in the MI border zone immediately after the induction of MI.

Macrophages polarized to M2 phenotype were used as additional control. We performed FACS analysis of the percentage of GFP⁺ cells in mice 5 days post-MI (Figure 4.2A, B). The percent of GFP⁺ cells between AAV2 vehicle MΦ, anti-inflammatory M2 MΦ, and AAV2 circ-cdr1as MΦ were similar (Figure 4.2B). We further investigated the percentage of GFP/CD206⁺ cells and GFP⁺CD206⁺ cells/gram of tissue in the border zone/infarcted region of these groups and found that anti-inflammatory M2 MΦ and AAV2 circ-cdr1as MΦ had a significant percentage of cells that were GFP/CD206⁺ (Figure 4.2C). We then examined the ratio of Ly6c⁺ (pro-inflammatory macrophage marker) or CD206⁺ (anti-inflammatory macrophage marker) cells. Anti-inflammatory M2 MΦ and AAV2 circ-cdr1as MΦ groups had the highest percentage of CD206⁺ cells compared to Ly6c⁺ cells (Figure 4.2D). We then validated our FACS analysis with immunohistochemistry staining for GFP and CD206 at 5 days post-MI. Anti-inflammatory M2 MΦ and AAV2 circ-cdr1as MΦ groups had the highest GFP/CD206⁺ cells. Additionally, we also stained with CD45 (leukocyte marker) and CD163 (anti-inflammatory macrophage marker) and found an increase in CD163⁺ cells in M2 MΦ and AAV2 circ-cdr1as MΦ groups compared to saline and AAV2 vehicle MΦ groups (Figure 4.2D, F). Taken together, these results demonstrate that either injection of anti-inflammatory MΦs or AAV2 circ-cdr1as MΦs directly into the injured heart promotes more anti-inflammatory macrophages and that these cells can maintain an M2-like phenotype in the initial stages of cardiac injury, during which inflammation is high.

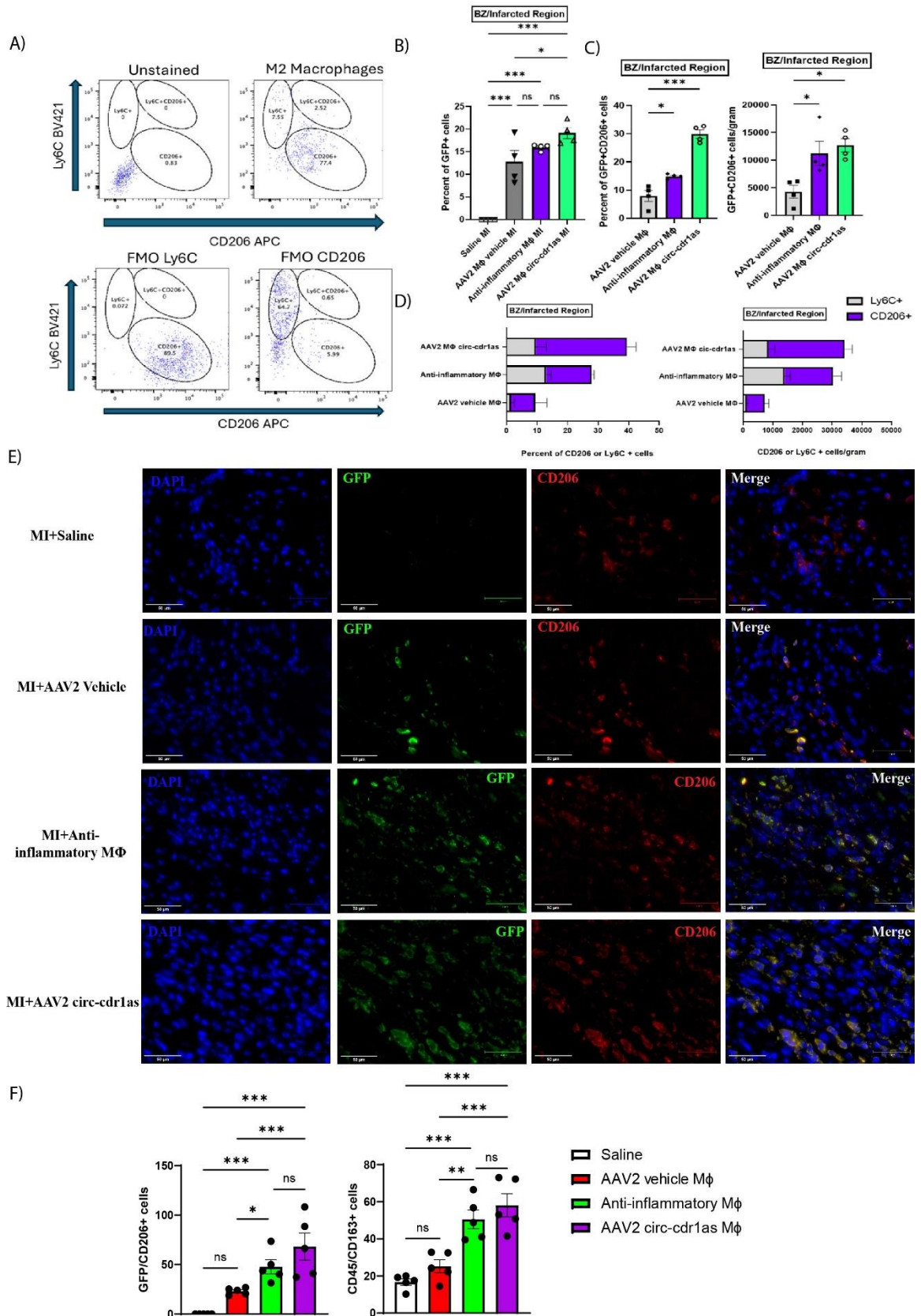


Figure 4.2. GFP+ circ-cdr1as overexpressing macrophages retain M2-like phenotype in ischemic heart. (A) FACS gating strategies for Ly6c (M1 marker) and CD206 (M2) marker with fluorescent minus one (FMOs) controls. (B) FACS analysis of %GFP+ cells in the LV MI region at 5D post-MI of all groups. (C) FACS analysis of %GFP/CD206+ cells in the LV MI region at 5D post-MI of all groups (left) and normalized cells/gram (right) for all groups. (D) FACS analysis of the percentage of CD206 or Ly6C cells found within the LV MI region 5D post-MI (left) and normalized cells/gram (right) for all groups. (E) Representative photomicrographs (50 μ m) of GFP (green) and CD206 (red) positive cells and nuclei DAPI (blue)/40X. (F) Quantification of GFP/CD206+ cells and CD45/CD163+ cells. Data are mean \pm SEM. N=5/group. NS, non-significant, *p<0.05, ** p<0.01, *** p<0.001. GFP, green-fluorescent protein; Ly6C, M1 macrophage marker; CD206, M2 macrophage marker; CD45, leukocyte marker; CD163, M2 macrophage marker

4.3.3 Injection of circ-cdr1as Overexpressing BMDMs into the Ischemic Myocardium Improved LV Function and Reduced Infarct Size.

Reduced levels of circ-cdr1as in the LV 3 days post-MI, in macrophages, and in cardiomyocytes suggested a possible physiological role for circ-cdr1as in MI pathophysiology. Therefore, we tested if exogenous delivery of circ-cdr1as overexpressing or anti-inflammatory macrophages at early stage of cardiac injury could promote an anti-inflammatory response and thereby, attenuate LV remodeling and dysfunction post-MI. 5x10⁵ AAV2 vehicle or AAV2 circ-cdr1as macrophages were injected intramyocardially in the border/infarct zone immediately post-left anterior descending artery (LAD) ligation. We then determined the effect of cell therapy on LV function by echocardiography at 7, 21-, and 28-days post-MI. Percent ejection fraction (EF) and fractional shortening (FS) at baseline and 7 days were similar in all groups. However, both circ-cdr1as overexpressing or anti-inflammatory macrophages significantly improved %EF and %FS at 21- and 28-days post-MI compared to saline and AAV2 M Φ vehicle (Figure 4.3A). Analysis of the LV end diastolic or systolic diameter indicated significant improvement with either circ-cdr1as overexpressing or anti-inflammatory macrophages treatments (Figure 4.3A). We next assessed infarct size by Masson's trichrome staining at 28 days post-MI in mice and found

a significant decrease in infarct size compared to AAV2 vehicle and saline groups (Figure 4.3B). In order to determine the effect of circ-cdr1as macrophages or anti-inflammatory macrophages on myocardial neovascularization, we stained sections with CD31 and α -SMA. We found increased capillary density and α -SMA+ arterioles in the border zone/infarcted area at 28 weeks post-MI in mice that received either circ-cdr1as macrophages or anti-inflammatory macrophages compared to mice that received AAV2 vehicle macrophages or saline (Figure 4.3C).

4.3.4 Administration of AAV9 circ-cdr1as by Tail Vein Injection Enhanced Cardiac circ-cdr1as Expression After Injury.

Upon examining circ-cdr1as expression at different time points and identifying a downregulation in expression in both macrophages and cardiomyocytes 3 days post MI, we examined if cardiac overexpression of circ-cdr1as would improve cardiac function and remodeling. We utilized AAV9 vector, which has a higher tropism for cardiomyocytes, to deliver circ-cdr1as by intravenous injection. We injected 1×10^{11} vp/mL by tail vein and examined the expression of circ-cdr1as in the LV tissue 14 days after tail vein injection and found a significant increase in the cardiac expression of circ-cdr1as. We then verified increased circ-cdr1as expression at 5- and 28-days post-MI by RT-qPCR (Figure 4.4A). Although AAV9 has a higher tropism for cardiomyocytes and highest expression of circ-cdr1as was found in the cardiomyocytes, since circ-cdr1as expression is driven by a CMV promoter, we also observed increased expression of circ-cdr1as in macrophages, endothelial cells, and fibroblast at 5 days post-MI, although to a lesser extent than cardiomyocytes (Figure 4.4B). We further validated cardiomyocyte tropism of AAV9 by intravenous injections of control AAV9-GFP vector and verifying the expression of GFP in cardiomyocytes by immunohistochemistry (Figure 4.4C).

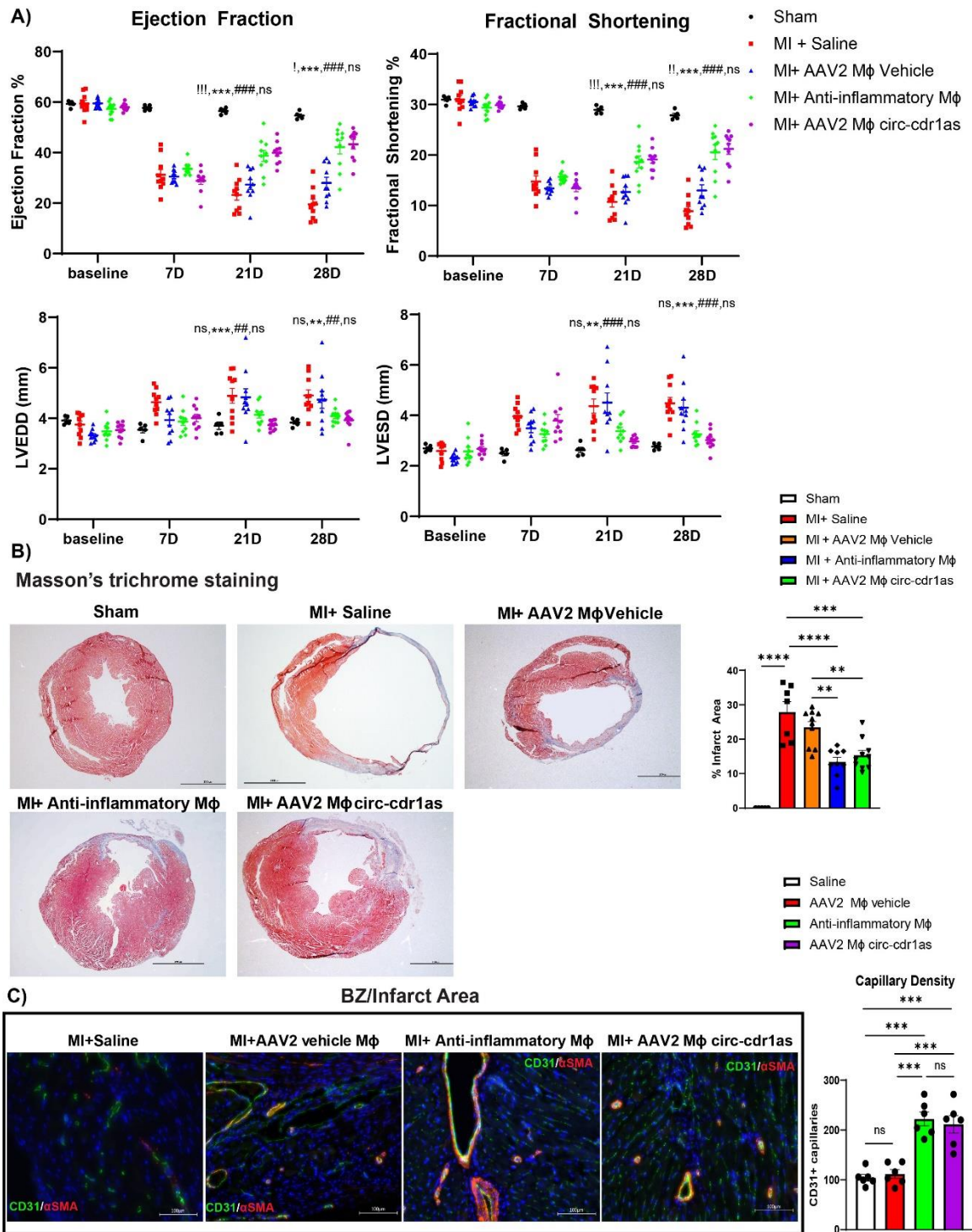


Figure 4.3. Circ-cdr1as overexpressing macrophages injected into the myocardium improved cardiac function and reduced infarct size 28 days post-MI in mice. (A) GFP+ circ-cdr1as overexpressing macrophages improved LV function (% ejection fraction, % fractional shortening, LVEDD (mm), and LVESD (mm)) measured by echocardiography. (!: sham vs AAV2 circ-cdr1as MΦ; *: MI+ Saline vs AAV2 circ-cdr1as MΦ; # AAV2 MΦ vehicle vs AAV2 circ-cdr1as MΦ) N= 5 (sham), N= 10 (all other groups) (B)

Representative Masson's Trichrome stained heart sections in sham, saline, AAV2 MΦ vehicle, anti-inflammatory MΦ, and AAV2 circ-cdr1as MΦ at 28 days post-MI. Quantification of infarct size at 28D days post-MI in each group. N=sham, N=7-10 (all other groups). (C) Representative images of capillary density in the border zone/infarcted area of the left ventricle at 28D post-MI. Capillaries were stained with CD31+ (green), arterioles stained with α SMA (red), and nuclei were stained with DAPI (blue). Capillary density was quantified as the number of CD31+ capillaries/20X. N=6/group. One-way ANOVA. Data are mean \pm SEM. NS, non-significant, * p <0.05, ** p <0.01, *** p <0.001.

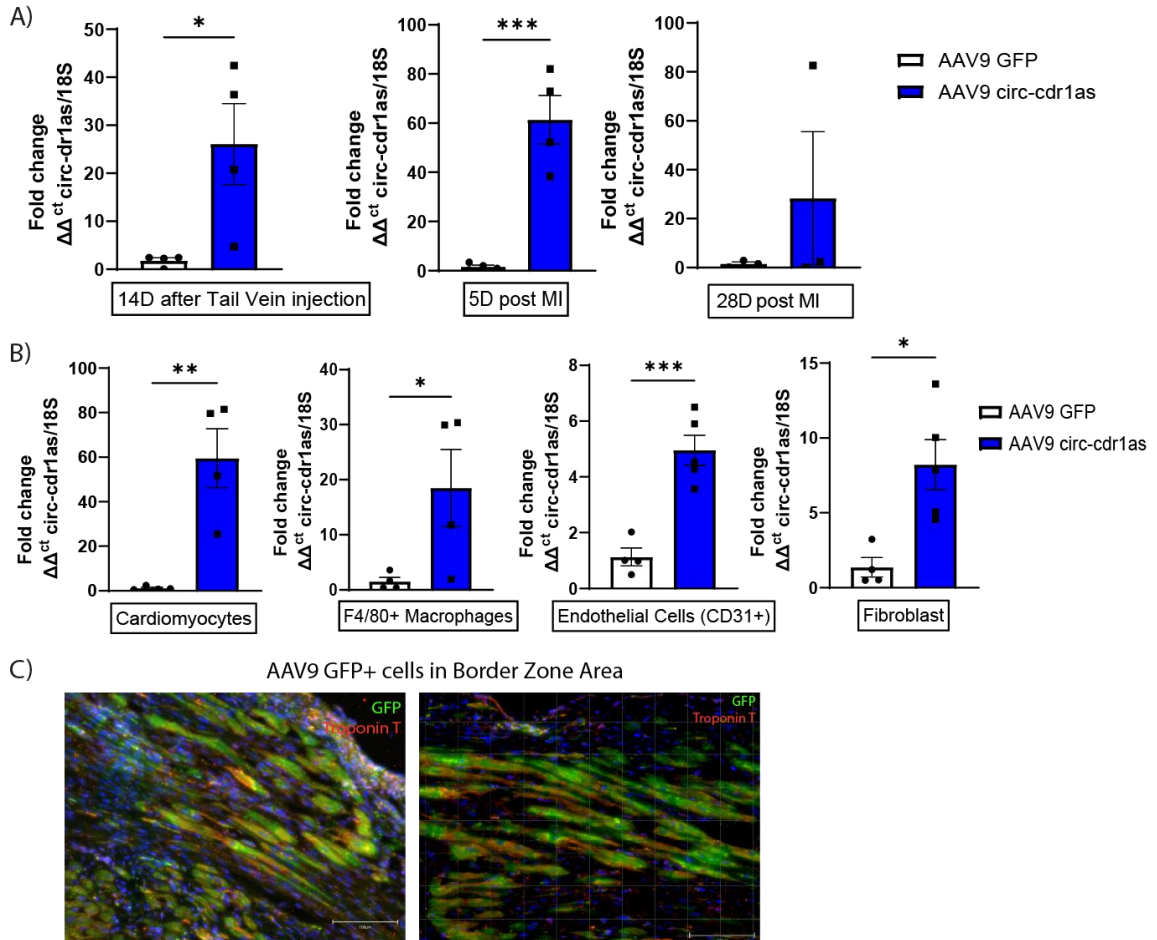


Figure 4.4. Validation of circ-cdr1as overexpression in the heart after tail vein injection. (A) qRT-PCR analysis of circ-cdr1as expression in AAV9 -GFP or AAV9 circ-cdr1as treated mice 14 days after tail vein injection and 5 days and 28 days after myocardial infarction, normalized to 18S. N=3-4/group. (B) qRT-qPCR analysis of circ-cdr1as expression in cardiac cells, cardiomyocytes, macrophages (Aria sorted F4/80+ cells), endothelial cells (CD31+), and fibroblast, isolated from LV-tissue 5 days post MI from AAV9-GFP or AAV9 circ-cdr1as treated mice, normalized to 18S. N= 4-5/group. Unpaired t-test. Data are mean \pm SEM. NS, non-significant, * p <0.05, ** p <0.01, *** p <0.001. (C) Representative images of GFP (green)/Troponin T (red) positive cells in border zone area in mice treated with AAV9-GFP.

4.3.5 Administration of AAV9 circ-cdr1as Attenuates LV Dysfunction and Reduces Infarct Size Post-MI.

Administration of AAV9 circ-cdr1as significantly improved cardiac LV functions examined by echocardiography. The percent EF and FS were similar at baseline for AAV9-GFP and AAV9 circ-cdr1as groups. There was a significant improvement in %EF and %FS for the AAV9 circ-cdr1as group at 21- and 28-days post-MI compared to the AAV9 vehicle group. Additionally, the LV end diastolic and systolic diameters indicated significant restoration of LV dimension at 28 days with AAV9 circ-cdr1as treatment (Figure 4.5A). We next examined the percentage of infarcted area between these groups by Masson's trichrome staining at 28 days post-MI and found a significant reduction in the infarcted area compared to the AAV9-GFP group (Figure 4.5B). We also found a significant increase in myocardial neovascularization reflected by increased capillary density and α -SMA+ arterioles in the border zone and infarcted areas at 28 days post-MI in mice treated with AAV9 circ-cdr1as compared to AAV9-GFP (Figure 4.5C). To determine if cardiomyocyte size (cardiomyocyte hypertrophy) was affected by AAV9 circ-cdr1as treatment at 28 days post-MI, we stained with WGA and quantified the area/cell. We found no significant change in cardiomyocyte size in mice treated with AAV9 circ-cdr1as or AAV9-GFP (Figure 4.5D).

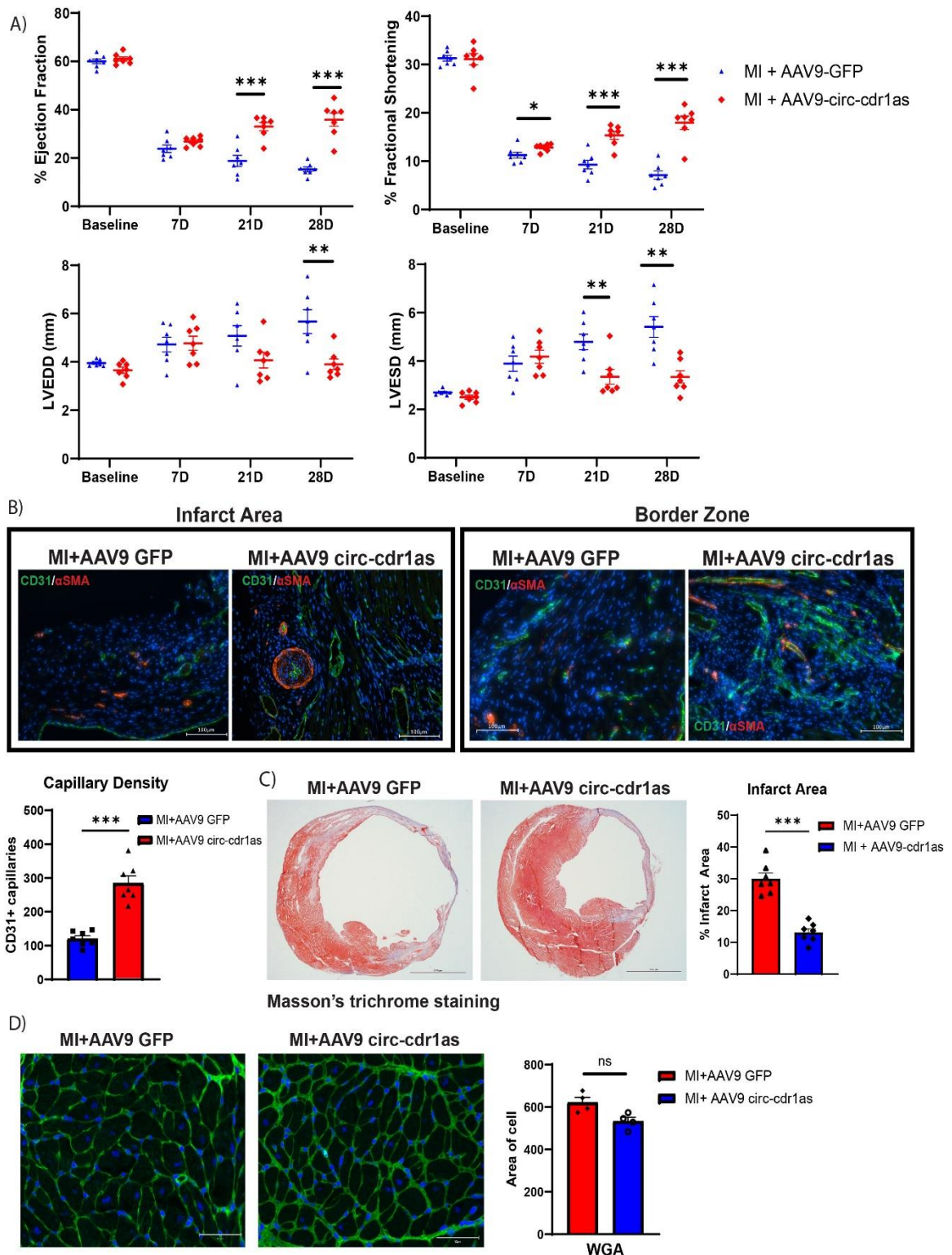


Figure 4.5. AAV9 circ-cdr1as tail vein injection improves cardiac function and reduces infarcted area in mice. (A) AAV9 circ-cdr1as significantly improved heart function (% ejection fraction, % fractional shortening, LVEDD (mm), and LVESD (mm)) measured by echocardiography compared to AAV9-GFP. N=7/group. (B) Representative images

(100 μ m) of capillary density measured in infarcted area and border zone area at 28 days post MI. Capillaries were stained with CD31 (green), arterioles stained with α SMA (red), and nuclei with DAPI (blue). Capillaries were quantified as the number of CD31+ cells/20X. N=7/group. (C) Representative images of Masson's Trichrome stained heart sections in AAV9 vehicle and AAV9 circ-cdr1as groups at 28 days post-MI and quantitative analysis of infarct size. N=7/group. (D) Representative images of WGA (50 μ m) staining indicating cardiomyocyte hypertrophy and quantification of the area/cell 40X. N=4/group. Unpaired t-test. Data are mean \pm SEM. NS, non-significant, *p<0.05, ** p<0.01, *** p<0.001.

4.3.6 Cardiac Overexpression of circ-cdr1as Reduces Cardiomyocyte Apoptosis and Increases Anti-Inflammatory Macrophages 5 days Post-MI

Anti-inflammatory macrophages exhibit a pro-regenerative phenotype and secrete high levels of anti-inflammatory cytokines including IL-10 and growth factors such as vascular endothelial growth factor VEGF and myeloid-derived growth factor known to be cardioprotective (17,19). Therefore, we assessed the role of circ-cdr1as on apoptosis of cardiomyocytes 5 days post-MI by TUNEL assay. We found a decrease in the percentage of cardiomyocyte apoptosis in mice treated with AAV9 circ-cdr1as compared to AAV9-GFP vehicle (Figure 4.6A). Interestingly, we found that treatment with AAV9 circ-cdr1as increased the number of anti-inflammatory macrophages present at the site of injury, indicated by increase in CD163 and CD206 positive cells 5 days post-MI (Figure 4.6B, C). We further validated these results by FACS analysis investigating the percentage of pro-(Ly6c) or anti-inflammatory (CD206) macrophages. We found that AAV9 circ-cdr1as treatment increased the ratio of CD206+ cells in the LV tissue compared to AAV9 vehicle at 5 days post-MI (Figure 4.6D).

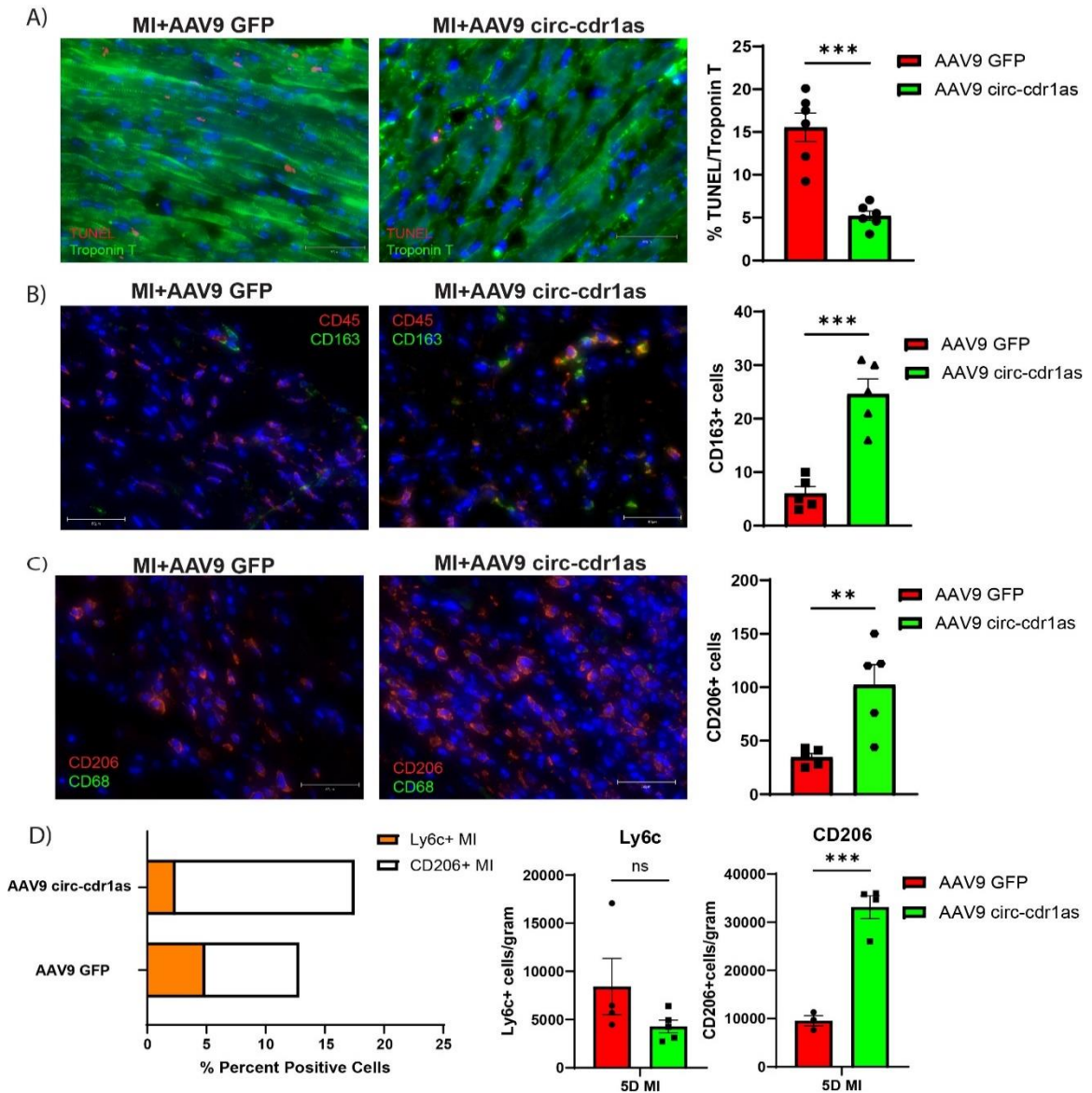


Figure 4.6. Cardiac overexpression of circ-cdr1as reduces cardiomyocyte cell death enhances anti-inflammatory macrophages 5 days post-MI. (A) Representative photomicrographs (50 μ m) of TUNEL (red)/Troponin T (green)staining in AAV9-GFP and AAV9 -circ-cdr1as treated mice and quantification of TUNEL/Troponin T + cells represented as the percent of TUNEL/Troponin T + cells and DAPI-stained nuclei/40X. N=6/group. (B) Representative photomicrographs (50 μ m) of CD163 (green) and CD45 (red) positive cells and quantification of CD163+ cells/40X. N=5/group (C) Representative photomicrographs (50 μ m) of CD68 (green) and CD206 (red) positive cells and quantification of CD206+ cells/40X. N=5/group. (D) FACS analysis of Ly6c+ (M1 M Φ marker) and CD206 (M2 M Φ marker) cells isolated from LV tissue 5 days post-MI and normalized cells/gram (right) for all groups. N=3-5/group. NS, non-significant, NS, non-significant, *p<0.05, ** p<0.01, *** p<0.001. GFP, green-fluorescent protein; Ly6C, M1 macrophage marker; CD206, M2 macrophage marker; CD45, leukocyte marker; CD163, M2 macrophage marker.

4.3.7 Circular RNA *cdrlas* Modulates miR-7 Expression in Injured Hearts and BMDMs

Published literature including *in silico* analysis in our most recent paper identified miRNA-7 as a circ-*cdrlas* target based on Arraystar's miRNA target prediction software utilizing TargetScan and miRanda (40,51,106,181,200,202,210). Circ-*cdrlas* is suggested to act as miR-7 sponge. Therefore, we investigated the expression of miR-7b-3p in the LV tissue, cardiomyocytes, and macrophages at 3 days post-MI. We identified a significant upregulation of miR-7b-3p in the LV tissue and cardiomyocytes (Figure 4.7A). Based on these results, we performed a pull-down assay with probes specifically designed to target the circ-*cdrlas* backsplicing junction covalently attached to the surface of magnetic particles. Using RAW264.7 macrophage cells polarized to pro- or anti-inflammatory phenotype, circ-*cdrlas* pulldown assays confirmed direct binding to miRNA-7b-3p (Figure 4.7B). To determine if miR-7b-3p plays a role in BMDM polarization, we treated BMDMs with antagonist of miR-7 or miR-7 mimic or their respective controls (Figure 4.7C). FACS analysis demonstrated that treatment of miR-7 mimics increased percentage of pro-inflammatory marker CD86 and reduction in anti-inflammatory marker CD206 in naïve, pro-, or anti-inflammatory macrophages (Figure 4.7 D, E). Meanwhile treatment with anti-miR-7 had the opposite effect (Figure 4.7 D, E). Transcriptional levels of anti-inflammatory lineage markers (Arg-1 and CD206) were upregulated, and transcriptional levels of pro-inflammatory markers (Ly6C and INOS) were downregulated in BMDMs treated with anti-miR-7. Meanwhile, treatment with miR-7 indicated the opposite effect (Figure 4.7F). These findings suggest that circ-*cdrlas* plays a role in regulating miR-7 that results in changes to polarization of macrophage phenotype.

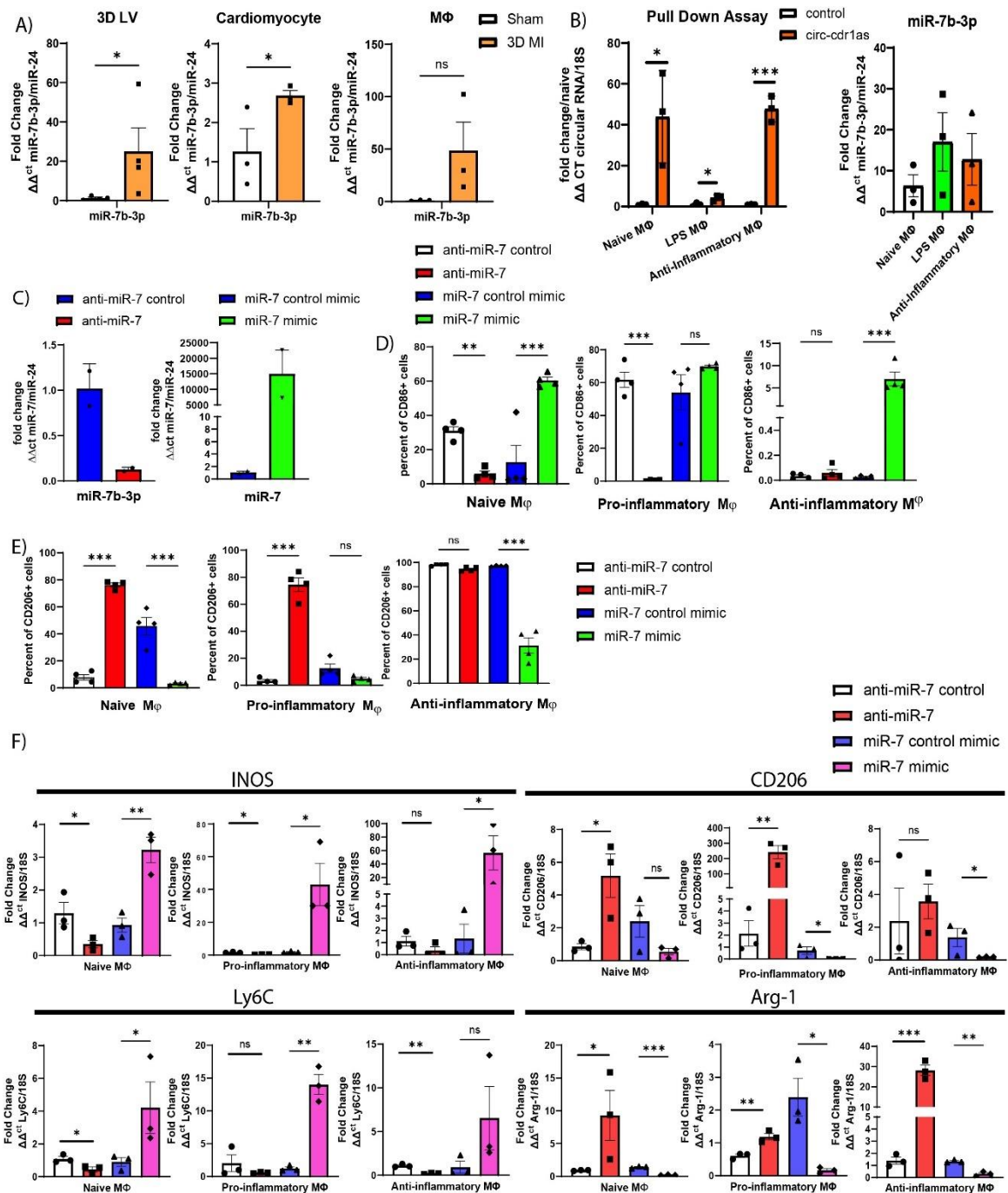


Figure 4.7. Reciprocal relationship between miR-7 and circ-cdr1as in injured hearts and macrophages. (A) qRT-qPCR of miR-7b-3p expression in 3D post-MI left ventricular (LV) tissue including isolated macrophages (MΦ) (Aria sorted for F4/80+ cells), cardiomyocytes (CM) compared to sham controls, normalized to miR-24. (Two-sided unpaired t-test). N=3-4/group. (B) Level of circ-cdr1as after pull-down and miR-7b-3p assessed by RT-qPCR in RAW 264.7 cells unpolarized or polarized with LPS or anti-inflammatory cytokines. (Two-sided unpaired t-test). N= 3/group. (C) Validation of miR-7b-3p expression or inhibition by miR mimic or anti-miR, respectively. N=2. FACS analysis of (D) F4/80/CD86 + cells

(pro-inflammatory MΦ marker) or (E) F4/80/CD206+ cells (anti-inflammatory MΦ marker) in naïve, pro-inflammatory, and anti-inflammatory macrophages treated with miR-7 mimic or anti-miR and their respective controls. N= 4/group (One way ANOVA) (F) qRT-qPCR analysis of transcriptional changes of macrophage markers in naïve, pro-inflammatory, and anti-inflammatory macrophages treated with miR-7 mimic or anti-miR and their respective controls, normalized to 18S. N=3/group. (Unpaired t-test) Data are mean ± SEM. NS, non-significant, *p<0.05, ** p<0.01, *** p<0.001. MΦ, macrophages; CM, cardiomyocytes; pro-inflammatory markers: Ly6C, lymphocyte antigen 6 family member C1; INOS, inducible nitric oxide synthase; anti-inflammatory markers: CD206; Arg-1, arginase 1.

4.3.8 MicroRNA-7 target KLF4 is Upregulated in BMDMs Treated with Anti-miR-7

Recent evidence has shown that a target of miRNA-7 is Krüppel-like factor 4 (KLF4), and miR-7 deficiency plays a role in macrophage phenotype in an acute lung injury model. KLF4 is associated with inflammatory responses and was indicated to be upregulated when miR-7 was inhibited (225). Thus, to explore the possible connection between miR-7 and KLF4 in macrophages, we assessed the comparative expression levels of KLF4 in the heart three days after myocardial infarction, in BMDMs subjected to circ-cdr1as or shRNA circ-cdr1as treatment, and in BMDMs treated with anti-miR-7 or miR-7 mimic. We observed downregulation of KLF4 that we also observed with circ-cdr1as in LV tissue 3 days post-MI (Figure 4.8A). Naïve, pro-, and anti-inflammatory macrophages had an upregulation of KLF4 expression when BDMDs were overexpressed with circ-cdr1as and a downregulation when circ-cdr1as was knocked down (Figure 4.8B). We saw the opposite relationship with miR-7 and KLF4. KLF4 expression was upregulated in Naïve, pro-, and anti-inflammatory macrophages when miR-7 was inhibited and a downregulation when BMDMs were treated with miR-7 mimic (Figure 4.8C). Collectively, our data indicates that circ-cdr1as modulates miR-7 to prevent interaction with KLF4 to alter macrophage phenotype.

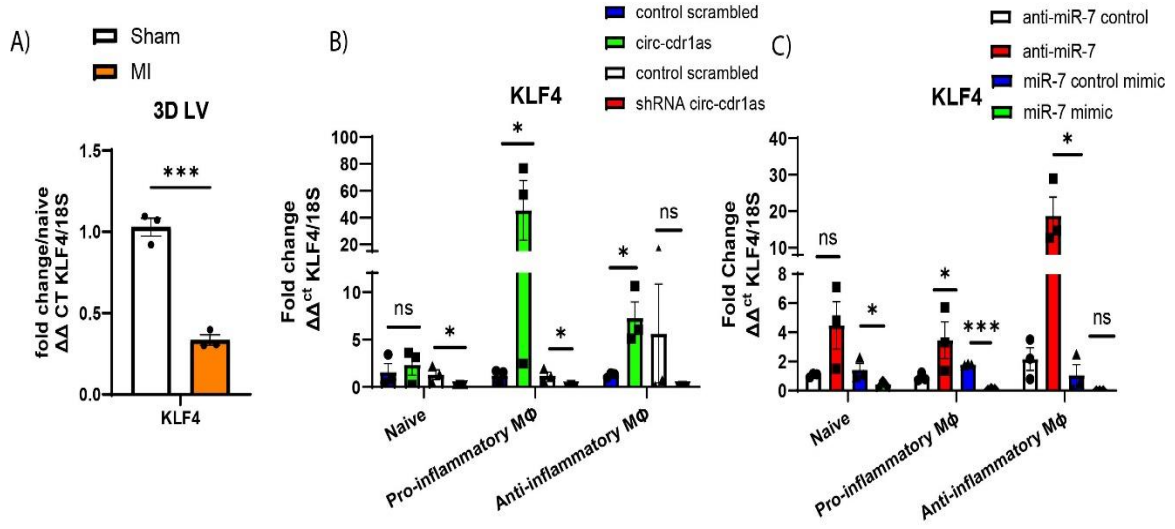


Figure 4.8. Changes in expression of miR-7b-3p target KLF4 in the heart 3D post-MI and in BMDMs. (A) qRT-qPCR of KLF4 expression in 3D post-MI left ventricular (LV) tissue compared to sham, normalized to 18S. N= 3/group. (Unpaired T-test) (B) Changes in KLF4 expression in naïve, pro-inflammatory, and anti-inflammatory macrophages overexpressing circ-cdr1as cells or in cells with knockdown of circ-cdr1as, normalized to 18S. N= 3/group. (One-way ANOVA) (C) Changes in KLF4 expression in naïve, pro-inflammatory, and anti-inflammatory macrophages treated with miR-7 mimic or anti-miR-7, normalized to miR-24. N= 3/group. (One-way ANOVA) Data are mean \pm SEM. NS, non-significant, * $p < 0.05$, ** $p < 0.01$, *** $p < 0.001$.

4.4 Discussion

Macrophages are key cellular elements of chronic inflammatory responses associated with cardiovascular disease and cancer (4,11,186,226). Blood derived and tissue resident macrophages exhibit both a pro-inflammatory (M1) and anti-inflammatory (M2) phenotypes, essential for removing injured tissue and facilitating repair. Sustained activation of pro-inflammatory macrophages increases adverse remodeling of cardiac tissue that ultimately leads to deterioration of cardiac function and heart failure (9-11). However, the molecular mechanism underlying functional polarization of macrophages into M1 or M2 phenotypes has yet to be fully understood.

Increasing studies have demonstrated that ncRNAs involvement in modulating macrophage polarization. Most studies have focused on the role of miRNAs and lncRNAs in shaping macrophage polarization and plasticity (227-230). Reportedly, miR-16 may be involved in repolarization of M1 macrophages by regulation of the tumor microenvironment through reduction of IL-16 and TGF β (230). Additionally, miR-511-3p could promote macrophage polarization to an M2 phenotype by inhibiting its direct targets (PTGDS, ROCK2, and LTBP1) in lung macrophages (229). Another study investigated lncRNAs expression profiles in human monocyte-derived macrophages (MDMs) polarized to either an M1 or M2 phenotype and found that lncRNA-TCONS_00019715 promotes macrophages polarization to M1 phenotype (228).

Circular RNAs (circRNAs) are a novel class of non-coding RNAs (ncRNAs). CircRNAs are abundant in the eukaryotic transcriptome and are differentially expressed in cardiovascular disease, cancer, and inflammatory diseases (52,178,231,232). A few studies have demonstrated the potential role of circular RNAs in macrophage polarization (40,46,163,233). Reportedly, circRNA-RNF19B expression in M1 macrophages was significantly higher than that in M2 macrophages. Interestingly, expression increased when M2 macrophages were polarized to an M1 phenotype. Knockdown of circRNF19B following M1 activation downregulated expression of M1 macrophages markers and elevated the expression of M2 macrophages markers (233). Another study found that circular antisense non-coding RNA in the INK4 locus (circANRIL) confers atheroprotection by regulating ribosomal biogenesis in macrophages. CircANRIL binds to pescadillo homologue 1 (PES1), an essential 60S-preribosomal assembly factor to prevent exonuclease-mediated pre-rRNA processing and ribosome biogenesis (46).

Additionally, we previously reported for the first time the role of circ-cdr1as in modulation of macrophage phenotype and overexpression of circ-cdr1as promotes phenotypic switching to an anti-inflammatory phenotype in BMDMs (40). However, the role of circ-cdr1as in modulation of macrophage function during cardiac injury has yet to be established.

In acute MI, circ-cdr1as was demonstrated to increase cardiac infarct size and apoptosis 24 hours after cardiac injury by LAD ligation. Further in vitro studies on mouse cardiac myocyte cell line supported circ-cdr1as as pro-apoptotic by preventing the inhibition of pro-apoptotic targets of miR-7, poly ADP ribose polymerase (PARP) and member of the SP/KLF family of transcription factors SP1(51). Although this study did reveal for the first time a possible role of circ-cdr1as/miR-7 in cardiomyocytes during acute MI, it is important to note that these observations were limited to the first initial 24 hours of cardiac injury. Another study between circ-cdr1as and post-MI cardiac function in pigs demonstrated a negative correlation between circ-cdr1as and infarct size. They observed a downregulation of circ-cdr1as 7 days post-MI (234). These findings support an integral role of circ-cdr1as in cardiac dysfunction. However, further comprehensive studies are needed to elucidate the role of circ-cdr1as in myocardial infarction.

The CDR1 (cerebellar degeneration related 1) gene is associated with cerebellar degeneration, Alzheimer's diseases, and hepatocellular carcinoma. The CDR1 gene is in the X chromosome and is highly conserved between humans and mice. The CDR1 protein is elevated in leukocytes in Alzheimer's patients (235). Circ-cdr1as is a closed circular RNA formed from the antisense transcript of the CDR1 gene and our previous work indicated that expression levels of circular form of circ-cdr1as were changed during

macrophage polarization without an effect to the linear transcript (40). Therefore, we focused on the role of circRNA *cdr1as* in the modulation of the inflammatory response during cardiac injury. In the current study, we demonstrate that circ-*cdr1as* is significantly repressed post-MI in mice and particularly in cardiomyocytes and macrophages. We show that exogenous delivery of circ-*cdr1as* plays a role in modulating the inflammatory response and cardiomyocyte apoptosis at the initial stages of cardiac injury and attenuating LV dysfunction in the later stages of MI in mice.

Bioinformatic analysis of the functional role of circ-*cdr1as* in cancer suggests that this circRNA plays a role in immune and stromal cell infiltration within the tumor tissue. Tissues with high circ-*CDR1as* expression had a higher ratio of anti-inflammatory macrophages and circ-*CDR1as* expression was negatively correlated with CD8⁺ T cells. Additionally, circ-*CDR1as* may also regulate the TGF- β signaling pathway and ECM-receptor interaction to serve as a mediator in reshaping the tumor microenvironment (181).

We observed that injection of macrophages overexpressing circ-*cdr1as* and anti-inflammatory M Φ s maintained their anti-inflammatory phenotype in inflammatory conditions following cardiac injury. Myocardial injection of circ-*cdr1as* M Φ s and anti-inflammatory M Φ s enhance angiogenesis, reduce infarct size, and attenuate LV dysfunction after MI. However, maintenance of improved cardiac function beyond 28 days remains unknown. Furthermore, a timeline of how long these macrophages maintain their phenotype post injury needs to be explored. Our second *in vivo* approach indicated that delivery of circ-*cdr1as* by tail vein injection increased the percentage of anti-inflammatory M Φ s at the site of injury. Anti-inflammatory M Φ s secrete high levels of anti-inflammatory cytokines and growth factors including VEGF, known to promote angiogenesis (4,197).

Anti-inflammatory MΦs can also produce myeloid-derived growth factor known to protect cardiomyocytes from cell death (19). Anti-inflammatory MΦs can secrete TGFβ1 leading to upregulation of α-SMA to aid in fibroblast differentiation and facilitate tissue repair (23). We observed that overexpression of circ-cdr1as by tail vein injection prior to MI attenuated LV dysfunction, reduced infarct size, enhanced angiogenesis, reduced cardiomyocyte apoptosis, and increased the percentage of anti-inflammatory macrophages. This could be the result of direct overexpression in cardiac cells or cross talk between cardiac cells to aid in the cardioprotective effects of circ-cdr1as. Notably, cardiomyocytes are known to release factors that promote phenotypic switching in macrophages, differentiation in fibroblast, and stimulate angiogenesis (4,236,237). However, more research is needed to understand the relationship between them.

The most established function of circRNAs located in the cytoplasm is acting as miRNAs sponges (49,102-104). Therefore, we investigated the potential relationship between circ-cdr1as and miRNAs and identified miR-7 as a target. Previous work has shown circ-cdr1as has over 70 binding sites and their interaction is highly conserved between species (83,106,181). In a diabetic mouse model, circ-cdr1as overexpression improved insulin secretion in pancreatic islet cells by inhibition of miR-7 (106). Functional studies on zebrafish demonstrated that overexpression of circ-cdr1as induced development defects in the midbrain through miR-7 dysregulation (104). Recent studies demonstrated that miR-7 is a key regulator of the immune response influencing T cell activation, macrophage function, and dendritic cell maturation in inflammation-related diseases (238-242). In a recent study, expression of miR-7 was significantly increased in bone marrow-derived macrophages activated by LPS through the TLR4 signaling pathway (240).

However, the role of miR-7 in modulation of the inflammatory response in cardiovascular disease is largely unexplored. In this study, we identify the reciprocal relationship between circ-cdr1as and miR-7 at 3 days post-MI and in naïve, pro-, and anti-inflammatory macrophages. We observed miR-7 is upregulated in the LV tissue, cardiomyocytes, and macrophages 3 days post-MI, during which circ-cdr1as is downregulated. We also identified that treatment with miR-7 mimic in BMDMs stimulated these cells to phenotypically switch to a more pro-inflammatory phenotype; meanwhile, treatment with anti-miR-7 has the opposite effect. We recognize that miR-7 may not be the only target of circ-cdr1as and thus we cannot attribute changes in macrophage polarization solely to targeting of miR-7.

Furthermore, we identified KLF4 as a miR-7 target previously known to play a role in acute lung injury. KLF4 is an evolutionarily conserved zinc finger-containing transcription factor that regulates cell growth, proliferation, and differentiation (243). Of note, miR-7 deficiency and KLF4 upregulation were associated with changes in immune cell composition and increase proportion of MHC anti-inflammatory macrophages in an acute lung injury model. Studies have previously reported that KLF4 is a critical regulator in LPS-induced inflammatory response (244), could potentially regulate the transduction of NF- κ B pathway (245), and may act as a transcriptional regulator to upregulate TGF β 1 and IL-10 (246,247). This study reports that KLF4 is downregulated in LV tissue 3 days post-MI. Overexpression of circ-cdr1as results in miR-7 inhibition leading to upregulation of KLF4 in naïve, pro-, and anti-inflammatory macrophages. Furthermore, modulation of circ-cdr1as levels in our study reveals a crucial role of circ-cdr1as/miR-7/KLF4 in cardiac injury and macrophage phenotype.

4.5 Conclusion

In summary, our findings highlight circ-cdr1as to be involved in the regulation of macrophage phenotype during cardiac injury and overexpression of circ-cdr1as resulted in cardioprotective effects by reducing cardiomyocyte apoptosis, enhancing angiogenesis, limiting infarct size, increasing percentage of anti-inflammatory macrophages, and overall preserving post-MI cardiac function. We suggest this occurs by circ-cdr1as modulation of miR-7 to prevent the inhibition of KLF4 (Figure 4.9). Therefore, circ-cdr1as may potentially be a therapeutic for the resolution of inflammation after cardiac injury.

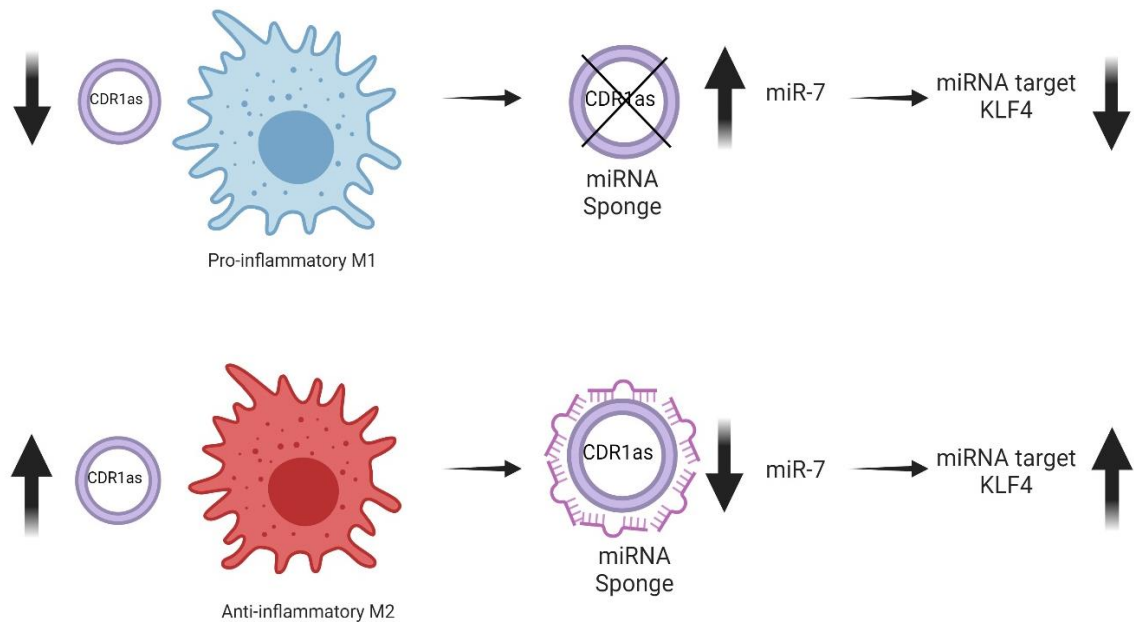


Figure 4.9. Graphical Summary.

CHAPTER 5

CONCLUDING REMARKS AND SIGNIFICANCE

The research described within this dissertation is aimed to 1) determine the specific role of circular RNA *cdrlas* in phenotypic modulation in macrophages, 2) determine whether functional regulation of *circ-cdrlas* plays a role in macrophage function after cardiac injury and repair, and 3) identify the possible molecular mechanism by which *circ-cdrlas* regulates macrophage phenotype. Although there have been advancements in treatment for cardiovascular disease, the prognosis remains poor. Macrophages are vital immune cells in the inflammatory response and are key cellular elements in chronic inflammatory diseases such as CVD and cancer. The challenges with immunomodulation during cardiac injury include increased risk of prolonging cardiac inflammation and impaired tissue remodeling. Therefore, an alternative strategy that could circumvent these challenges could be to alter macrophage phenotype to an anti-inflammatory phenotype in the initial stages of cardiac injury to modulate the inflammatory response and to promote cardiac repair at an earlier time point and prevent further cell death.

In recent years, non-coding RNAs have been implicated in cardiovascular disease, cancer, and inflammation. Our study focused on a newer family of non-coding RNAs, circular RNAs, due to their resistance to exonuclease degradation, capability to regulate gene expression by modulation miRNA activity, conservation between species, and differential expression in cardiovascular and immune-related diseases. Therefore, comprehensive characterization of circRNA and functional examination in macrophages of different phenotypes may aid in the identification of circRNAs involved in macrophage polarization and provide specific targets for the modulation of macrophage phenotype.

There are several significant findings from our investigation. First, we performed circular RNA expression profiling to identify circular RNAs that are differentially expressed in naïve, pro-, and anti-inflammatory macrophages. This led us to identify circ-cdr1as as the most upregulated circRNA in anti-inflammatory macrophages. Functional studies demonstrated that overexpression of circ-cdr1as promotes a shift to an anti-inflammatory phenotype in unpolarized and pro-inflammatory phenotype polarized macrophages. Based on circRNA profiling we also identified differentially expressed circular RNAs between pro- and anti-inflammatory macrophages associated with gene interaction networks involved in cell death and activation of master inflammatory regulators like NF- κ B, INF α , and IL-10. Although, we did not comprehensively investigate whether circ-cdr1as plays a role in cell death or activation of inflammatory regulators, we did observe an increase in transcription of anti-inflammatory cytokines IL-10 and TGF β . In the future, investigating if circ-cdr1as is involved in these processes will provide a more detailed characterization of how circ-cdr1as modulates macrophage function. It should also be noted that there could be other circular RNA not investigated in this study that could be involved in macrophage polarization.

Given the relevance of circRNAs in cardiovascular disease and our IPA disease enrichment analysis of the circRNAs, we further investigated whether circ-cdr1as could modulate macrophage function during cardiac injury and potentially regulate post-injury cardiac inflammation. Our studies investigated circular cdr1as in the regulation of macrophage function *in vivo* using a myocardial infarction mouse model. We first identified circ-cdr1as expression in the LV tissue 3 days post MI and found a downregulation of circ-cdr1as in the MI region, cardiomyocytes, and macrophages. And

so, for our first approach, we overexpressed circ-cdr1as in macrophages and injected these macrophages into the myocardium at time of MI. Using this cell based therapeutic approach, we observed that macrophages retained their anti-inflammatory M2 like phenotype in the initial stages of MI, during which inflammation is high, but also attenuated LV dysfunction in the later stages of MI. Our next approach focused on overexpression of circ-cdr1as by tail vein injection primarily targeting cardiomyocytes by utilizing AAV9. Interestingly, we observed increase percentage of anti-inflammatory macrophages at site of injury and a reduction of cardiomyocyte cell death in the initial stages of MI. We also observed attenuation of LV dysfunction, decrease of infarct size, and increase in angiogenesis. These observations could be a result of anti-inflammatory macrophages secreting high levels of anti-inflammatory cytokines and growth factors known to promote angiogenesis, fibroblast differentiation, prevent cardiomyocyte cell death, and promote cardiac remodeling. Additionally, cardiomyocytes are also able to secrete factors that promote phenotypic switching in macrophages, differentiation in fibroblast, and stimulate angiogenesis. Overall, the interplay between cardiac cells and upregulation of circ-cdr1as needs to be further investigated. Future studies may include investigating if overexpression of circ-cdr1as in cardiomyocytes affect polarization of macrophages, how circ-cdr1as affects cell death in macrophages and cardiomyocytes, and determining the factors secreted by either cardiomyocytes or macrophages when they overexpress circ-cdr1as.

Lastly, we investigated the potential mechanism of circ-cdr1as as a miRNA sponge for miR-7 and its target KLF4. We identified a reciprocal relationship between circ-cdr1as and miR-7 at 3 days post-MI and in naïve, pro-, and anti-inflammatory macrophages.

We observed a downregulation of circ-cdr1as, upregulation of miR-7 and downregulation KLF4 in LV tissue, cardiomyocytes, and macrophages 3 days post-MI during. We observed the same trend in naïve, pro-, and anti-inflammatory macrophages. We identified treatment with miR-7 mimic in BMDMs stimulated these macrophages to favor a pro-inflammatory phenotype and inhibition of miR-7 favored an anti-inflammatory phenotype. Interestingly, we observed that overexpression of circ-cdr1as, downregulated miR-7, and upregulated miR-7 target KLF4. Meanwhile, knockdown of circ-cdr1as has the opposite effect. We recognize that miR-7 may not be the only target of circ-cdr1as and thus we cannot attribute changes in macrophage polarization solely to targeting of miR-7. Although this study indicates the crucial role of circ-cdr1as/miR-7/KLF4 in cardiac injury and macrophage phenotype, further research is needed in how modulation of circ-cdr1as in conjunction with modulation of miR-7 modulate macrophage phenotype.

Overall, these studies shed light on the regulatory roles of circRNAs, particularly circ-cdr1as, in modulating macrophage phenotype and function, overexpression of circ-cdr1as may be cardioprotective by reducing cardiomyocyte apoptosis, enhancing angiogenesis, limiting infarct size, increasing percentage of anti-inflammatory macrophages, and overall preserving post-MI cardiac function. Therefore, utilizing circular RNAs as a potential therapeutic target may offer potential avenues for therapeutic intervention in inflammatory diseases.

REFERENCES

1. Martin, S. S., Aday, A. W., Almarzooq, Z. I., Anderson, C. A. M., Arora, P., Avery, C. L., et al. (2024). 2024 Heart Disease and Stroke Statistics: A Report of US and Global Data From the American Heart Association. *Circulation*, *149*(8), e347-e913. doi:10.1161/CIR.0000000000001209
2. Frangogiannis, N. G. (2015). Pathophysiology of Myocardial Infarction. *Compr Physiol*, *5*(4), 1841-75. doi:10.1002/cphy.c150006
3. Schirone, L., Forte, M., D'Ambrosio, L., Valenti, V., Vecchio, D., Schiavon, S., et al. (2022). An Overview of the Molecular Mechanisms Associated with Myocardial Ischemic Injury: State of the Art and Translational Perspectives. *Cells*, *11*(7). doi:10.3390/cells11071165
4. Jian, Y., Zhou, X., Shan, W., Chen, C., Ge, W., Cui, J., et al. (2023). Crosstalk between macrophages and cardiac cells after myocardial infarction. *Cell Commun Signal*, *21*(1), 109. doi:10.1186/s12964-023-01105-4
5. Daseke, M. J., 2nd, Tenkorang, M. A. A., Chalise, U., Konfrst, S. R., Lindsey, M. L. (2020). Cardiac fibroblast activation during myocardial infarction wound healing: Fibroblast polarization after MI. *Matrix Biol*, *91-92*, 109-16. doi:10.1016/j.matbio.2020.03.010
6. Ojha, N., Dhamoon, A. S. (2024). Myocardial Infarction. In *StatPearls*. Treasure Island (FL) ineligible companies. Disclosure: Amit Dhamoon declares no relevant financial relationships with ineligible companies.
7. Ye, Q., Zhang, J., Ma, L. (2020). Predictors of all-cause 1-year mortality in myocardial infarction patients. *Medicine (Baltimore)*, *99*(29), e21288. doi:10.1097/MD.00000000000021288
8. Levine, B., Kalman, J., Mayer, L., Fillit, H. M., Packer, M. (1990). Elevated circulating levels of tumor necrosis factor in severe chronic heart failure. *N Engl J Med*, *323*(4), 236-41. doi:10.1056/NEJM199007263230405
9. Lavine, K. J., Pinto, A. R., Epelman, S., Kopecky, B. J., Clemente-Casares, X., Godwin, J., et al. (2018). The Macrophage in Cardiac Homeostasis and Disease: JACC Macrophage in CVD Series (Part 4). *J Am Coll Cardiol*, *72*(18), 2213-30. doi:10.1016/j.jacc.2018.08.2149
10. Mann, D. L. (2015). Innate immunity and the failing heart: the cytokine hypothesis revisited. *Circ Res*, *116*(7), 1254-68. doi:10.1161/CIRCRESAHA.116.302317

11. O'Rourke, S. A., Dunne, A., Monaghan, M. G. (2019). The Role of Macrophages in the Infarcted Myocardium: Orchestrators of ECM Remodeling. *Front Cardiovasc Med*, 6, 101. doi:10.3389/fcvm.2019.00101
12. Halade, G. V., Lee, D. H. (2022). Inflammation and resolution signaling in cardiac repair and heart failure. *EBioMedicine*, 79, 103992. doi:10.1016/j.ebiom.2022.103992
13. Fang, L., Moore, X. L., Dart, A. M., Wang, L. M. (2015). Systemic inflammatory response following acute myocardial infarction. *J Geriatr Cardiol*, 12(3), 305-12. doi:10.11909/j.issn.1671-5411.2015.03.020
14. Feng, Q., Li, Q., Zhou, H., Sun, L., Lin, C., Jin, Y., et al. (2022). The role of major immune cells in myocardial infarction. *Front Immunol*, 13, 1084460. doi:10.3389/fimmu.2022.1084460
15. Frangogiannis, N. G. (2014). The inflammatory response in myocardial injury, repair, and remodelling. *Nat Rev Cardiol*, 11(5), 255-65. doi:10.1038/nrcardio.2014.28
16. Duncan, S. E., Gao, S., Sarhene, M., Coffie, J. W., Linhua, D., Bao, X., et al. (2020). Macrophage Activities in Myocardial Infarction and Heart Failure. *Cardiol Res Pract*, 2020, 4375127. doi:10.1155/2020/4375127
17. Shapouri-Moghaddam, A., Mohammadian, S., Vazini, H., Taghadosi, M., Esmaeili, S. A., Mardani, F., et al. (2018). Macrophage plasticity, polarization, and function in health and disease. *J Cell Physiol*, 233(9), 6425-40. doi:10.1002/jcp.26429
18. Yan, X., Anzai, A., Katsumata, Y., Matsushashi, T., Ito, K., Endo, J., et al. (2013). Temporal dynamics of cardiac immune cell accumulation following acute myocardial infarction. *J Mol Cell Cardiol*, 62, 24-35. doi:10.1016/j.yjmcc.2013.04.023
19. Korf-Klingebiel, M., Reboll, M. R., Klede, S., Brod, T., Pich, A., Polten, F., et al. (2015). Myeloid-derived growth factor (C19orf10) mediates cardiac repair following myocardial infarction. *Nat Med*, 21(2), 140-9. doi:10.1038/nm.3778
20. Bajpai, G., Schneider, C., Wong, N., Bredemeyer, A., Hulsmans, M., Nahrendorf, M., et al. (2018). The human heart contains distinct macrophage subsets with divergent origins and functions. *Nat Med*, 24(8), 1234-45. doi:10.1038/s41591-018-0059-x
21. Zhang, S., Yeap, X. Y., DeBerge, M., Naresh, N. K., Wang, K., Jiang, Z., et al. (2017). Acute CD47 Blockade During Ischemic Myocardial Reperfusion Enhances Phagocytosis-Associated Cardiac Repair. *JACC Basic Transl Sci*, 2(4), 386-97. doi:10.1016/j.jacbts.2017.03.013

22. Hulsmans, M., Clauss, S., Xiao, L., Aguirre, A. D., King, K. R., Hanley, A., et al. (2017). Macrophages Facilitate Electrical Conduction in the Heart. *Cell*, 169(3), 510-22 e20. doi:10.1016/j.cell.2017.03.050
23. Braga, T. T., Agudelo, J. S., Camara, N. O. (2015). Macrophages During the Fibrotic Process: M2 as Friend and Foe. *Front Immunol*, 6, 602. doi:10.3389/fimmu.2015.00602
24. Alonso-Herranz, L., Sahun-Espanol, A., Paredes, A., Gonzalo, P., Gkontra, P., Nunez, V., et al. (2020). Macrophages promote endothelial-to-mesenchymal transition via MT1-MMP/TGFbeta1 after myocardial infarction. *Elife*, 9. doi:10.7554/eLife.57920
25. Kuang, Y., Li, X., Liu, X., Wei, L., Chen, X., Liu, J., et al. (2021). Vascular endothelial S1pr1 ameliorates adverse cardiac remodelling via stimulating reparative macrophage proliferation after myocardial infarction. *Cardiovasc Res*, 117(2), 585-99. doi:10.1093/cvr/cvaa046
26. Gruzdeva, O., Uchasova, E., Dyleva, Y., Akbasheva, O., Matveeva, V., Karetnikova, V., et al. (2017). Relationship key factor of inflammation and the development of complications in the late period of myocardial infarction in patients with visceral obesity. *BMC Cardiovasc Disord*, 17(1), 36. doi:10.1186/s12872-017-0473-x
27. Frangogiannis, N. G., Dewald, O., Xia, Y., Ren, G., Haudek, S., Leucker, T., et al. (2007). Critical role of monocyte chemoattractant protein-1/CC chemokine ligand 2 in the pathogenesis of ischemic cardiomyopathy. *Circulation*, 115(5), 584-92. doi:10.1161/CIRCULATIONAHA.106.646091
28. Ait-Oufella, H., Herbin, O., Bouaziz, J. D., Binder, C. J., Uyttenhove, C., Laurans, L., et al. (2010). B cell depletion reduces the development of atherosclerosis in mice. *J Exp Med*, 207(8), 1579-87. doi:10.1084/jem.20100155
29. Peet, C., Ivetic, A., Bromage, D. I., Shah, A. M. (2020). Cardiac monocytes and macrophages after myocardial infarction. *Cardiovasc Res*, 116(6), 1101-12. doi:10.1093/cvr/cvz336
30. Colpaert, R. M. W., Calore, M. (2021). Epigenetics and microRNAs in cardiovascular diseases. *Genomics*, 113(2), 540-51. doi:10.1016/j.ygeno.2020.12.042
31. Fang, Y., Xu, Y., Wang, R., Hu, L., Guo, D., Xue, F., et al. (2020). Recent advances on the roles of LncRNAs in cardiovascular disease. *J Cell Mol Med*, 24(21), 12246-57. doi:10.1111/jcmm.15880

32. Liu, W., Hu, J., Lu, S., Wang, Z. (2022). The role of non-coding RNAs in myocarditis: a narrative review. *Ann Transl Med*, 10(18), 1022. doi:10.21037/atm-21-6116
33. Marinescu, M. C., Lazar, A. L., Marta, M. M., Cozma, A., Catana, C. S. (2022). Non-Coding RNAs: Prevention, Diagnosis, and Treatment in Myocardial Ischemia-Reperfusion Injury. *Int J Mol Sci*, 23(5). doi:10.3390/ijms23052728
34. Tang, Y., Bao, J., Hu, J., Liu, L., Xu, D. Y. (2021). Circular RNA in cardiovascular disease: Expression, mechanisms and clinical prospects. *J Cell Mol Med*, 25(4), 1817-24. doi:10.1111/jcmm.16203
35. Zhang, C., Xiong, Y., Zeng, L., Peng, Z., Liu, Z., Zhan, H., et al. (2020). The Role of Non-coding RNAs in Viral Myocarditis. *Front Cell Infect Microbiol*, 10, 312. doi:10.3389/fcimb.2020.00312
36. Consortium, E. P. (2012). An integrated encyclopedia of DNA elements in the human genome. *Nature*, 489(7414), 57-74. doi:10.1038/nature11247
37. Sallam, T., Sandhu, J., Tontonoz, P. (2018). Long Noncoding RNA Discovery in Cardiovascular Disease: Decoding Form to Function. *Circ Res*, 122(1), 155-66. doi:10.1161/CIRCRESAHA.117.311802
38. Cai, B., Ma, W., Ding, F., Zhang, L., Huang, Q., Wang, X., et al. (2018). The Long Noncoding RNA CAREL Controls Cardiac Regeneration. *J Am Coll Cardiol*, 72(5), 534-50. doi:10.1016/j.jacc.2018.04.085
39. Garikipati, V. N. S., Verma, S. K., Cheng, Z., Liang, D., Truongcao, M. M., Cimini, M., et al. (2019). Circular RNA CircFndc3b modulates cardiac repair after myocardial infarction via FUS/VEGF-A axis. *Nat Commun*, 10(1), 4317. doi:10.1038/s41467-019-11777-7
40. Gonzalez, C., Cimini, M., Cheng, Z., Benedict, C., Wang, C., Trungcao, M., et al. (2022). Role of circular RNA cdr1as in modulation of macrophage phenotype. *Life Sci*, 309, 121003. doi:10.1016/j.lfs.2022.121003
41. Huang, G., Garikipati, V. N. S., Zhou, Y., Benedict, C., Houser, S. R., Koch, W. J., et al. (2020). Identification and Comparison of Hyperglycemia-Induced Extracellular Vesicle Transcriptome in Different Mouse Stem Cells. *Cells*, 9(9). doi:10.3390/cells9092098
42. Piccoli, M. T., Gupta, S. K., Viereck, J., Foinquinos, A., Samolovac, S., Kramer, F. L., et al. (2017). Inhibition of the Cardiac Fibroblast-Enriched lncRNA Meg3 Prevents Cardiac Fibrosis and Diastolic Dysfunction. *Circ Res*, 121(5), 575-83. doi:10.1161/CIRCRESAHA.117.310624

43. Ranjan, P., Kumari, R., Goswami, S. K., Li, J., Pal, H., Suleiman, Z., et al. (2021). Myofibroblast-Derived Exosome Induce Cardiac Endothelial Cell Dysfunction. *Front Cardiovasc Med*, 8, 676267. doi:10.3389/fcvm.2021.676267
44. Wu, G., Cai, J., Han, Y., Chen, J., Huang, Z. P., Chen, C., et al. (2014). LincRNA-p21 regulates neointima formation, vascular smooth muscle cell proliferation, apoptosis, and atherosclerosis by enhancing p53 activity. *Circulation*, 130(17), 1452-65. doi:10.1161/CIRCULATIONAHA.114.011675
45. Chen, Y. G., Kim, M. V., Chen, X., Batista, P. J., Aoyama, S., Wilusz, J. E., et al. (2017). Sensing Self and Foreign Circular RNAs by Intron Identity. *Mol Cell*, 67(2), 228-38 e5. doi:10.1016/j.molcel.2017.05.022
46. Holdt, L. M., Stahringer, A., Sass, K., Pichler, G., Kulak, N. A., Wilfert, W., et al. (2016). Circular non-coding RNA ANRIL modulates ribosomal RNA maturation and atherosclerosis in humans. *Nat Commun*, 7, 12429. doi:10.1038/ncomms12429
47. Werfel, S., Nothjunge, S., Schwarzmayr, T., Strom, T. M., Meitinger, T., Engelhardt, S. (2016). Characterization of circular RNAs in human, mouse and rat hearts. *J Mol Cell Cardiol*, 98, 103-7. doi:10.1016/j.yjmcc.2016.07.007
48. Chen, L. L. (2016). The biogenesis and emerging roles of circular RNAs. *Nat Rev Mol Cell Biol*, 17(4), 205-11. doi:10.1038/nrm.2015.32
49. Greene, J., Baird, A. M., Brady, L., Lim, M., Gray, S. G., McDermott, R., et al. (2017). Circular RNAs: Biogenesis, Function and Role in Human Diseases. *Front Mol Biosci*, 4, 38. doi:10.3389/fmolb.2017.00038
50. Beermann, J., Piccoli, M. T., Viereck, J., Thum, T. (2016). Non-coding RNAs in Development and Disease: Background, Mechanisms, and Therapeutic Approaches. *Physiol Rev*, 96(4), 1297-325. doi:10.1152/physrev.00041.2015
51. Geng, H. H., Li, R., Su, Y. M., Xiao, J., Pan, M., Cai, X. X., et al. (2016). The Circular RNA Cdr1as Promotes Myocardial Infarction by Mediating the Regulation of miR-7a on Its Target Genes Expression. *PLoS One*, 11(3), e0151753. doi:10.1371/journal.pone.0151753
52. Kishore, R., Garikipati, V. N. S., Gonzalez, C. (2020). Role of Circular RNAs in Cardiovascular Disease. *J Cardiovasc Pharmacol*, 76(2), 128-37. doi:10.1097/FJC.0000000000000841
53. Ng, W. L., Marinov, G. K., Chin, Y. M., Lim, Y. Y., Ea, C. K. (2017). Transcriptomic analysis of the role of RasGEF1B circular RNA in the TLR4/LPS pathway. *Sci Rep*, 7(1), 12227. doi:10.1038/s41598-017-12550-w

54. Ng, W. L., Marinov, G. K., Liau, E. S., Lam, Y. L., Lim, Y. Y., Ea, C. K. (2016). Inducible RasGEF1B circular RNA is a positive regulator of ICAM-1 in the TLR4/LPS pathway. *RNA Biol*, 13(9), 861-71. doi:10.1080/15476286.2016.1207036
55. Chen, L. L., Yang, L. (2015). Regulation of circRNA biogenesis. *RNA Biol*, 12(4), 381-8. doi:10.1080/15476286.2015.1020271
56. Liang, Y., Liu, N., Yang, L., Tang, J., Wang, Y., Mei, M. (2021). A Brief Review of circRNA Biogenesis, Detection, and Function. *Curr Genomics*, 22(7), 485-95. doi:10.2174/1389202922666210331130722
57. Carrara, M., Fuschi, P., Ivan, C., Martelli, F. (2018). Circular RNAs: Methodological challenges and perspectives in cardiovascular diseases. *J Cell Mol Med*, 22(11), 5176-87. doi:10.1111/jcmm.13789
58. Szabo, L., Salzman, J. (2016). Detecting circular RNAs: bioinformatic and experimental challenges. *Nat Rev Genet*, 17(11), 679-92. doi:10.1038/nrg.2016.114
59. Roy, C. K., Olson, S., Graveley, B. R., Zamore, P. D., Moore, M. J. (2015). Assessing long-distance RNA sequence connectivity via RNA-templated DNA-DNA ligation. *Elife*, 4. doi:10.7554/eLife.03700
60. Schneider, T., Schreiner, S., Preusser, C., Bindereif, A., Rossbach, O. (2018). Northern Blot Analysis of Circular RNAs. *Methods Mol Biol*, 1724, 119-33. doi:10.1007/978-1-4939-7562-4_10
61. Glazar, P., Papavasileiou, P., Rajewsky, N. (2014). circBase: a database for circular RNAs. *RNA*, 20(11), 1666-70. doi:10.1261/rna.043687.113
62. Dudekula, D. B., Panda, A. C., Grammatikakis, I., De, S., Abdelmohsen, K., Gorospe, M. (2016). CircInteractome: A web tool for exploring circular RNAs and their interacting proteins and microRNAs. *RNA Biol*, 13(1), 34-42. doi:10.1080/15476286.2015.1128065
63. Zhang, X. O., Dong, R., Zhang, Y., Zhang, J. L., Luo, Z., Zhang, J., et al. (2016). Diverse alternative back-splicing and alternative splicing landscape of circular RNAs. *Genome Res*, 26(9), 1277-87. doi:10.1101/gr.202895.115
64. Ghosal, S., Das, S., Sen, R., Basak, P., Chakrabarti, J. (2013). Circ2Traits: a comprehensive database for circular RNA potentially associated with disease and traits. *Front Genet*, 4, 283. doi:10.3389/fgene.2013.00283
65. Fan, C., Lei, X., Fang, Z., Jiang, Q., Wu, F. X. (2018). CircR2Disease: a manually curated database for experimentally supported circular RNAs associated with various diseases. *Database (Oxford)*, 2018. doi:10.1093/database/bay044

66. Ivanov, A., Memczak, S., Wyler, E., Torti, F., Porath, H. T., Orejuela, M. R., et al. (2015). Analysis of intron sequences reveals hallmarks of circular RNA biogenesis in animals. *Cell Rep*, *10*(2), 170-7. doi:10.1016/j.celrep.2014.12.019
67. Salzman, J. (2016). Circular RNA Expression: Its Potential Regulation and Function. *Trends Genet*, *32*(5), 309-16. doi:10.1016/j.tig.2016.03.002
68. Kristensen, L. S., Andersen, M. S., Stagsted, L. V. W., Ebbesen, K. K., Hansen, T. B., Kjems, J. (2019). The biogenesis, biology and characterization of circular RNAs. *Nat Rev Genet*, *20*(11), 675-91. doi:10.1038/s41576-019-0158-7
69. Zhang, Y., Zhang, X. O., Chen, T., Xiang, J. F., Yin, Q. F., Xing, Y. H., et al. (2013). Circular intronic long noncoding RNAs. *Mol Cell*, *51*(6), 792-806. doi:10.1016/j.molcel.2013.08.017
70. Conn, S. J., Pillman, K. A., Toubia, J., Conn, V. M., Salmanidis, M., Phillips, C. A., et al. (2015). The RNA binding protein quaking regulates formation of circRNAs. *Cell*, *160*(6), 1125-34. doi:10.1016/j.cell.2015.02.014
71. Ashwal-Fluss, R., Meyer, M., Pamudurti, N. R., Ivanov, A., Bartok, O., Hanan, M., et al. (2014). circRNA biogenesis competes with pre-mRNA splicing. *Mol Cell*, *56*(1), 55-66. doi:10.1016/j.molcel.2014.08.019
72. Zhang, X. O., Wang, H. B., Zhang, Y., Lu, X., Chen, L. L., Yang, L. (2014). Complementary sequence-mediated exon circularization. *Cell*, *159*(1), 134-47. doi:10.1016/j.cell.2014.09.001
73. Petkovic, S., Muller, S. (2015). RNA circularization strategies in vivo and in vitro. *Nucleic Acids Res*, *43*(4), 2454-65. doi:10.1093/nar/gkv045
74. Hedberg, A., Johansen, S. D. (2013). Nuclear group I introns in self-splicing and beyond. *Mob DNA*, *4*(1), 17. doi:10.1186/1759-8753-4-17
75. Lambowitz, A. M., Zimmerly, S. (2011). Group II introns: mobile ribozymes that invade DNA. *Cold Spring Harb Perspect Biol*, *3*(8), a003616. doi:10.1101/cshperspect.a003616
76. Lehmann, K., Schmidt, U. (2003). Group II introns: structure and catalytic versatility of large natural ribozymes. *Crit Rev Biochem Mol Biol*, *38*(3), 249-303. doi:10.1080/713609236
77. Aktas, T., Avsar Ilik, I., Maticzka, D., Bhardwaj, V., Pessoa Rodrigues, C., Mittler, G., et al. (2017). DHX9 suppresses RNA processing defects originating from the Alu invasion of the human genome. *Nature*, *544*(7648), 115-9. doi:10.1038/nature21715

78. Wang, X., Dong, J., Li, X., Cheng, Z., Zhu, Q. (2021). CPSF4 regulates circRNA formation and microRNA mediated gene silencing in hepatocellular carcinoma. *Oncogene*, 40(25), 4338-51. doi:10.1038/s41388-021-01867-6
79. Chen, L., Huang, C., Wang, X., Shan, G. (2015). Circular RNAs in Eukaryotic Cells. *Curr Genomics*, 16(5), 312-8. doi:10.2174/1389202916666150707161554
80. Huang, C., Shan, G. (2015). What happens at or after transcription: Insights into circRNA biogenesis and function. *Transcription*, 6(4), 61-4. doi:10.1080/21541264.2015.1071301
81. Liang, D., Wilusz, J. E. (2014). Short intronic repeat sequences facilitate circular RNA production. *Genes Dev*, 28(20), 2233-47. doi:10.1101/gad.251926.114
82. Li, X., Yang, L., Chen, L. L. (2018). The Biogenesis, Functions, and Challenges of Circular RNAs. *Mol Cell*, 71(3), 428-42. doi:10.1016/j.molcel.2018.06.034
83. Memczak, S., Jens, M., Elefsinioti, A., Torti, F., Krueger, J., Rybak, A., et al. (2013). Circular RNAs are a large class of animal RNAs with regulatory potency. *Nature*, 495(7441), 333-8. doi:10.1038/nature11928
84. Zhang, Y., Xue, W., Li, X., Zhang, J., Chen, S., Zhang, J. L., et al. (2016). The Biogenesis of Nascent Circular RNAs. *Cell Rep*, 15(3), 611-24. doi:10.1016/j.celrep.2016.03.058
85. Jeck, W. R., Sorrentino, J. A., Wang, K., Slevin, M. K., Burd, C. E., Liu, J., et al. (2013). Circular RNAs are abundant, conserved, and associated with ALU repeats. *RNA*, 19(2), 141-57. doi:10.1261/rna.035667.112
86. Tan, W. L., Lim, B. T., Anene-Nzeli, C. G., Ackers-Johnson, M., Dashi, A., See, K., et al. (2017). A landscape of circular RNA expression in the human heart. *Cardiovasc Res*, 113(3), 298-309. doi:10.1093/cvr/cvw250
87. Lasda, E., Parker, R. (2014). Circular RNAs: diversity of form and function. *RNA*, 20(12), 1829-42. doi:10.1261/rna.047126.114
88. Rybak-Wolf, A., Stottmeister, C., Glazar, P., Jens, M., Pino, N., Giusti, S., et al. (2015). Circular RNAs in the Mammalian Brain Are Highly Abundant, Conserved, and Dynamically Expressed. *Mol Cell*, 58(5), 870-85. doi:10.1016/j.molcel.2015.03.027
89. Salzman, J., Gawad, C., Wang, P. L., Lacayo, N., Brown, P. O. (2012). Circular RNAs are the predominant transcript isoform from hundreds of human genes in diverse cell types. *PLoS One*, 7(2), e30733. doi:10.1371/journal.pone.0030733

90. You, X., Vlatkovic, I., Babic, A., Will, T., Epstein, I., Tushev, G., et al. (2015). Neural circular RNAs are derived from synaptic genes and regulated by development and plasticity. *Nat Neurosci*, 18(4), 603-10. doi:10.1038/nn.3975
91. Abu, N., Jamal, R. (2016). Circular RNAs as Promising Biomarkers: A Mini-Review. *Front Physiol*, 7, 355. doi:10.3389/fphys.2016.00355
92. Xu, T., Wu, J., Han, P., Zhao, Z., Song, X. (2017). Circular RNA expression profiles and features in human tissues: a study using RNA-seq data. *BMC Genomics*, 18(Suppl 6), 680. doi:10.1186/s12864-017-4029-3
93. Li, Z., Huang, C., Bao, C., Chen, L., Lin, M., Wang, X., et al. (2015). Exon-intron circular RNAs regulate transcription in the nucleus. *Nat Struct Mol Biol*, 22(3), 256-64. doi:10.1038/nsmb.2959
94. Wesselhoeft, R. A., Kowalski, P. S., Parker-Hale, F. C., Huang, Y., Bisaria, N., Anderson, D. G. (2019). RNA Circularization Diminishes Immunogenicity and Can Extend Translation Duration In Vivo. *Mol Cell*, 74(3), 508-20 e4. doi:10.1016/j.molcel.2019.02.015
95. Yang, Y., Fan, X., Mao, M., Song, X., Wu, P., Zhang, Y., et al. (2017). Extensive translation of circular RNAs driven by N(6)-methyladenosine. *Cell Res*, 27(5), 626-41. doi:10.1038/cr.2017.31
96. Abe, N., Matsumoto, K., Nishihara, M., Nakano, Y., Shibata, A., Maruyama, H., et al. (2015). Rolling Circle Translation of Circular RNA in Living Human Cells. *Sci Rep*, 5, 16435. doi:10.1038/srep16435
97. Pamudurti, N. R., Bartok, O., Jens, M., Ashwal-Fluss, R., Stottmeister, C., Ruhe, L., et al. (2017). Translation of CircRNAs. *Mol Cell*, 66(1), 9-21 e7. doi:10.1016/j.molcel.2017.02.021
98. Stagsted, L. V., Nielsen, K. M., Dugaard, I., Hansen, T. B. (2019). Noncoding AUG circRNAs constitute an abundant and conserved subclass of circles. *Life Sci Alliance*, 2(3). doi:10.26508/lsa.201900398
99. Nicolet, B. P., Jansen, S. B. G., Heideveld, E., Ouweland, W. H., van den Akker, E., von Lindern, M., et al. (2022). Circular RNAs exhibit limited evidence for translation, or translation regulation of the mRNA counterpart in terminal hematopoiesis. *RNA*, 28(2), 194-209. doi:10.1261/rna.078754.121
100. Ho-Xuan, H., Glazar, P., Latini, C., Heizler, K., Haase, J., Hett, R., et al. (2020). Comprehensive analysis of translation from overexpressed circular RNAs reveals pervasive translation from linear transcripts. *Nucleic Acids Res*, 48(18), 10368-82. doi:10.1093/nar/gkaa704

101. Abdelmohsen, K., Panda, A. C., Munk, R., Grammatikakis, I., Dudekula, D. B., De, S., et al. (2017). Identification of HuR target circular RNAs uncovers suppression of PABPN1 translation by CircPABPN1. *RNA Biol*, 14(3), 361-9. doi:10.1080/15476286.2017.1279788
102. Liu, K. S., Pan, F., Mao, X. D., Liu, C., Chen, Y. J. (2019). Biological functions of circular RNAs and their roles in occurrence of reproduction and gynecological diseases. *Am J Transl Res*, 11(1), 1-15. Retrieved from <https://www.ncbi.nlm.nih.gov/pubmed/30787966>
103. Yu, C. Y., Kuo, H. C. (2019). The emerging roles and functions of circular RNAs and their generation. *J Biomed Sci*, 26(1), 29. doi:10.1186/s12929-019-0523-z
104. Hansen, T. B., Jensen, T. I., Clausen, B. H., Bramsen, J. B., Finsen, B., Damgaard, C. K., et al. (2013). Natural RNA circles function as efficient microRNA sponges. *Nature*, 495(7441), 384-8. doi:10.1038/nature11993
105. Piwecka, M., Glazar, P., Hernandez-Miranda, L. R., Memczak, S., Wolf, S. A., Rybak-Wolf, A., et al. (2017). Loss of a mammalian circular RNA locus causes miRNA deregulation and affects brain function. *Science*, 357(6357). doi:10.1126/science.aam8526
106. Xu, H., Guo, S., Li, W., Yu, P. (2015). The circular RNA Cdr1as, via miR-7 and its targets, regulates insulin transcription and secretion in islet cells. *Sci Rep*, 5, 12453. doi:10.1038/srep12453
107. Chen, G., Shi, Y., Liu, M., Sun, J. (2018). circHIPK3 regulates cell proliferation and migration by sponging miR-124 and regulating AQP3 expression in hepatocellular carcinoma. *Cell Death Dis*, 9(2), 175. doi:10.1038/s41419-017-0204-3
108. Zheng, Q., Bao, C., Guo, W., Li, S., Chen, J., Chen, B., et al. (2016). Circular RNA profiling reveals an abundant circHIPK3 that regulates cell growth by sponging multiple miRNAs. *Nat Commun*, 7, 11215. doi:10.1038/ncomms11215
109. Boeckel, J. N., Jae, N., Heumuller, A. W., Chen, W., Boon, R. A., Stellos, K., et al. (2015). Identification and Characterization of Hypoxia-Regulated Endothelial Circular RNA. *Circ Res*, 117(10), 884-90. doi:10.1161/CIRCRESAHA.115.306319
110. Militello, G., Weirick, T., John, D., Doring, C., Dimmeler, S., Uchida, S. (2017). Screening and validation of lncRNAs and circRNAs as miRNA sponges. *Brief Bioinform*, 18(5), 780-8. doi:10.1093/bib/bbw053
111. Guo, J. U., Agarwal, V., Guo, H., Bartel, D. P. (2014). Expanded identification and characterization of mammalian circular RNAs. *Genome Biol*, 15(7), 409. doi:10.1186/s13059-014-0409-z

112. Huang, A., Zheng, H., Wu, Z., Chen, M., Huang, Y. (2020). Circular RNA-protein interactions: functions, mechanisms, and identification. *Theranostics*, 10(8), 3503-17. doi:10.7150/thno.42174
113. Du, W. W., Yang, W., Liu, E., Yang, Z., Dhaliwal, P., Yang, B. B. (2016). Foxo3 circular RNA retards cell cycle progression via forming ternary complexes with p21 and CDK2. *Nucleic Acids Res*, 44(6), 2846-58. doi:10.1093/nar/gkw027
114. Yang, Q., Du, W. W., Wu, N., Yang, W., Awan, F. M., Fang, L., et al. (2017). A circular RNA promotes tumorigenesis by inducing c-myc nuclear translocation. *Cell Death Differ*, 24(9), 1609-20. doi:10.1038/cdd.2017.86
115. Zeng, Y., Du, W. W., Wu, Y., Yang, Z., Awan, F. M., Li, X., et al. (2017). A Circular RNA Binds To and Activates AKT Phosphorylation and Nuclear Localization Reducing Apoptosis and Enhancing Cardiac Repair. *Theranostics*, 7(16), 3842-55. doi:10.7150/thno.19764
116. Du, W. W., Fang, L., Yang, W., Wu, N., Awan, F. M., Yang, Z., et al. (2017). Induction of tumor apoptosis through a circular RNA enhancing Foxo3 activity. *Cell Death Differ*, 24(2), 357-70. doi:10.1038/cdd.2016.133
117. Kishore, R., Garikipati, V. N. S., Gumpert, A. (2016). Tiny Shuttles for Information Transfer: Exosomes in Cardiac Health and Disease. *J Cardiovasc Transl Res*, 9(3), 169-75. doi:10.1007/s12265-016-9682-4
118. Li, Y., Zheng, Q., Bao, C., Li, S., Guo, W., Zhao, J., et al. (2015). Circular RNA is enriched and stable in exosomes: a promising biomarker for cancer diagnosis. *Cell Res*, 25(8), 981-4. doi:10.1038/cr.2015.82
119. Lasda, E., Parker, R. (2016). Circular RNAs Co-Precipitate with Extracellular Vesicles: A Possible Mechanism for circRNA Clearance. *PLoS One*, 11(2), e0148407. doi:10.1371/journal.pone.0148407
120. Vausort, M., Salgado-Somoza, A., Zhang, L., Leszek, P., Scholz, M., Teren, A., et al. (2016). Myocardial Infarction-Associated Circular RNA Predicting Left Ventricular Dysfunction. *J Am Coll Cardiol*, 68(11), 1247-8. doi:10.1016/j.jacc.2016.06.040
121. Liu, L., Chen, X., Chen, Y. H., Zhang, K. (2020). Identification of Circular RNA hsa_Circ_0003391 in Peripheral Blood Is Potentially Associated With Alzheimer's Disease. *Front Aging Neurosci*, 12, 601965. doi:10.3389/fnagi.2020.601965
122. Cheng, Z., Zhang, Y., Wu, S., Zhao, R., Yu, Y., Zhou, Y., et al. (2022). Peripheral blood circular RNA hsa_circ_0058493 as a potential novel biomarker for silicosis

- and idiopathic pulmonary fibrosis. *Ecotoxicol Environ Saf*, 236, 113451. doi:10.1016/j.ecoenv.2022.113451
123. Li, Q., Wang, Y., An, Y., Wang, J., Gao, Y. (2022). The Particular Expression Profiles of Circular RNA in Peripheral Blood of Myocardial Infarction Patients by RNA Sequencing. *Front Cardiovasc Med*, 9, 810257. doi:10.3389/fcvm.2022.810257
 124. Zhao, Z., Li, X., Gao, C., Jian, D., Hao, P., Rao, L., et al. (2017). Peripheral blood circular RNA hsa_circ_0124644 can be used as a diagnostic biomarker of coronary artery disease. *Sci Rep*, 7, 39918. doi:10.1038/srep39918
 125. Bao, X., Zheng, S., Mao, S., Gu, T., Liu, S., Sun, J., et al. (2018). A potential risk factor of essential hypertension in case-control study: Circular RNA hsa_circ_0037911. *Biochem Biophys Res Commun*, 498(4), 789-94. doi:10.1016/j.bbrc.2018.03.059
 126. Zaiou, M. (2019). Circular RNAs in hypertension: challenges and clinical promise. *Hypertens Res*, 42(11), 1653-63. doi:10.1038/s41440-019-0294-7
 127. Li, B., Li, Y., Hu, L., Liu, Y., Zhou, Q., Wang, M., et al. (2020). Role of Circular RNAs in the Pathogenesis of Cardiovascular Disease. *J Cardiovasc Transl Res*, 13(4), 572-83. doi:10.1007/s12265-019-09912-2
 128. Wang, L., Xu, G. E., Spanos, M., Li, G., Lei, Z., Sluijter, J. P. G., et al. (2023). Circular RNAs in Cardiovascular Diseases: Regulation and Therapeutic Applications. *Research (Wash D C)*, 6, 0038. doi:10.34133/research.0038
 129. Negi, S., Anand, A. (2010). Atherosclerotic coronary heart disease-epidemiology, classification and management. *Cardiovasc Hematol Disord Drug Targets*, 10(4), 257-61. doi:10.2174/187152910793743832
 130. Wang, L., Shen, C., Wang, Y., Zou, T., Zhu, H., Lu, X., et al. (2019). Identification of circular RNA Hsa_circ_0001879 and Hsa_circ_0004104 as novel biomarkers for coronary artery disease. *Atherosclerosis*, 286, 88-96. doi:10.1016/j.atherosclerosis.2019.05.006
 131. Wu, W. P., Pan, Y. H., Cai, M. Y., Cen, J. M., Chen, C., Zheng, L., et al. (2020). Plasma-Derived Exosomal Circular RNA hsa_circ_0005540 as a Novel Diagnostic Biomarker for Coronary Artery Disease. *Dis Markers*, 2020, 3178642. doi:10.1155/2020/3178642
 132. Cheng, C., Wang, Y., Xue, Q., Huang, Y., Wang, X., Liao, F., et al. (2023). CircRnas in atherosclerosis, with special emphasis on the spongy effect of circRnas on miRnas. *Cell Cycle*, 22(5), 527-41. doi:10.1080/15384101.2022.2133365

133. Hall, I. F., Climent, M., Quintavalle, M., Farina, F. M., Schorn, T., Zani, S., et al. (2019). Circ_Lrp6, a Circular RNA Enriched in Vascular Smooth Muscle Cells, Acts as a Sponge Regulating miRNA-145 Function. *Circ Res*, 124(4), 498-510. doi:10.1161/CIRCRESAHA.118.314240
134. Sun, Y., Zhang, S., Yue, M., Li, Y., Bi, J., Liu, H. (2019). Angiotensin II inhibits apoptosis of mouse aortic smooth muscle cells through regulating the circNRG-1/miR-193b-5p/NRG-1 axis. *Cell Death Dis*, 10(5), 362. doi:10.1038/s41419-019-1590-5
135. Yang, L., Yang, F., Zhao, H., Wang, M., Zhang, Y. (2019). Circular RNA circCHFR Facilitates the Proliferation and Migration of Vascular Smooth Muscle via miR-370/FOXO1/Cyclin D1 Pathway. *Mol Ther Nucleic Acids*, 16, 434-41. doi:10.1016/j.omtn.2019.02.028
136. Zhuang, J. B., Li, T., Hu, X. M., Ning, M., Gao, W. Q., Lang, Y. H., et al. (2020). Circ_CHFR expedites cell growth, migration and inflammation in ox-LDL-treated human vascular smooth muscle cells via the miR-214-3p/Wnt3/beta-catenin pathway. *Eur Rev Med Pharmacol Sci*, 24(6), 3282-92. doi:10.26355/eurev_202003_20696
137. Samak, M., Fatullayev, J., Sabashnikov, A., Zeriouh, M., Schmack, B., Farag, M., et al. (2016). Cardiac Hypertrophy: An Introduction to Molecular and Cellular Basis. *Med Sci Monit Basic Res*, 22, 75-9. doi:10.12659/MSMBR.900437
138. Wang, K., Long, B., Liu, F., Wang, J. X., Liu, C. Y., Zhao, B., et al. (2016). A circular RNA protects the heart from pathological hypertrophy and heart failure by targeting miR-223. *Eur Heart J*, 37(33), 2602-11. doi:10.1093/eurheartj/ehv713
139. Lim, T. B., Aliwarga, E., Luu, T. D. A., Li, Y. P., Ng, S. L., Annadoray, L., et al. (2019). Targeting the highly abundant circular RNA circSlc8a1 in cardiomyocytes attenuates pressure overload induced hypertrophy. *Cardiovasc Res*, 115(14), 1998-2007. doi:10.1093/cvr/cvz130
140. Du, W. W., Xu, J., Yang, W., Wu, N., Li, F., Zhou, L., et al. (2021). A Neuroligin Isoform Translated by circNlgn Contributes to Cardiac Remodeling. *Circ Res*, 129(5), 568-82. doi:10.1161/CIRCRESAHA.120.318364
141. Khan, M. A., Reckman, Y. J., Aufiero, S., van den Hoogenhof, M. M., van der Made, I., Beqqali, A., et al. (2016). RBM20 Regulates Circular RNA Production From the Titin Gene. *Circ Res*, 119(9), 996-1003. doi:10.1161/CIRCRESAHA.116.309568
142. Lu, D., Chatterjee, S., Xiao, K., Riedel, I., Huang, C. K., Costa, A., et al. (2022). A circular RNA derived from the insulin receptor locus protects against doxorubicin-

- induced cardiotoxicity. *Eur Heart J*, 43(42), 4496-511. doi:10.1093/eurheartj/ehac337
143. Yang, F., Li, A., Qin, Y., Che, H., Wang, Y., Lv, J., et al. (2019). A Novel Circular RNA Mediates Pyroptosis of Diabetic Cardiomyopathy by Functioning as a Competing Endogenous RNA. *Mol Ther Nucleic Acids*, 17, 636-43. doi:10.1016/j.omtn.2019.06.026
 144. Jiang, J., Gao, G., Pan, Q., Liu, J., Tian, Y., Zhang, X. (2022). Circular RNA circHIPK3 is downregulated in diabetic cardiomyopathy and overexpression of circHIPK3 suppresses PTEN to protect cardiomyocytes from high glucose-induced cell apoptosis. *Bioengineered*, 13(3), 6272-9. doi:10.1080/21655979.2022.2031395
 145. Zhou, B., Yu, J. W. (2017). A novel identified circular RNA, circRNA_010567, promotes myocardial fibrosis via suppressing miR-141 by targeting TGF-beta1. *Biochem Biophys Res Commun*, 487(4), 769-75. doi:10.1016/j.bbrc.2017.04.044
 146. Li, H., Xu, J. D., Fang, X. H., Zhu, J. N., Yang, J., Pan, R., et al. (2020). Circular RNA circRNA_000203 aggravates cardiac hypertrophy via suppressing miR-26b-5p and miR-140-3p binding to Gata4. *Cardiovasc Res*, 116(7), 1323-34. doi:10.1093/cvr/cvz215
 147. Tang, C. M., Zhang, M., Huang, L., Hu, Z. Q., Zhu, J. N., Xiao, Z., et al. (2017). CircRNA_000203 enhances the expression of fibrosis-associated genes by derepressing targets of miR-26b-5p, Col1a2 and CTGF, in cardiac fibroblasts. *Sci Rep*, 7, 40342. doi:10.1038/srep40342
 148. Ni, H., Li, W., Zhuge, Y., Xu, S., Wang, Y., Chen, Y., et al. (2019). Inhibition of circHIPK3 prevents angiotensin II-induced cardiac fibrosis by sponging miR-29b-3p. *Int J Cardiol*, 292, 188-96. doi:10.1016/j.ijcard.2019.04.006
 149. Zhu, Y., Pan, W., Yang, T., Meng, X., Jiang, Z., Tao, L., et al. (2019). Upregulation of Circular RNA CircNFIB Attenuates Cardiac Fibrosis by Sponging miR-433. *Front Genet*, 10, 564. doi:10.3389/fgene.2019.00564
 150. Du, W. W., Yang, W., Chen, Y., Wu, Z. K., Foster, F. S., Yang, Z., et al. (2017). Foxo3 circular RNA promotes cardiac senescence by modulating multiple factors associated with stress and senescence responses. *Eur Heart J*, 38(18), 1402-12. doi:10.1093/eurheartj/ehw001
 151. Shao, Y., Li, M., Yu, Q., Gong, M., Wang, Y., Yang, X., et al. (2022). CircRNA CDR1as promotes cardiomyocyte apoptosis through activating hippo signaling pathway in diabetic cardiomyopathy. *Eur J Pharmacol*, 922, 174915. doi:10.1016/j.ejphar.2022.174915

152. Li, M., Ding, W., Tariq, M. A., Chang, W., Zhang, X., Xu, W., et al. (2018). A circular transcript of *ncx1* gene mediates ischemic myocardial injury by targeting miR-133a-3p. *Theranostics*, 8(21), 5855-69. doi:10.7150/thno.27285
153. Si, X., Zheng, H., Wei, G., Li, M., Li, W., Wang, H., et al. (2020). circRNA *Hipk3* Induces Cardiac Regeneration after Myocardial Infarction in Mice by Binding to *Notch1* and miR-133a. *Mol Ther Nucleic Acids*, 21, 636-55. doi:10.1016/j.omtn.2020.06.024
154. Huang, S., Li, X., Zheng, H., Si, X., Li, B., Wei, G., et al. (2019). Loss of Super-Enhancer-Regulated circRNA *Nfix* Induces Cardiac Regeneration After Myocardial Infarction in Adult Mice. *Circulation*, 139(25), 2857-76. doi:10.1161/CIRCULATIONAHA.118.038361
155. Huang, Z. K., Yao, F. Y., Xu, J. Q., Deng, Z., Su, R. G., Peng, Y. P., et al. (2018). Microarray Expression Profile of Circular RNAs in Peripheral Blood Mononuclear Cells from Active Tuberculosis Patients. *Cell Physiol Biochem*, 45(3), 1230-40. doi:10.1159/000487454
156. Chen, Y. G., Chen, R., Ahmad, S., Verma, R., Kasturi, S. P., Amaya, L., et al. (2019). N6-Methyladenosine Modification Controls Circular RNA Immunity. *Mol Cell*, 76(1), 96-109 e9. doi:10.1016/j.molcel.2019.07.016
157. Liu, C. X., Li, X., Nan, F., Jiang, S., Gao, X., Guo, S. K., et al. (2019). Structure and Degradation of Circular RNAs Regulate PKR Activation in Innate Immunity. *Cell*, 177(4), 865-80 e21. doi:10.1016/j.cell.2019.03.046
158. Corey, S., Luo, Y. (2019). Circular RNAs and neutrophils: Key factors in tackling asymptomatic moyamoya disease. *Brain Circ*, 5(3), 150-5. doi:10.4103/bc.bc_38_19
159. Chen, Q., Mang, G., Wu, J., Sun, P., Li, T., Zhang, H., et al. (2020). Circular RNA circ*Snx5* Controls Immunogenicity of Dendritic Cells through the miR-544/SOCS1 Axis and PU.1 Activity Regulation. *Mol Ther*, 28(11), 2503-18. doi:10.1016/j.ymthe.2020.07.001
160. Zhang, Y., Zhang, G., Liu, Y., Chen, R., Zhao, D., McAlister, V., et al. (2018). GDF15 Regulates Malat-1 Circular RNA and Inactivates NFkappaB Signaling Leading to Immune Tolerogenic DCs for Preventing Alloimmune Rejection in Heart Transplantation. *Front Immunol*, 9, 2407. doi:10.3389/fimmu.2018.02407
161. Li, S., Abu Omar, A., Greasley, A., Wang, B., Wang, T. Z., Chahal, S., et al. (2024). Circular RNA MAP2K2-modified immunosuppressive dendritic cells for preventing alloimmune rejection in organ transplantation. *Bioeng Transl Med*, 9(1), e10615. doi:10.1002/btm2.10615

162. Amaya, L., Grigoryan, L., Li, Z., Lee, A., Wender, P. A., Pulendran, B., et al. (2023). Circular RNA vaccine induces potent T cell responses. *Proc Natl Acad Sci U S A*, *120*(20), e2302191120. doi:10.1073/pnas.2302191120
163. Zhang, Y., Zhang, Y., Li, X., Zhang, M., Lv, K. (2017). Microarray analysis of circular RNA expression patterns in polarized macrophages. *Int J Mol Med*, *39*(2), 373-9. doi:10.3892/ijmm.2017.2852
164. Wang, X., Bai, M. (2021). CircTM7SF3 contributes to oxidized low-density lipoprotein-induced apoptosis, inflammation and oxidative stress through targeting miR-206/ASPH axis in atherosclerosis cell model in vitro. *BMC Cardiovasc Disord*, *21*(1), 51. doi:10.1186/s12872-020-01800-x
165. He, Q., Shao, D., Hao, S., Yuan, Y., Liu, H., Liu, F., et al. (2021). CircSCAP Aggravates Oxidized Low-density Lipoprotein-induced Macrophage Injury by Upregulating PDE3B by miR-221-5p in Atherosclerosis. *J Cardiovasc Pharmacol*, *78*(5), e749-e60. doi:10.1097/FJC.0000000000001118
166. Bonilla, F. A., Oettgen, H. C. (2010). Adaptive immunity. *J Allergy Clin Immunol*, *125*(2 Suppl 2), S33-40. doi:10.1016/j.jaci.2009.09.017
167. Zhang, C., Wang, X., Chen, Y., Wu, Z., Zhang, C., Shi, W. (2018). The down-regulation of hsa_circ_0012919, the sponge for miR-125a-3p, contributes to DNA methylation of CD11a and CD70 in CD4(+) T cells of systemic lupus erythematosus. *Clin Sci (Lond)*, *132*(21), 2285-98. doi:10.1042/CS20180403
168. Huang, Z., Cao, Y., Zhou, M., Qi, X., Fu, B., Mou, Y., et al. (2019). Hsa_circ_0005519 increases IL-13/IL-6 by regulating hsa-let-7a-5p in CD4(+) T cells to affect asthma. *Clin Exp Allergy*, *49*(8), 1116-27. doi:10.1111/cea.13445
169. Tagawa, T., Gao, S., Koparde, V. N., Gonzalez, M., Spouge, J. L., Serquina, A. P., et al. (2018). Discovery of Kaposi's sarcoma herpesvirus-encoded circular RNAs and a human antiviral circular RNA. *Proc Natl Acad Sci U S A*, *115*(50), 12805-10. doi:10.1073/pnas.1816183115
170. Chen, T. C., Tallo-Parra, M., Cao, Q. M., Kadener, S., Bottcher, R., Perez-Vilaro, G., et al. (2020). Host-derived circular RNAs display proviral activities in Hepatitis C virus-infected cells. *PLoS Pathog*, *16*(8), e1008346. doi:10.1371/journal.ppat.1008346
171. Lu, S., Zhu, N., Guo, W., Wang, X., Li, K., Yan, J., et al. (2020). RNA-Seq Revealed a Circular RNA-microRNA-mRNA Regulatory Network in Hantaan Virus Infection. *Front Cell Infect Microbiol*, *10*, 97. doi:10.3389/fcimb.2020.00097

172. Huang, Y., Xue, Q., Cheng, C., Wang, Y., Wang, X., Chang, J., et al. (2023). Circular RNA in autoimmune diseases: special emphasis on regulation mechanism in RA and SLE. *J Pharm Pharmacol*, 75(3), 370-84. doi:10.1093/jpp/rgac096
173. Ouyang, Q., Wu, J., Jiang, Z., Zhao, J., Wang, R., Lou, A., et al. (2017). Microarray Expression Profile of Circular RNAs in Peripheral Blood Mononuclear Cells from Rheumatoid Arthritis Patients. *Cell Physiol Biochem*, 42(2), 651-9. doi:10.1159/000477883
174. Ouyang, Q., Liu, C., Lu, X., Liang, R., Zhao, J., Yang, M. (2021). Identification of Circular RNAs Circ_0005008 and Circ_0005198 in Plasma as Novel Biomarkers for New-Onset Rheumatoid Arthritis. *Front Pharmacol*, 12, 722017. doi:10.3389/fphar.2021.722017
175. Yang, J., Cheng, M., Gu, B., Wang, J., Yan, S., Xu, D. (2020). CircRNA_09505 aggravates inflammation and joint damage in collagen-induced arthritis mice via miR-6089/AKT1/NF-kappaB axis. *Cell Death Dis*, 11(10), 833. doi:10.1038/s41419-020-03038-z
176. Iparraguirre, L., Munoz-Culla, M., Prada-Luengo, I., Castillo-Trivino, T., Olascoaga, J., Otaegui, D. (2017). Circular RNA profiling reveals that circular RNAs from ANXA2 can be used as new biomarkers for multiple sclerosis. *Hum Mol Genet*, 26(18), 3564-72. doi:10.1093/hmg/ddx243
177. Carlos-Reyes, A., Romero-Garcia, S., Contreras-Sanzon, E., Ruiz, V., Prado-Garcia, H. (2022). Role of Circular RNAs in the Regulation of Immune Cells in Response to Cancer Therapies. *Front Genet*, 13, 823238. doi:10.3389/fgene.2022.823238
178. Li, Z., Cheng, Y., Wu, F., Wu, L., Cao, H., Wang, Q., et al. (2020). The emerging landscape of circular RNAs in immunity: breakthroughs and challenges. *Biomark Res*, 8, 25. doi:10.1186/s40364-020-00204-5
179. Ma, Y., Zhang, C., Zhang, B., Yu, H., Yu, Q. (2019). circRNA of AR-suppressed PABPC1 91 bp enhances the cytotoxicity of natural killer cells against hepatocellular carcinoma via upregulating UL16 binding protein 1. *Oncol Lett*, 17(1), 388-97. doi:10.3892/ol.2018.9606
180. Katopodi, T., Petanidis, S., Domvri, K., Zarogoulidis, P., Anastakis, D., Charalampidis, C., et al. (2021). Kras-driven intratumoral heterogeneity triggers infiltration of M2 polarized macrophages via the circHIPK3/PTK2 immunosuppressive circuit. *Sci Rep*, 11(1), 15455. doi:10.1038/s41598-021-94671-x

181. Zou, Y., Zheng, S., Deng, X., Yang, A., Xie, X., Tang, H., et al. (2019). The Role of Circular RNA CDR1as/ciRS-7 in Regulating Tumor Microenvironment: A Pan-Cancer Analysis. *Biomolecules*, 9(9). doi:10.3390/biom9090429
182. Hong, W., Xue, M., Jiang, J., Zhang, Y., Gao, X. (2020). Circular RNA circ-CPA4/let-7 miRNA/PD-L1 axis regulates cell growth, stemness, drug resistance and immune evasion in non-small cell lung cancer (NSCLC). *J Exp Clin Cancer Res*, 39(1), 149. doi:10.1186/s13046-020-01648-1
183. Parisi, L., Gini, E., Baci, D., Tremolati, M., Fanuli, M., Bassani, B., et al. (2018). Macrophage Polarization in Chronic Inflammatory Diseases: Killers or Builders? *J Immunol Res*, 2018, 8917804. doi:10.1155/2018/8917804
184. Steinbach, E. C., Plevy, S. E. (2014). The role of macrophages and dendritic cells in the initiation of inflammation in IBD. *Inflamm Bowel Dis*, 20(1), 166-75. doi:10.1097/MIB.0b013e3182a69dca
185. Das, A., Sinha, M., Datta, S., Abas, M., Chaffee, S., Sen, C. K., et al. (2015). Monocyte and macrophage plasticity in tissue repair and regeneration. *Am J Pathol*, 185(10), 2596-606. doi:10.1016/j.ajpath.2015.06.001
186. Mantovani, A., Biswas, S. K., Galdiero, M. R., Sica, A., Locati, M. (2013). Macrophage plasticity and polarization in tissue repair and remodelling. *J Pathol*, 229(2), 176-85. doi:10.1002/path.4133
187. Ponzoni, M., Pastorino, F., Di Paolo, D., Perri, P., Brignole, C. (2018). Targeting Macrophages as a Potential Therapeutic Intervention: Impact on Inflammatory Diseases and Cancer. *Int J Mol Sci*, 19(7). doi:10.3390/ijms19071953
188. Krishnamurthy, P., Thal, M., Verma, S., Hoxha, E., Lambers, E., Ramirez, V., et al. (2011). Interleukin-10 deficiency impairs bone marrow-derived endothelial progenitor cell survival and function in ischemic myocardium. *Circ Res*, 109(11), 1280-9. doi:10.1161/CIRCRESAHA.111.248369
189. Cimini, M., Garikipati, V. N. S., de Lucia, C., Cheng, Z., Wang, C., Truongcao, M. M., et al. (2019). Podoplanin neutralization improves cardiac remodeling and function after acute myocardial infarction. *JCI Insight*, 5(15). doi:10.1172/jci.insight.126967
190. Ying, W., Cheruku, P. S., Bazer, F. W., Safe, S. H., Zhou, B. (2013). Investigation of macrophage polarization using bone marrow derived macrophages. *J Vis Exp*(76). doi:10.3791/50323
191. Bender, A. T., Ostenson, C. L., Giordano, D., Beavo, J. A. (2004). Differentiation of human monocytes in vitro with granulocyte-macrophage colony-stimulating factor and macrophage colony-stimulating factor produces distinct changes in

- cGMP phosphodiesterase expression. *Cell Signal*, 16(3), 365-74. doi:10.1016/j.cellsig.2003.08.009
192. Kramer, M. C., Liang, D., Tatomer, D. C., Gold, B., March, Z. M., Cherry, S., et al. (2015). Combinatorial control of Drosophila circular RNA expression by intronic repeats, hnRNPs, and SR proteins. *Genes Dev*, 29(20), 2168-82. doi:10.1101/gad.270421.115
 193. Lo, H. L., Yee, J. K. (2007). Production of vesicular stomatitis virus G glycoprotein (VSV-G) pseudotyped retroviral vectors. *Curr Protoc Hum Genet*, Chapter 12, Unit 12 7. doi:10.1002/0471142905.hg1207s52
 194. Kutner, R. H., Zhang, X. Y., Reiser, J. (2009). Production, concentration and titration of pseudotyped HIV-1-based lentiviral vectors. *Nat Protoc*, 4(4), 495-505. doi:10.1038/nprot.2009.22
 195. Benskey, M. J., Manfredsson, F. P. (2016). Lentivirus Production and Purification. *Methods Mol Biol*, 1382, 107-14. doi:10.1007/978-1-4939-3271-9_8
 196. Sica, A., Erreni, M., Allavena, P., Porta, C. (2015). Macrophage polarization in pathology. *Cell Mol Life Sci*, 72(21), 4111-26. doi:10.1007/s00018-015-1995-y
 197. Gombozhapova, A., Rogovskaya, Y., Shurupov, V., Rebenkova, M., Kzhyshkowska, J., Popov, S. V., et al. (2017). Macrophage activation and polarization in post-infarction cardiac remodeling. *J Biomed Sci*, 24(1), 13. doi:10.1186/s12929-017-0322-3
 198. Krenkel, O., Tacke, F. (2017). Liver macrophages in tissue homeostasis and disease. *Nat Rev Immunol*, 17(5), 306-21. doi:10.1038/nri.2017.11
 199. Arnaiz, E., Sole, C., Manterola, L., Iparraguirre, L., Otaegui, D., Lawrie, C. H. (2019). CircRNAs and cancer: Biomarkers and master regulators. *Semin Cancer Biol*, 58, 90-9. doi:10.1016/j.semcancer.2018.12.002
 200. Chen, H., Mao, M., Jiang, J., Zhu, D., Li, P. (2019). Circular RNA CDR1as acts as a sponge of miR-135b-5p to suppress ovarian cancer progression. *Onco Targets Ther*, 12, 3869-79. doi:10.2147/OTT.S207938
 201. Cheng, D., Wang, J., Dong, Z., Li, X. (2021). Cancer-related circular RNA: diverse biological functions. *Cancer Cell Int*, 21(1), 11. doi:10.1186/s12935-020-01703-z
 202. Jiang, J., Li, R., Wang, J., Hou, J., Qian, H., Xu, W. (2021). Circular RNA CDR1as Inhibits the Metastasis of Gastric Cancer through Targeting miR-876-5p/GNG7 Axis. *Gastroenterol Res Pract*, 2021, 5583029. doi:10.1155/2021/5583029

203. Martinez, F. O., Sica, A., Mantovani, A., Locati, M. (2008). Macrophage activation and polarization. *Front Biosci*, *13*, 453-61. doi:10.2741/2692
204. Orecchioni, M., Ghosheh, Y., Pramod, A. B., Ley, K. (2019). Macrophage Polarization: Different Gene Signatures in M1(LPS+) vs. Classically and M2(LPS-) vs. Alternatively Activated Macrophages. *Front Immunol*, *10*, 1084. doi:10.3389/fimmu.2019.01084
205. Liu, Y., Xiao, J., Cai, J., Li, R., Sui, X., Zhang, J., et al. (2024). Single-cell immune profiling of mouse liver aging reveals Cxcl2+ macrophages recruit neutrophils to aggravate liver injury. *Hepatology*, *79*(3), 589-605. doi:10.1097/HEP.0000000000000590
206. Agarwal, V., Bell, G. W., Nam, J. W., Bartel, D. P. (2015). Predicting effective microRNA target sites in mammalian mRNAs. *Elife*, *4*. doi:10.7554/eLife.05005
207. Dorrington, M. G., Fraser, I. D. C. (2019). NF-kappaB Signaling in Macrophages: Dynamics, Crosstalk, and Signal Integration. *Front Immunol*, *10*, 705. doi:10.3389/fimmu.2019.00705
208. Chuang, Y., Hung, M. E., Cangelose, B. K., Leonard, J. N. (2016). Regulation of the IL-10-driven macrophage phenotype under incoherent stimuli. *Innate Immun*, *22*(8), 647-57. doi:10.1177/1753425916668243
209. Ward, Z., Pearson, J., Schmeier, S., Cameron, V., Pilbrow, A. (2021). Insights into circular RNAs: their biogenesis, detection, and emerging role in cardiovascular disease. *RNA Biol*, *18*(12), 2055-72. doi:10.1080/15476286.2021.1891393
210. Li, R., Xu, X., Gao, S., Wang, J., Hou, J., Xie, Z., et al. (2023). Circular RNA CDR1as Mediated by Human Antigen R (HuR) Promotes Gastric Cancer Growth via miR-299-3p/TGIF1 Axis. *Cancers (Basel)*, *15*(23). doi:10.3390/cancers15235556
211. Azizoglu, M., Ayaz, L., Bayrak, G., Yilmaz, B. C., Birbicer, H., Doruk, N. (2020). Evaluation of miRNAs Related with Nuclear Factor Kappa B Pathway in Lipopolysaccharide Induced Acute Respiratory Distress Syndrome. *Int J Mol Cell Med*, *9*(2), 130-9. doi:10.22088/IJMCM.BUMS.9.2.130
212. Ye, T., Yang, M., Huang, D., Wang, X., Xue, B., Tian, N., et al. (2019). MicroRNA-7 as a potential therapeutic target for aberrant NF-kappaB-driven distant metastasis of gastric cancer. *J Exp Clin Cancer Res*, *38*(1), 55. doi:10.1186/s13046-019-1074-6
213. Hoque, P., Romero, B., Akins, R. E., Batish, M. (2023). Exploring the Multifaceted Biologically Relevant Roles of circRNAs: From Regulation, Translation to Biomarkers. *Cells*, *12*(24). doi:10.3390/cells12242813

214. Schaefer, B. C., Schaefer, M. L., Kappler, J. W., Marrack, P., Kedl, R. M. (2001). Observation of antigen-dependent CD8+ T-cell/ dendritic cell interactions in vivo. *Cell Immunol*, 214(2), 110-22. doi:10.1006/cimm.2001.1895
215. Liu, S., Lockhart, J. R., Fontenard, S., Berlett, M., Ryan, T. M. (2020). Mapping the Chromosomal Insertion Site of the GFP Transgene of UBC-GFP Mice to the MHC Locus. *J Immunol*, 204(7), 1982-7. doi:10.4049/jimmunol.1901338
216. Yano, J., Lilly, E. A., Noverr, M. C., Fidel, P. L. (2020). A Contemporary Warming/Restraining Device for Efficient Tail Vein Injections in a Murine Fungal Sepsis Model. *J Vis Exp*(165). doi:10.3791/61961
217. Diehl, K. H., Hull, R., Morton, D., Pfister, R., Rabemampianina, Y., Smith, D., et al. (2001). A good practice guide to the administration of substances and removal of blood, including routes and volumes. *J Appl Toxicol*, 21(1), 15-23. doi:10.1002/jat.727
218. Turner, P. V., Brabb, T., Pekow, C., Vasbinder, M. A. (2011). Administration of substances to laboratory animals: routes of administration and factors to consider. *J Am Assoc Lab Anim Sci*, 50(5), 600-13. Retrieved from <https://www.ncbi.nlm.nih.gov/pubmed/22330705>
219. Turner, P. V., Pekow, C., Vasbinder, M. A., Brabb, T. (2011). Administration of substances to laboratory animals: equipment considerations, vehicle selection, and solute preparation. *J Am Assoc Lab Anim Sci*, 50(5), 614-27. Retrieved from <https://www.ncbi.nlm.nih.gov/pubmed/22330706>
220. Gray, S. J., Choi, V. W., Asokan, A., Haberman, R. A., McCown, T. J., Samulski, R. J. (2011). Production of recombinant adeno-associated viral vectors and use in in vitro and in vivo administration. *Curr Protoc Neurosci*, Chapter 4, Unit 4 17. doi:10.1002/0471142301.ns0417s57
221. Xiao, X., Li, J., Samulski, R. J. (1998). Production of high-titer recombinant adeno-associated virus vectors in the absence of helper adenovirus. *J Virol*, 72(3), 2224-32. doi:10.1128/JVI.72.3.2224-2232.1998
222. Rabinowitz, J. E., Rolling, F., Li, C., Conrath, H., Xiao, W., Xiao, X., et al. (2002). Cross-packaging of a single adeno-associated virus (AAV) type 2 vector genome into multiple AAV serotypes enables transduction with broad specificity. *J Virol*, 76(2), 791-801. doi:10.1128/jvi.76.2.791-801.2002
223. Ackers-Johnson, M., Li, P. Y., Holmes, A. P., O'Brien, S. M., Pavlovic, D., Foo, R. S. (2016). A Simplified, Langendorff-Free Method for Concomitant Isolation of Viable Cardiac Myocytes and Nonmyocytes From the Adult Mouse Heart. *Circ Res*, 119(8), 909-20. doi:10.1161/CIRCRESAHA.116.309202

224. Yue, Y., Garikipati, V. N. S., Verma, S. K., Goukassian, D. A., Kishore, R. (2017). Interleukin-10 Deficiency Impairs Reparative Properties of Bone Marrow-Derived Endothelial Progenitor Cell Exosomes. *Tissue Eng Part A*, 23(21-22), 1241-50. doi:10.1089/ten.TEA.2017.0084
225. Zhao, J., Chen, C., Guo, M., Tao, Y., Cui, P., Zhou, Y., et al. (2016). MicroRNA-7 Deficiency Ameliorates the Pathologies of Acute Lung Injury through Elevating KLF4. *Front Immunol*, 7, 389. doi:10.3389/fimmu.2016.00389
226. Yang, S., Yuan, H. Q., Hao, Y. M., Ren, Z., Qu, S. L., Liu, L. S., et al. (2020). Macrophage polarization in atherosclerosis. *Clin Chim Acta*, 501, 142-6. doi:10.1016/j.cca.2019.10.034
227. Mohapatra, S., Pioppini, C., Ozpolat, B., Calin, G. A. (2021). Non-coding RNAs regulation of macrophage polarization in cancer. *Mol Cancer*, 20(1), 24. doi:10.1186/s12943-021-01313-x
228. Huang, Z., Luo, Q., Yao, F., Qing, C., Ye, J., Deng, Y., et al. (2016). Identification of Differentially Expressed Long Non-coding RNAs in Polarized Macrophages. *Sci Rep*, 6, 19705. doi:10.1038/srep19705
229. Zhou, Y., Do, D. C., Ishmael, F. T., Squadrito, M. L., Tang, H. M., Tang, H. L., et al. (2018). Mannose receptor modulates macrophage polarization and allergic inflammation through miR-511-3p. *J Allergy Clin Immunol*, 141(1), 350-64 e8. doi:10.1016/j.jaci.2017.04.049
230. Jang, J. Y., Lee, J. K., Jeon, Y. K., Kim, C. W. (2013). Exosome derived from epigallocatechin gallate treated breast cancer cells suppresses tumor growth by inhibiting tumor-associated macrophage infiltration and M2 polarization. *BMC Cancer*, 13, 421. doi:10.1186/1471-2407-13-421
231. Fang, G., Xu, D., Zhang, T., Wang, G., Qiu, L., Gao, X., et al. (2023). Biological functions, mechanisms, and clinical significance of circular RNA in colorectal cancer. *Front Oncol*, 13, 1138481. doi:10.3389/fonc.2023.1138481
232. Yin, J., Hu, T., Xu, L., Li, P., Li, M., Ye, Y., et al. (2019). Circular RNA expression profile in peripheral blood mononuclear cells from Crohn disease patients. *Medicine (Baltimore)*, 98(26), e16072. doi:10.1097/MD.00000000000016072
233. Zhou, R. M., Shi, Z. H., Shan, K., Zhang, S. J., Zhang, Y. H., Liang, Y., et al. (2022). Comparative Analysis of Differentially Expressed Circular RNAs in Polarized Macrophages. *Front Genet*, 13, 823517. doi:10.3389/fgene.2022.823517
234. Mester-Tonczar, J., Winkler, J., Einzinger, P., Hasimbegovic, E., Kastner, N., Lukovic, D., et al. (2020). Association between Circular RNA CDR1as and Post-

- Infarction Cardiac Function in Pig Ischemic Heart Failure: Influence of the Anti-Fibrotic Natural Compounds Bufalin and Lycorine. *Biomolecules*, 10(8). doi:10.3390/biom10081180
235. Bosco, P., Spada, R., Caniglia, S., Salluzzo, M. G., Salemi, M. (2014). Cerebellar degeneration-related autoantigen 1 (CDR1) gene expression in Alzheimer's disease. *Neurol Sci*, 35(10), 1613-4. doi:10.1007/s10072-014-1805-6
236. Lodrini, A. M., Goumans, M. J. (2021). Cardiomyocytes Cellular Phenotypes After Myocardial Infarction. *Front Cardiovasc Med*, 8, 750510. doi:10.3389/fcvm.2021.750510
237. Gladka, M. M., Kohela, A., Molenaar, B., Versteeg, D., Kooijman, L., Monshouwer-Kloots, J., et al. (2021). Cardiomyocytes stimulate angiogenesis after ischemic injury in a ZEB2-dependent manner. *Nat Commun*, 12(1), 84. doi:10.1038/s41467-020-20361-3
238. Zhao, J., Chu, F., Xu, H., Guo, M., Shan, S., Zheng, W., et al. (2021). C/EBPalpha/miR-7 Controls CD4(+) T-Cell Activation and Function and Orchestrates Experimental Autoimmune Hepatitis in Mice. *Hepatology*, 74(1), 379-96. doi:10.1002/hep.31607
239. Kong, D., Piao, Y. S., Yamashita, S., Oshima, H., Oguma, K., Fushida, S., et al. (2012). Inflammation-induced repression of tumor suppressor miR-7 in gastric tumor cells. *Oncogene*, 31(35), 3949-60. doi:10.1038/onc.2011.558
240. Chen, H., Guo, M., Yue, D., Zhao, J., Zhou, Y., Chen, C., et al. (2021). MicroRNA-7 negatively regulates Toll-like receptor 4 signaling pathway through FAM177A. *Immunology*, 162(1), 44-57. doi:10.1111/imm.13252
241. Banerjee, S., Xie, N., Cui, H., Tan, Z., Yang, S., Icyuz, M., et al. (2013). MicroRNA let-7c regulates macrophage polarization. *J Immunol*, 190(12), 6542-9. doi:10.4049/jimmunol.1202496
242. Safari, A., Madadi, S., Schwarzenbach, H., Soleimani, M., Safari, A., Ahmadi, M., et al. (2023). MicroRNAs and their Implications in CD4+ T-cells, Oligodendrocytes and Dendritic Cells in Multiple Sclerosis Pathogenesis. *Curr Mol Med*, 23(7), 630-47. doi:10.2174/1566524022666220525150259
243. Ghaleb, A. M., Yang, V. W. (2017). Kruppel-like factor 4 (KLF4): What we currently know. *Gene*, 611, 27-37. doi:10.1016/j.gene.2017.02.025
244. Liu, J., Liu, Y., Zhang, H., Chen, G., Wang, K., Xiao, X. (2008). KLF4 promotes the expression, translocation, and release of HMGB1 in RAW264.7 macrophages in response to LPS. *Shock*, 30(3), 260-6. doi:10.1097/shk.0b013e318162bef7

245. Yoshida, T., Yamashita, M., Iwai, M., Hayashi, M. (2016). Endothelial Kruppel-Like Factor 4 Mediates the Protective Effect of Statins against Ischemic AKI. *J Am Soc Nephrol*, 27(5), 1379-88. doi:10.1681/ASN.2015040460
246. Zahlten, J., Steinicke, R., Bertrams, W., Hocke, A. C., Scharf, S., Schmeck, B., et al. (2013). TLR9- and Src-dependent expression of Krueppel-like factor 4 controls interleukin-10 expression in pneumonia. *Eur Respir J*, 41(2), 384-91. doi:10.1183/09031936.00196311
247. Zhang, Y., Wang, Y., Liu, Y., Wang, N., Qi, Y., Du, J. (2013). Kruppel-like factor 4 transcriptionally regulates TGF-beta1 and contributes to cardiac myofibroblast differentiation. *PLoS One*, 8(4), e63424. doi:10.1371/journal.pone.0063424